琉球大学学術リポジトリ

合成極厚無筋壁で補強されたRC造ピロティ建築物の耐震評価

メタデータ	
	言語:
	出版者: Javadi, Pasha
	公開日: 2021-12-15
	キーワード (Ja):
	キーワード (En):
	作成者: Javadi, Pasha
	メールアドレス:
	所属:
URL	http://hdl.handle.net/20.500.12000/18527

SEISMIC EVALUATION OF SOFT-FIRST-STORY RC BUILDINGS RETROFITTED BY THICK HYBRID WALL TECHNIQUE

by

PASHA JAVADI

A Thesis
Submitted to the Division of Material, Structural and Energy Engineering
in Partial Fulfillment of the Requirements for the Degree of

DOCTOR OF PHILOSOPHY
IN
STRUCTURAL ENGINEERING

Supervised by

Prof. TETSUO YAMAKAWA
Professor of Department of Civil Engineering and Architecture

University of the Ryukyus
Okinawa, Japan

August 2009

ABSTRACT

This thesis focuses on seismic evaluation and retrofit of soft-first-story RC buildings. Seismic evaluations are conducted through the experimental investigations and dynamic response analyses. Experimental investigations were carried out on one-bay two-story RC frames retrofitted by thick hybrid wall technique. One specimen is a non-retrofitted benchmark specimen to verify the effectiveness of the retrofit method. Three specimens were retrofitted by thick hybrid wing-wall with different retrofit schemes and one specimen was retrofitted by thick hybrid panel-wall. In the proposed retrofit technique, channel-shaped steel plates jacket the boundary columns of RC frame and extend to the bay of the frame through the additional steel plates. The steel plates at both sides of frame are stitched together by means of PC bars (high-strength bolts) crossing the body of thick hybrid wall. The depth of wing-wall can be readily decided to obtain a desired lateral strength and stiffness. The experimental investigations proved the effectiveness of the proposed retrofit technique. The design frameworks for calculations the lateral strengths of the retrofitted columns are suggested. To find out the seismic response of the building retrofitted by thick hybrid wall, an existing soft-first-story building in Okinawa, where the soft-first-story buildings are commonly built, is selected. The seismic evaluation of the building is implemented based on the retrofit guideline by Japan Building Disaster Prevention Association and nonlinear dynamic response analyses. It was assumed that the building was retrofitted by conventional method (shear wall) and by thick hybrid wall. Nonlinear dynamic analyses were implemented under three earthquake excitations including Taft, Kobe and El Centro scaled to two levels of intensity. Seismic performance of the building retrofitted by thick hybrid wall exhibited a superior performance in compared to the conventional one.

ACKNOWLEDGMENTS

I would like to express gratitude to several persons, for their roles during the elaboration of this work, and without them it should be difficult to achieve the final objectives:

- First of all, to my tireless supervisor, Professor Tetsuo Yamakawa, who has introduced me the world of retrofit of buildings and help me to conduct an interesting research. I am really thankful of my supervisor for all of the knowledge, advices and suggestions gave me during doctoral course, and also his kind relationship which leaded to a perfect working and confident ambience.
- To Dr K. Nakada, for his instant and important supports, and his patient treatment.
- To Prof. A. J. Carr from university of the Canterbury that help me to implement nonlinear dynamic analyses during his stay in Okinawa.
- To all undergraduate students, graduated students and technicians of Prof. Yamakawa laboratory. Certainly, without a friendly group work, carrying out the experimental loading tests is not possible.
- To my father, mother, brother and sister that always encouraged me to continue the study.
- To Prof. M. R. Alsharif, Iranian Professor of the Engineering Department, who introduced me research activities of Prof. Yamakawa laboratory, and greatly helped me to stay in Okinawa.
- To my aunt and my cousins for their kindness and their supports during this time.
- To Japanese Government for providing a situation accompanying advanced research and enjoyable life.
- To all of the persons that directly or indirectly help me, but I don't mention their names here.

TABLE OF CONTENTS

LIST OF FIGURES

LIST OF TABLES

x

1. INTRODUCTION

1.1 General

In recent years, damage to buildings with low seismic capacities has occurred in a number of earthquake-prone countries, for example, in the Kocaeli Earthquake and 1999 Chi-chi Earthquake, which represent the requiring technical development for improvement of the seismic capacity of such buildings. Japan is located in an earthquake-prone region and during its history has experienced serious disaster caused by a number of major earthquakes. Thus, ensuring the seismic safety of building is a matter of concern not only to construction engineering including the administrative authorities responsible for construction, but also the general public.

The 1968 Tokachi-oki earthquake caused significant damages, for the first time in Japan, to reinforced concrete buildings, which had been believed by engineers, researchers and the general public to be earthquake resistant since the 1923 Kanto earthquake. Reinforced concrete columns failed in shear in school buildings in the earthquake. The concern was expressed by many organizations about the earthquakes safety of existing reinforced concrete buildings; e. g., the Ministry of Education about school buildings, the Ministry of Construction about government buildings, and construction companies about their clients buildings. Various methods were developed for the seismic vulnerability assessment of existing buildings against future earthquakes [1]. The Ministry of construction organized a committee in 1976 to develop an integrated method to evaluate the seismic vulnerability of existing low-to-mid-rise reinforced concrete buildings. The committee published "Standard for Seismic Vulnerability Assessment of Existing Reinforced Concrete Buildings" [2]. The standard was revised in December 1990. The reliability of the method was tested after several earthquakes including the 1978 Miyagi-ken Oki earthquake and the 1995 Hyogo-ken Nanbu Earthquake for school buildings.

The ministry of construction sponsored a coordinated technical project (1981-1985) for the development of post earthquake measures and the development of repairing and strengthening

technique [3]. The guidelines [4] for post earthquake inspection and assessment of earthquake damages were published in February 1991. The guidelines were used after the 1995 Hyogo-ken Nanbu earthquake to evaluate the damage level of affected buildings and the need for strengthening. After the 1995 Hyogo-ken Nanbu earthquake, the government, recognizing the urgent importance of improving seismic resistance of existing buildings, proclaimed a law [5] to promote the seismic strengthening of existing buildings. The law, enforced on December 25 1995, requires that the owner of a "specially designated building" should make efforts to strengthen the structure if needed.

Sever earthquakes disasters occurred in Turkey and Taiwan 1999, and in Iran 2003. Old buildings collapsed in these events, which re-emphasized the importance of seismic vulnerability assessment of existing buildings in seismic regions. In the most recent destructive earthquake in Japan, Kobe earthquake, it was observed that many RC structures are still vulnerable under strong earthquakes. Among different types of failures, soft-story mechanism was the most common. In soft-story building, one story has low strength and stiffness in compared to its adjacent stories. Damage usually concentrated in the soft story and cause sway mechanism with high local ductility demand. Nowadays, a great number of reinforced concrete structures in use have similar characteristics to those that collapsed during the past earthquakes. Considering this fact, it is an urgent at present to find out the vulnerability of the existing structures and consequently try to propose adequate rehabilitation methods.

1.2 Background

A large number of RC structures received destructive damages during the past earthquakes. Since, at present, many buildings have the characteristics of those buildings, it is necessary that their seismic performance will carefully be verified. When a structural engineer encounter to a

Fig. 1.1 Pilotis RC building damaged by shear-compression failure in Geiyo EQ (M=6.7), Hiroshima, 2001

Fig1.2 Pilotis RC building damaged by flexural failure in Hyogoken-nanbu EQ (M=6.7), Hiroshima, 2001

building designed according to insufficient seismic design, the attentions most be focused on two problems. The first is that which retrofitting scheme is suitable for the existing building. In this choice, the common usage of the building and its architecture provide some limitations. In the second problem, the approach to numerically analysis the building before and after retrofit should be verified. There are different ways to analyze a building that each one has its simplicity and aqua racy. Certainly, a simple method to evaluate the vulnerability of buildings is more suitable if it provides an acceptable accuracy. Among different ways of analyses, nonlinear dynamic response analysis can superiorly predict the seismic response of a building under a special time-history excitation.

There are different methods to rehabilitee a soft-story frame. The primary concern is a technique to upgrade the lateral strength, and the secondary one is to improve the lateral ductility. One of major deficiency in existing reinforced concrete building, constructed before the 1971 revision of the Building Standard Law of Japan, were not provided with sufficient amount of lateral reinforcement and may fail in shear at relative small deformation. Therefore, one of the most common retrofitting strategies is to install new structural walls to increase the stiffness and the strength of the structure so that the lateral deformation of these columns can be limited during

earthquakes. This strengthening includes the installation of new reinforced concrete shear walls in open frames, adding thickness to existing walls, or filling openings in existing walls. Placements of stiff walls affect the location of resistance center in plane; therefore, the walls should be properly placed to balance the stiffness distribution in plan [1]. Three different types of shear wall can be designed including flexural-behavior wall, shear-dominant wall and uplifting-rotation wall.

Addition of steel diagonal braced frames to an existing concrete moment frame building is another method of adding strength and/or stiffness to the structural system. The steel braces can be added without a significant increase in the building weight. A significant concern associated with installing a new steel braced frame in a concrete building is the connection of the beam at the top of the frame in each story to the underside of the existing concrete diaphragm overhead. The primary concern is that a relatively large shear force must be transferred from the overhead diaphragm into the new steel bracing below through a relatively localized connection using discreet anchors/bolts [1], [6].

Also, an existing column may be stiffened and strengthened by adding wing walls on both sides and one side of the column. The addition of wing-wall can increase the shear strength or flexural strength of the column. The important point in this approach is that the brittle shear failure is likely to happen in the wing-wall-column. By increasing the width and thickness of wing-wall, it is possible to reach to the flexural yielding of wing-wall-column. In this method, the wing-wall must be carefully connected to the RC column.

In addition to the mentioned methods that increased the lateral strength. The lateral strength of the frame can be increased with altering the possible mechanism. For example, in case of RC column that shear failure is likely to happen, with utilizing fiber reinforced plastics (FRP) , steel plate jacketing, PC bar prestressing and etc., the brittle shear failure can be changed to ductile flexural mode which accompanies with increasing the lateral strength. So, considering different approaches in enhancing the lateral strength, a appropriate retrofitting system should be chosen to satisfy the required capacity for building during an expected strong earthquake.

As explained previously, the way of analysis a building before and after retrofit has important role in estimating its response during an earthquake. Japan Building Disaster Prevention Association (JBDPA) suggested simplified analysis approach in evaluating the vulnerability of a building. The standard uses three-level screening procedures. A simple screening procedure is intended to identify majority of earthquake resistant buildings by examining story shear strength provided by columns and structural walls. Those buildings, identified as questionable by the simple procedure, must be

analyzed by more sophisticated second-level procedure considering deformation capacity of vertical members. The third-level procedure is a general and detail procedure and requires the nonlinear static and dynamic analysis of the entire structure.

When the RC structures subjected to sever earthquake excitations they are expected to deform well into the inelastic range and dissipate the large seismic energy input into the structure through large but controllable inelastic deformation at critical region. In order to predict the distribution of forces and deformations in these structures under the maximum credible earthquake that can occur at the site, accurate models of the hysteretic behavior of the different critical regions of the structure are necessary [7].

Many analytical models have been proposed to date for the nonlinear analysis of reinforced concrete frame structures. These range from very refined and complex local models to simplified global models. Refined analytical models are typically used in predicting the response of small structures or structural subassemblies. On the other hand simplified global models have been typically used in the dynamic response analysis of large structures. While simple component models are unreliable and incapable of simulating the local behavior of critical inelastic regions in the structure and cannot yield accurate estimates of strain or curvature ductilities, the computational cost associated with the use of refined finite element models in nonlinear dynamic response studies of high-rise concrete frames is very high [7]. So, in order to obtain reasonable dynamic responses of buildings during earthquake excitations, the potential-critical plastic hinges of the structures should be carefully recognized and modeled. Certainly, a correct modeling of the plastic hinges zones can be confirmed through the comparison between the experimentally observed mechanism and the related model of critical plastic hinge zones which strongly generate the deformations of the structures. In the most RC buildings, the major source of deformations are flexural plastic hinges while some other mechanism, such as shear deformation or fixed-end rotation due to bond splitting failure can slightly to greatly contribute in the response of the members.

1.3 Review of previous studies

Application of thick hybrid wall in retrofitting shear-dominant wing-wall column was first proposed by Yamakawa et al [8]. The research conducted on shear-dominant wing-wall columns exhibited that by application thick hybrid wall, the brittle shear failure perfectly prevents and the retrofitted specimens show a ductile flexural response even for large drift angle. In following the investigations conducted on wing-wall-column, a study was carried out on soft-story frames [9].

As mentioned previously, application of shear-dominant wall is a one retrofitting method in increase the lateral strength and stiffness of soft-story frames. The most important concern in application of this retrofitting scheme is that the shear failure is likely to happen in the utilized shear wall under unexpected strong earthquakes. A schematic view of utilizing shear wall as a convenient

Non-retrofitted bare frame

Non-retrofitted bare frame

Conventional retrofit technique by installing wing-wall into bare frame

Proposed retrofit technique by installing wing-wall into bare frame

Conventional retrofit technique by installing panel wall into bare frame

Proposed retrofit technique by installing panel wall into bare frame
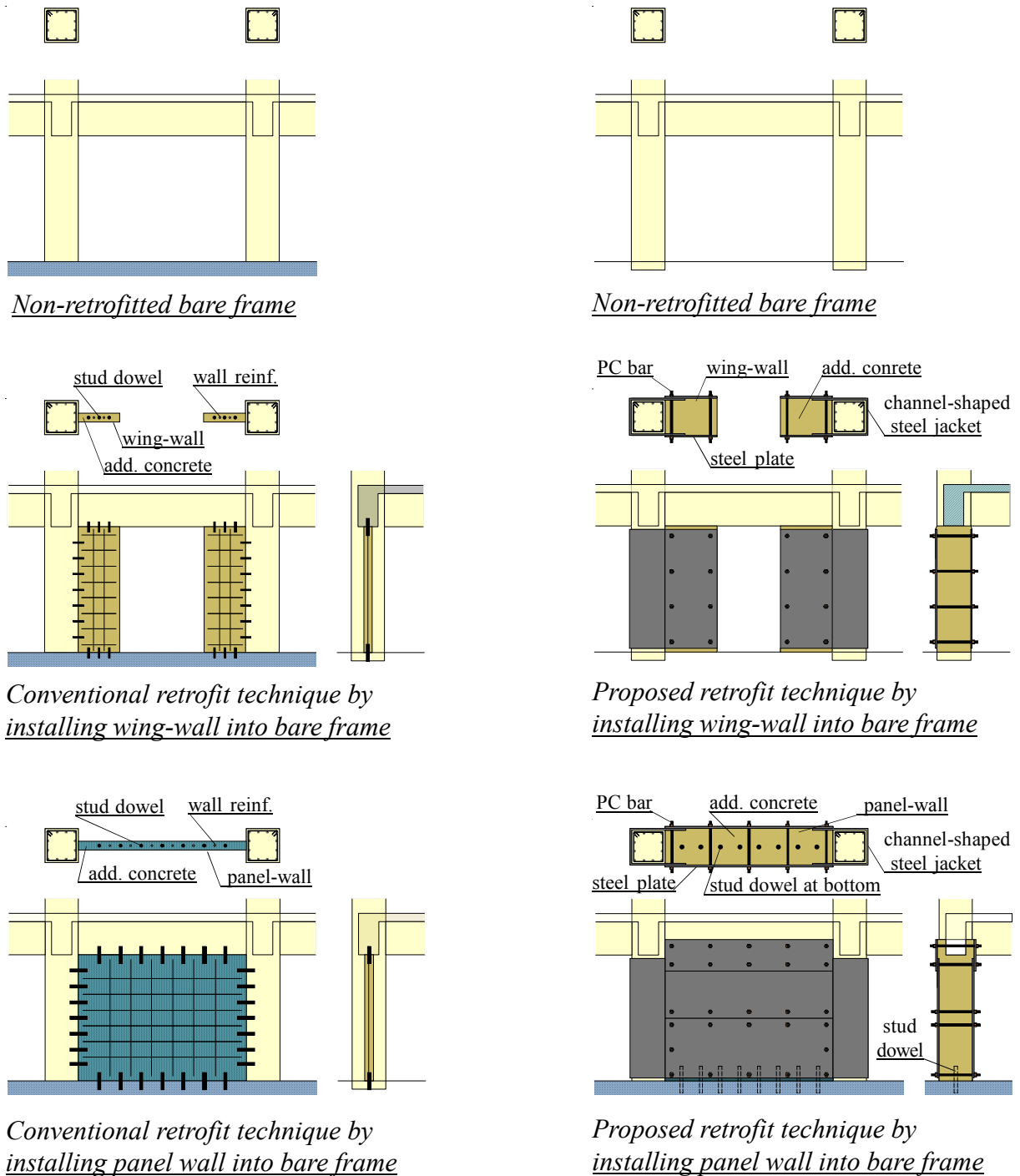
Fig. 1.3 Example of conventional and proposed retrofit techniques [9]

retrofitting method is illustrated in **Fig. 1.3**. A convenient approach in connecting the shear wall to the RC frame is installation of stud dowels. At first, on the surrounding RC frame holes are provided. After that, the holes are filled with epoxy grout. The stud dowels are inserted to the epoxy-injected holes. Then, the reinforcement arranged on the frame vertically and horizontally. Finally, the concrete are cast in the bay of frame. In this approach, in addition to shear failure that likely to happen in shear wall, another weak point is the connection of shear wall to the surrounding RC frame. Transferring high shear force from a localized connection needs a large number of stud dowels which, in some practical cases, might be impossible to use. Moreover, making holes on the surrounding RC frame is a noisy and dusty procedure that provides some hesitancy to operate the retrofitting procedures.

The proposed method by Yamakawa et al. [8,9] can be categorized into two type retrofit including wing-wall type and panel-wall type. In the first approach channel-shaped steel plates jacket the boundary columns and extend into the bay of the frame through the additional steel plates. The depth of the wing-wall depends on the demand of the lateral strength. In another method (panel-wall type) channel-shaped steel plates jacket the boundary columns and cover the whole length of the bay. The installed steel plates at both sides of the frame stitch together with PC bars. By applying this method, the RC column and the additional wing-wall or panel-wall behave as a relatively unified member with high shear resistance. In this method, in addition to increasing the lateral strength and stiffness of the frame, its ductility also improves considerably. On the other hand, in case of RC columns that the shear failure is likely to happen, by application of thick hybrid wall, the mechanism change from the brittle shear failure to the ductile flexural behavior.

1.4 Objectives

Capacity-based deign is commonly used as a method of design new structures and for retrofitting of existing structures. In the capacity design of structures for earthquake resistance, distinct elements of the primary lateral force resisting system are chosen and suitably designed and detailed for energy dissipation under sever imposed deformations. The critical regions of these members, often termed plastic hinges, are detailed for inelastic flexural action, and shear failure is inhibited by a suitable strength differential. All other structural elements are then protected against actions that could cause failure, by providing them with strength greater than that corresponding to development of maximum feasible strength in the potential plastic hinge regions.
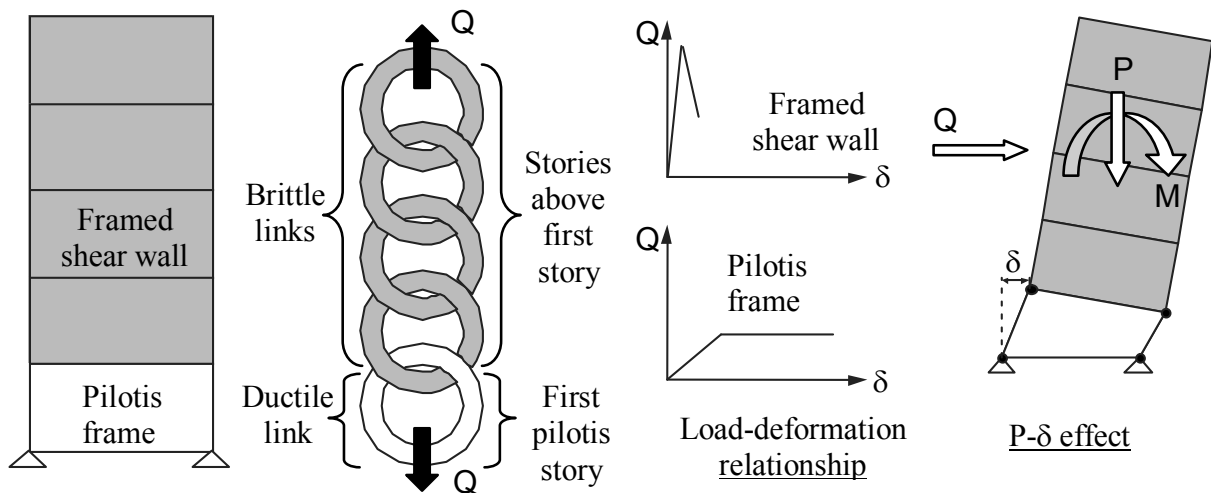
Fig. 1.4 Principle of strength limitation in case of soft-first-story frame

To highlight the simple concept of capacity-based design for soft-first-story frames, a chain shown in Fig. 1.4 will be considered. A soft-first-story frame is modeled by a chain. In the considered frame, the first story include open frame with low strength and high ductility, and the upper stories include shear wall with high strength and low ductility. The base shear force induced during an earthquake can be assumed to apply at the ends of the chain. The global strength of the chain will be determined by the link with low strength and high ductility. It should be noted that if the brittle links were designed to have the same nominal strength as the ductile link, the randomness of strength variation between all links, including the ductile link, would imply a high probability that failure would occur in a brittle link and the chain would no ductility. Failure of all other links can, however, be prevented if their strength is in excess of the maximum feasible strength of the weak link, corresponding to the level of ductility envisaged.

Regarding the concept of capacity-based design, since in soft-first-story frames the lateral strength and stiffness of the first story is considerably less than those of upper stories, the lateral deformations during an earthquake will be concentrated at the first story. The concerning problem is that if the induced lateral displacement in the first story be significantly large, secondary deformations due to the P-δ effect can accelerate the lateral displacement and consequently it leads to collapse the first story. Considering this fact, application of a retrofit system that controllably increases the lateral strength and stiffness of first story is valuable.

In following the previous investigations on soft story frames [9], in this study the attention mainly focuses on a retrofit technique for soft-first-story frames. The main objective is to obtain a desired retrofitting scheme for this building type. Generally, two types of retrofit methods including application of wing-wall and panel-wall for soft-first-story frames will be verified. In

view points of practical engineering, the most important points in utilizing a retrofit system are its simplicity in understanding the physical mechanism and its ease in construction.

When an applied retrofit project can be effective, the vulnerability assessment of existing building carefully carried out before and after retrofitting. Even though there is a simplified vulnerability assessment in the retrofit guideline by Japan Building Disaster Prevention Association, it will be interesting to verify responses of the building through nonlinear dynamic analysis. In performing the dynamic analysis, the critical region of the proposed retrofit scheme should be carefully recognized and modeled. So, in this study, the hysteretic models of the retrofitted columns by the proposed method are described according to experimentally observed mechanisms. In the most design codes or retrofit guidelines, the demand forces of buildings are calculated according to seismic zone activity. But, it will be worthy to check the response of the building according to probable earthquakes, and comparing the results with the simplified methods.

1.5 Outlines of thesis

The present thesis contains five chapters. It covers a brief introduction about the problems of soft story frames and the conducted previous studies. In chapter two, the state-of-art of experimental investigations on soft-first-story frames are detailed and discussed. The experimental results will be explained and the fundamental mechanisms will be discussed. Among different types of retrofitting schemes, the desired one will be introduced. Also, the simplified design equations are presented for the proposed methods. In Chapter 3, the hysteretic behavior of the columns retrofitted with wing-wall and panel-wall are verified and appropriate rules are obtained. The hysteretic models are calibrated with the experimentally observed mechanisms. In Chapter 4, an existing soft-first-story building is evaluated before and after retrofit through the simplified screening procedure suggested by Japan Building Disaster Prevention Association. Also, nonlinear dynamic analyses are conducted for the building under three excitations including Taft, El Centro and Kobe Earthquakes. The results of simplified screening procedure and the results obtained by nonlinear dynamic analysis are compared. In Chapter 5, summary of conclusions of the experimental tests and seismic analyses will be presented.

2. EXPERIMENTAL INVESTIGATION ON PILOTIS RC FRAMES RETROFITTED WITH THICK HYBRID WALL

2.1 General

In the recent strong earthquakes such as the 1995 Kobe earthquake, a large number of RC buildings severely damaged in Japan. Among different type of failures, the soft story mechanism was one of the common features of the failures. Where one level, typically the lowest, is weaker than upper levels, a column sway mechanism can develop with high local ductility demand. This often resulted from a functional desire to open the lowest level to the maximum extent possible for retail shopping or parking requirements. Nowadays, a great number of RC buildings have the characteristics of soft-first-story buildings. So, retrofit of this building type is an urgent at present. There are different types of retrofit methods for soft-first-story building such as application of shear wall or steel braced frame, etc.

In the previous investigations by Yamakawa et al. and Rahman et al. [8, 9, 10], it was found out that application of thick hybrid wing-wall and panel-wall are suitable for soft story frames. In thick hybrid wall technique, the lateral strength and stiffness of RC frames considerably increase and also the lateral ductility significantly improves. Regarding the concept of thick hybrid wall technique, in this study, thick hybrid wall technique is applied in case of soft first story frames. A series of experimental investigations were conducted on one-bay two-story pilotis RC frames retrofitted by thick hybrid wall which will be discussed in great details in this chapter.

2.2 Test plan

In order to obtain a desired retrofitting scheme of soft-first-story RC frames retrofitted by thick hybrid wall technique, five one-bay one-story pilotis RC frames were testes. The specimens were tested under constant axial force ($0.2\,\sigma_B bD$, where b and D are dimensions of columns, and σ_B is the cylinder strength of concrete) and horizontal cyclic loading test. The details of

reinforcements are given in **Fig, 2.1**. The scale factor of the test specimens is 1/4~1/3 of a low-rise school building designed according to the pre-1971 Japanese design code. Sectional dimensions of the columns of the test specimens are 175x175mm and their height are h=875mm. The dimensions of the RC columns in the first and second stories are the same. The shear span to depth ratio (M/(VD)) for the columns was 2.5 and that for the top beam of the first story was 2.65. The ratio of the longitudinal reinforcements of the columns was p_g=1.85% and the ratio of their transverse reinforcements was p_w=0.12%. Since the ratio of transverse reinforcements of
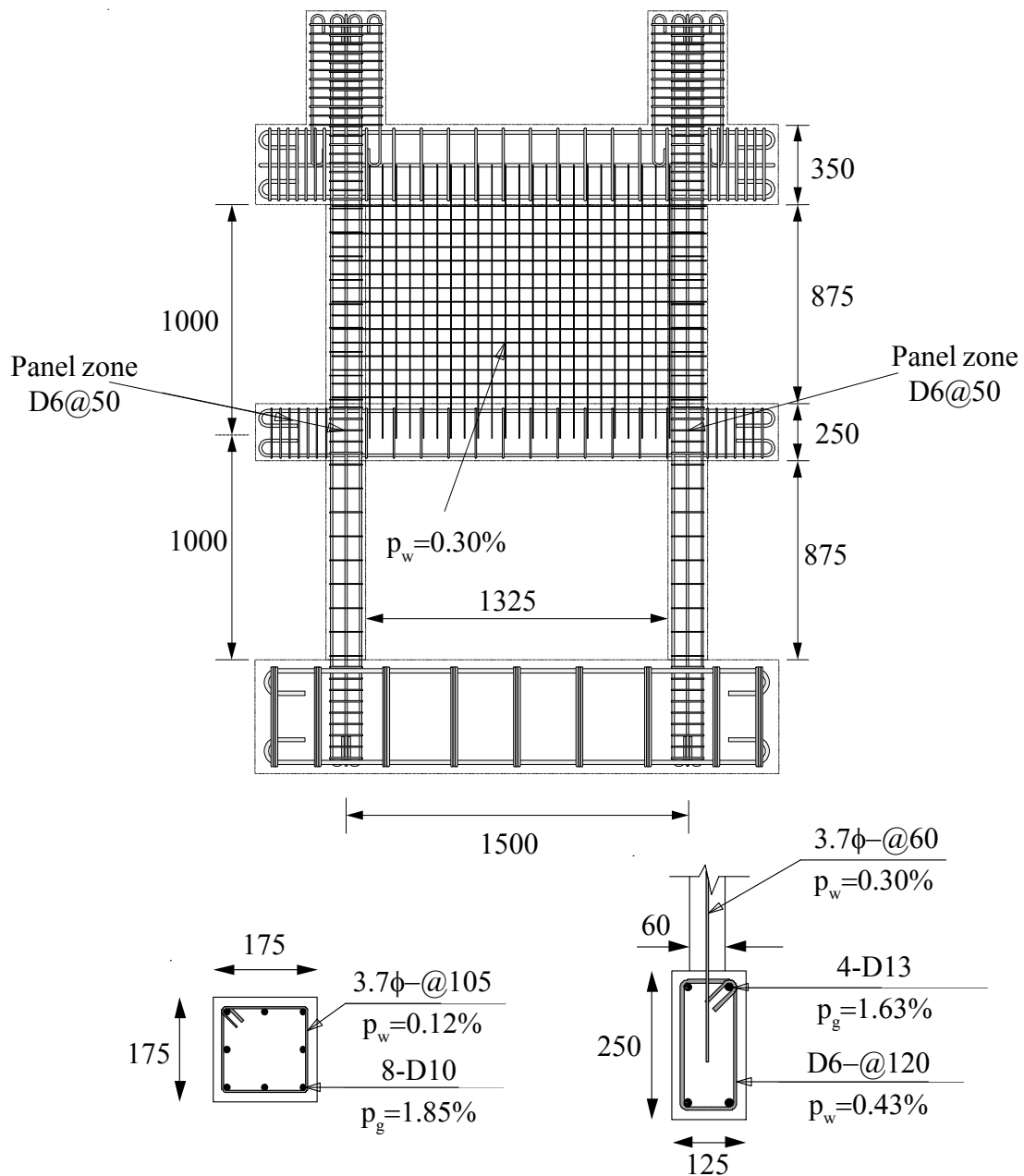
Fig 2.1 Details of reinforcements (unit:mm)

the columns was the poor value of p_w=0.12%, the shear failure of the columns are likely to happen in the columns of the first story. In order to detect the local strain of the reinforcements, a series of electric resistance strain gauges were placed on the critical regions of the tests specimens. The strain gauges were attached on the longitudinal reinforcements at the ends of the RC columns to exactly find out at which drift angle the longitudinal reinforcements yielded and flexural plastic hinges form. The histories of variations of the strain gauges were completely monitored during the loading test. The details of arrangements of strain gauges are shown in **Fig. 2.2**. The details of the test specimens will be discussed in the following.
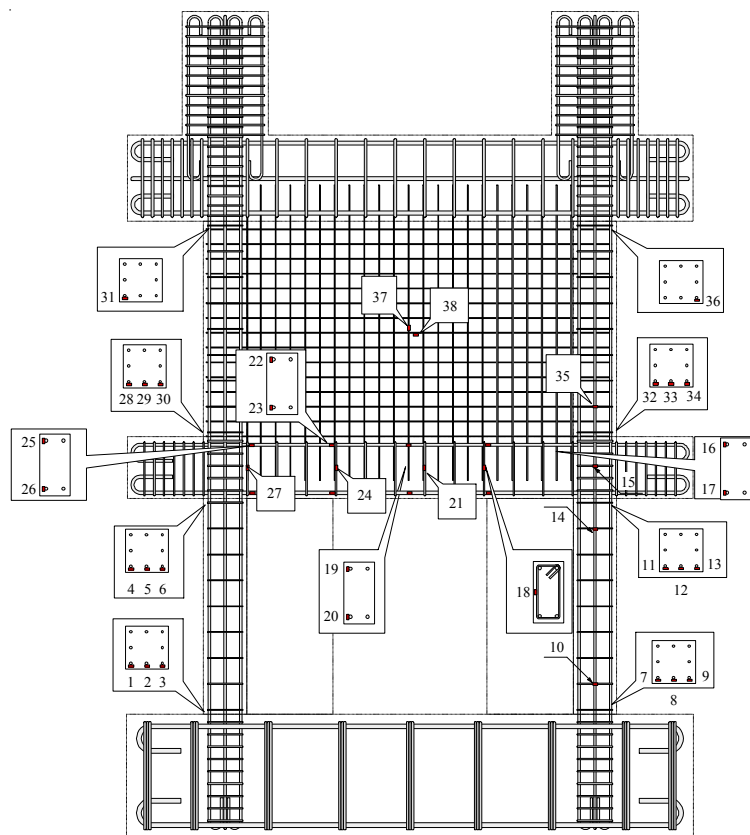
Fig. 2.2 Details of strain gauges

As mentioned previously, four one-bay two-story specimens were made and retrofitted with the thick hybrid wall technique. One specimen is non-retrofitted specimen which is used as a benchmark specimen to verify the effectiveness of the proposed method in increasing the lateral strength and also improving the lateral ductility. Three specimens were retrofitted by thick hybrid wing-wall with a depth equal of that of the RC column. In the retrofitting procedure, both boundary RC columns were retrofitted by wing-wall. Moreover, one specimen is retrofitted by thick hybrid

panel-wall. In all of the test specimens, at first the original RC frame was cast and cured and then after at least 28 days, the retrofitting procedures were implemented.

The specimen R07P-P0 is the benchmark specimen. The first story consists of bar frame and the second story includes shear wall. There is considerable difference between the lateral strength and stiffness of the first and second story, so it is expected the behavior of the test specimen will be same as a building with soft-first-story. In construction of the test specimen, at first the first story was cast and in the next stage concrete of the second story was cast and cured.

σ_B =24.1 MPa, for first story

σ_B =17.9 MPa, for second story

Axial force: N=0.2σ_BbD (σ_B for first story)

3.7ϕ–@60
p_w=0.30%

D6–@120
p_w=0.43%

4-D13
p_g=1.63%

8-D10
p_g=1.85%

3.7ϕ–@105
p_w=0.12%
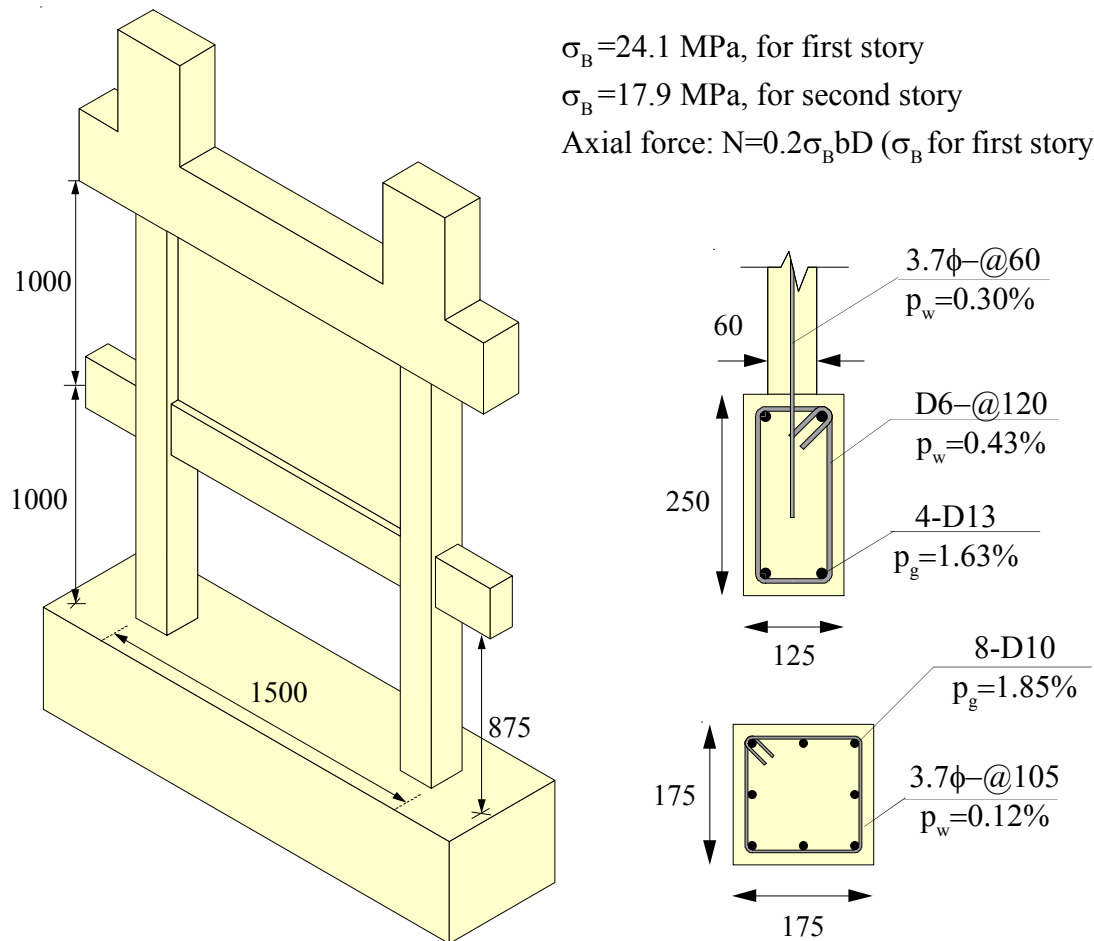
Fig. 2.3Detail of the benchmark specimen R07P-P0 (unit:mm)

Specimen R06P-WW was retrofitted with wing-wall type thick hybrid wall. The details of retrofit are illustrated in **Fig. 2.4**. In the retrofitting procedure, channel-shaped steel plates (thickness=2.3mm) jacketed the boundary RC columns. A gap about 10 mm exists between the channel-shaped steel plates and the faces of the RC columns. Two pieces of deck plates (t=1.2mm)

Long. reinf. of columns: 8-D10 (p_g=1.855)

Trans. reinf. of columns: 3.7ϕ–@105(p_w=0.12%)

Long. reinf. of beam of 1th story: 8-D10 (p_g=1.855)

Trans. reinf. of beam of 1th story: 3.7ϕ–@105 (p_w=0.12%)

Reinforcement of shear wall: 3.7ϕ–@60 (p_w=0.30%)

Axial force: N=0.2σ_BbD (σ_B for first story)

σ_B=34.0 MPa, for first story

σ_B=28.7 MPa, for second story

σ_B=30.4 MPa, for additional concrete
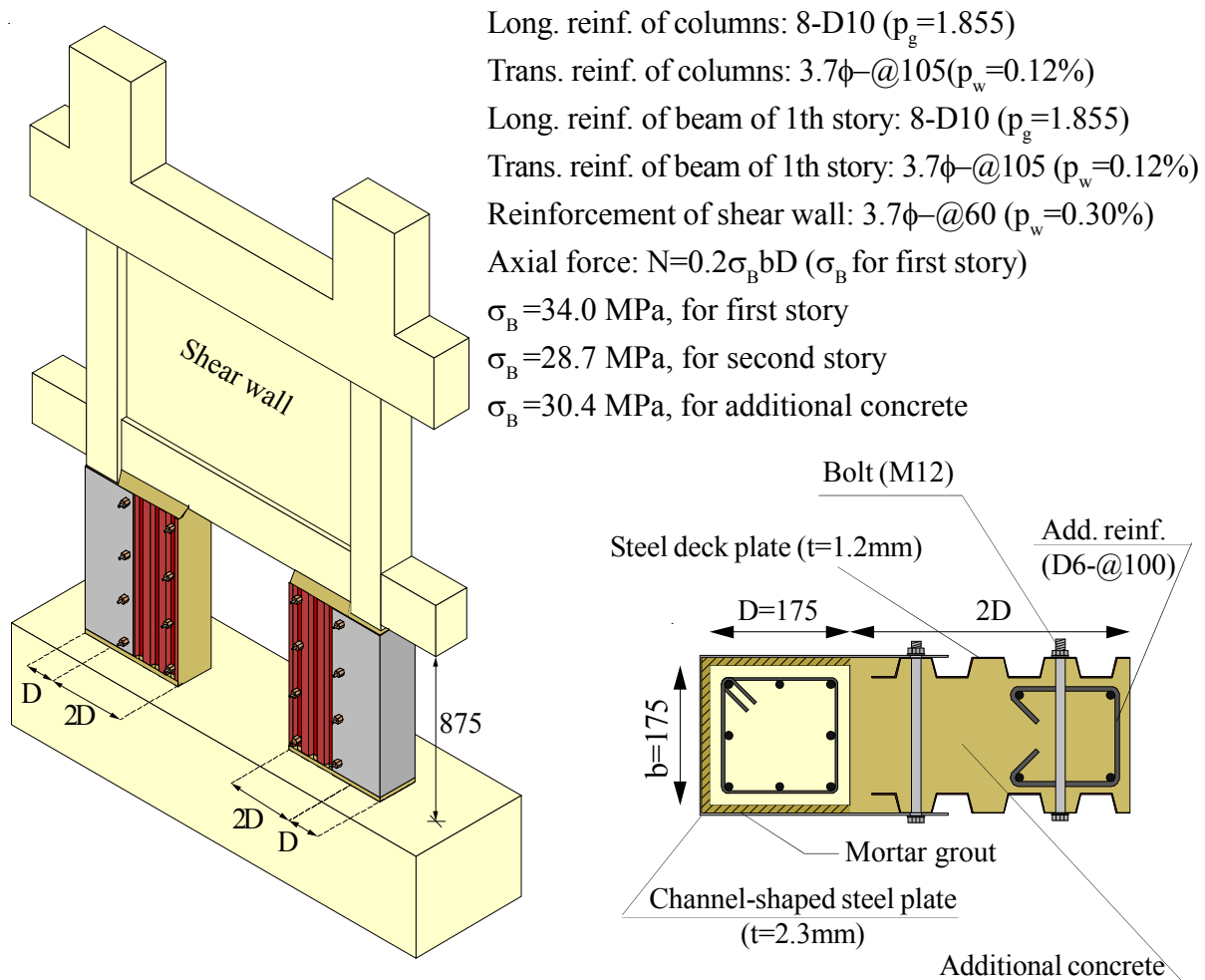
Fig. 2.4 Detail of retrofit scheme of specimen R06P-WW (unit:mm)

were installed at both sides of the steel plate and they were connect to each other by the means of bolts (M12). After installation of deck plates and jacketing steel plates, the additional concrete was cast. After hardening of additional concrete, the gap between the RC column and jacketing steel plate was filled by the grout. In this case study the depth of the additional wing-wall was twice the depth of the column. To prevent the spalling of concrete at exposed face of wing-wall, the transverse reinforcements (D6-@100) were arranged at that zone.

Specimen R08P-WN was retrofitted by wing-wall type thick hybrid wall. The retrofit procedure of this specimen is almost same as that carried for specimen R06P-WW with some differences. In specimen R08P-WN, the steel plain plate (thickness=2.3mm) was used instead of steel deck plate (thickness 1.2mm). Also, the steel plates at both sides of the wing-wall were stitched together through the high strength bolts (PC bars, 13ϕ) instead of ordinary bolts (M12). After hardening

Long. reinf. of columns: 8-D10 (p_g=1.855)

Trans. reinf. of columns: 3.7ϕ–@105(p_w=0.12%)

Long. reinf. of beam of 1th story: 8-D10 (p_g=1.855)

Trans. reinf. of beam of 1th story: 3.7ϕ–@105 (p_w=0.12%)

Reinforcement of shear wall: 3.7ϕ–@60 (p_w=0.30%)

Axial force: N=0.2σ_BbD (σ_B for first story)

σ_B=25.1 MPa, for the first story

σ_B=18.5 MPa, for the second story

σ_B=32.9 MPa, for the additional concrete
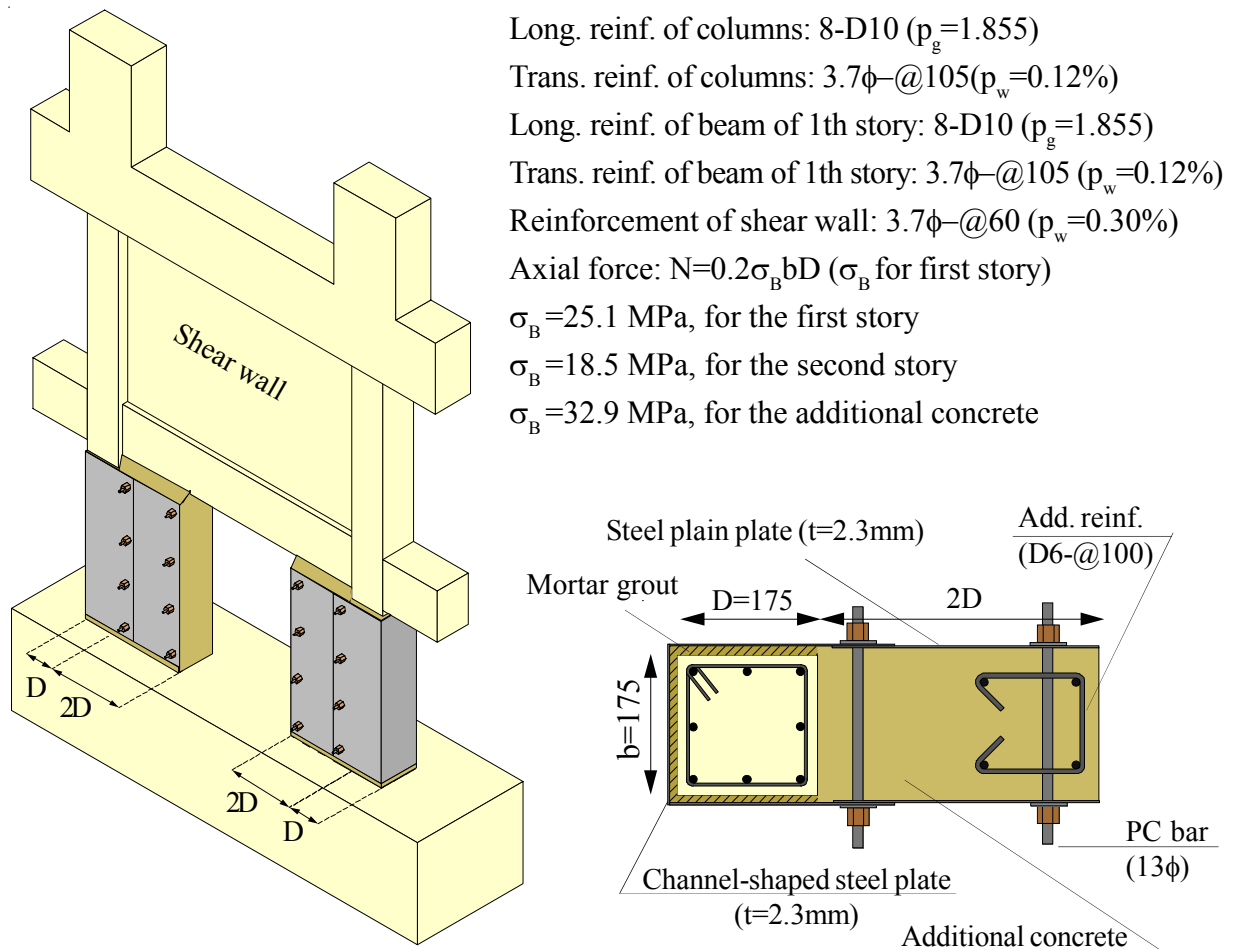
Fig. 2.5 Detail of retrofit scheme of specimen R08P-WN (unit:mm)

the additional concrete and before the loading test, the PC bars were fasten with hand force. The detail of the specimen R08P-WN is given in the **Fig. 2.5**.

Specimen R08P-WA is retrofitted with wing-wall type thick hybrid wall. The additional length of wing-wall was twice the depth of the column. The details of the test specimen are given in **Fig. 2.6**. The retrofit procedure of the specimen R0P-WA is the same as that described for specimen R06P-WW with some differences. In specimen R08P-WA, since it is probable that the shear sliding at the top of the wing-wall will be a dominant mechanism, it was decided that the steel plates of the wing-wall part extended up to the middle height of the top beam. In this zone, a steel plate at each side was anchored to the wing-wall and also to the top beam. Also, at the bottom of each wing-wall one disk-anchor was installed. The disks anchors were provided to prevent the possible shear sliding at the base. The disk-anchors were designed and detailed according to the manufacturer's instructions. Detail of the disk-anchor is shown in **Fig. 2.7**. The resistance

Long. reinf. of columns: 8-D10 (p_g=1.855)

Trans. reinf. of columns: 3.7ϕ–@105(p_w=0.12%)

Long. reinf. of beam of 1th story: 8-D10 (p_g=1.855)

Trans. reinf. of beam of 1th story: 3.7ϕ–@105 (p_w=0.12%)

Reinforcement of shear wall: 3.7ϕ–@60 (p_w=0.30%)

Axial force: N=0.2σ_BbD (σ_B for first story)

σ_B=24.6 MPa, for first story

σ_B=28.7 MPa, for second story

σ_B=30.4 MPa, for additional concrete
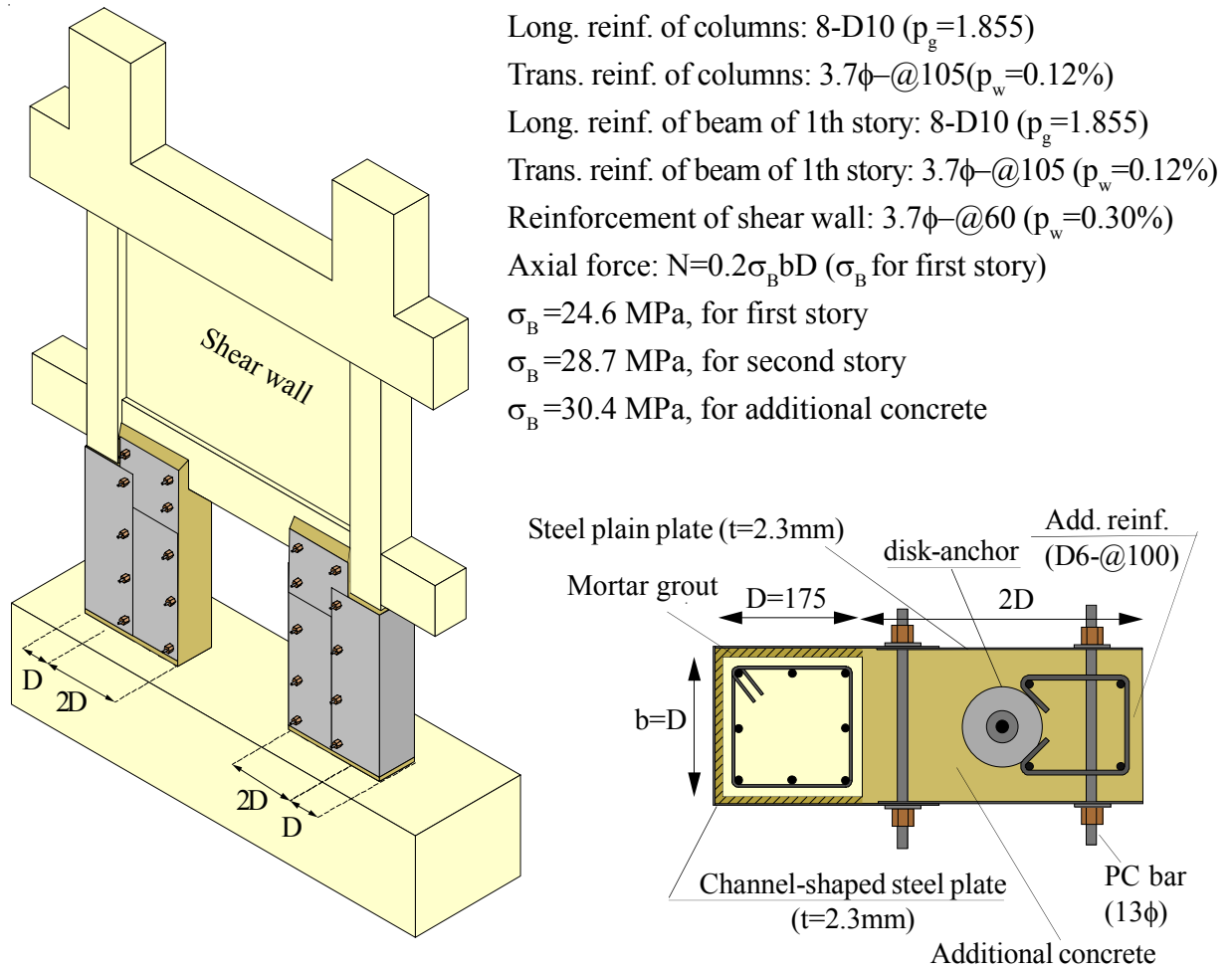
Fig. 2.6 Detail of retrofit scheme of specimen R08P-WA (unit:mm)
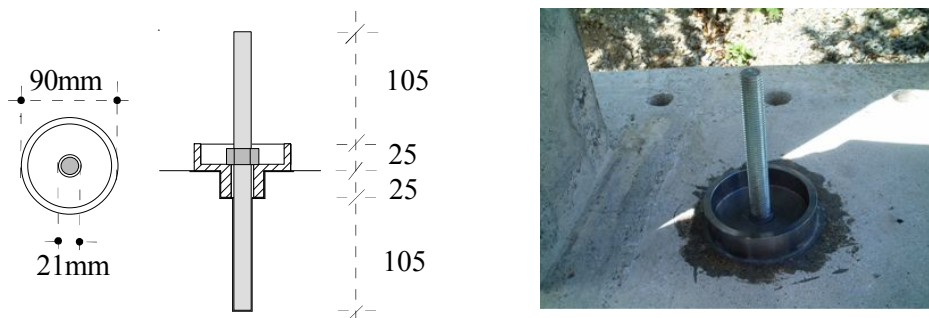
Fig. 2.7 Detail of disk-anchor (unit:mm)

mechanism of the disk-anchor is in such a way that since at the interface of wing-wall and stub, relatively high shear force transfer from wing-wall to the anchor and consequently to the stub, disk play an important role in distributing the induce shear force. On the other hand, the disk-anchor reduces the concentration of the applied shear sliding stresses.

Long. reinf. of columns: 8-D10 (p_g=1.855)

Trans. reinf. of columns: 3.7ϕ–@105(p_w=0.12%)

Long. reinf. of beam of 1th story: 8-D10 (p_g=1.855)

Trans. reinf. of beam of 1th story: 3.7ϕ–@105 (p_w=0.12%)

Reinforcement of shear wall: 3.7ϕ–@60 (p_w=0.30%)

Axial force: N=0.2σ_BbD (σ_B for first story)

σ_B=33.5 MPa, for first story

σ_B=28.7 MPa, for second story

σ_B=20.7 MPa, for additional concrete
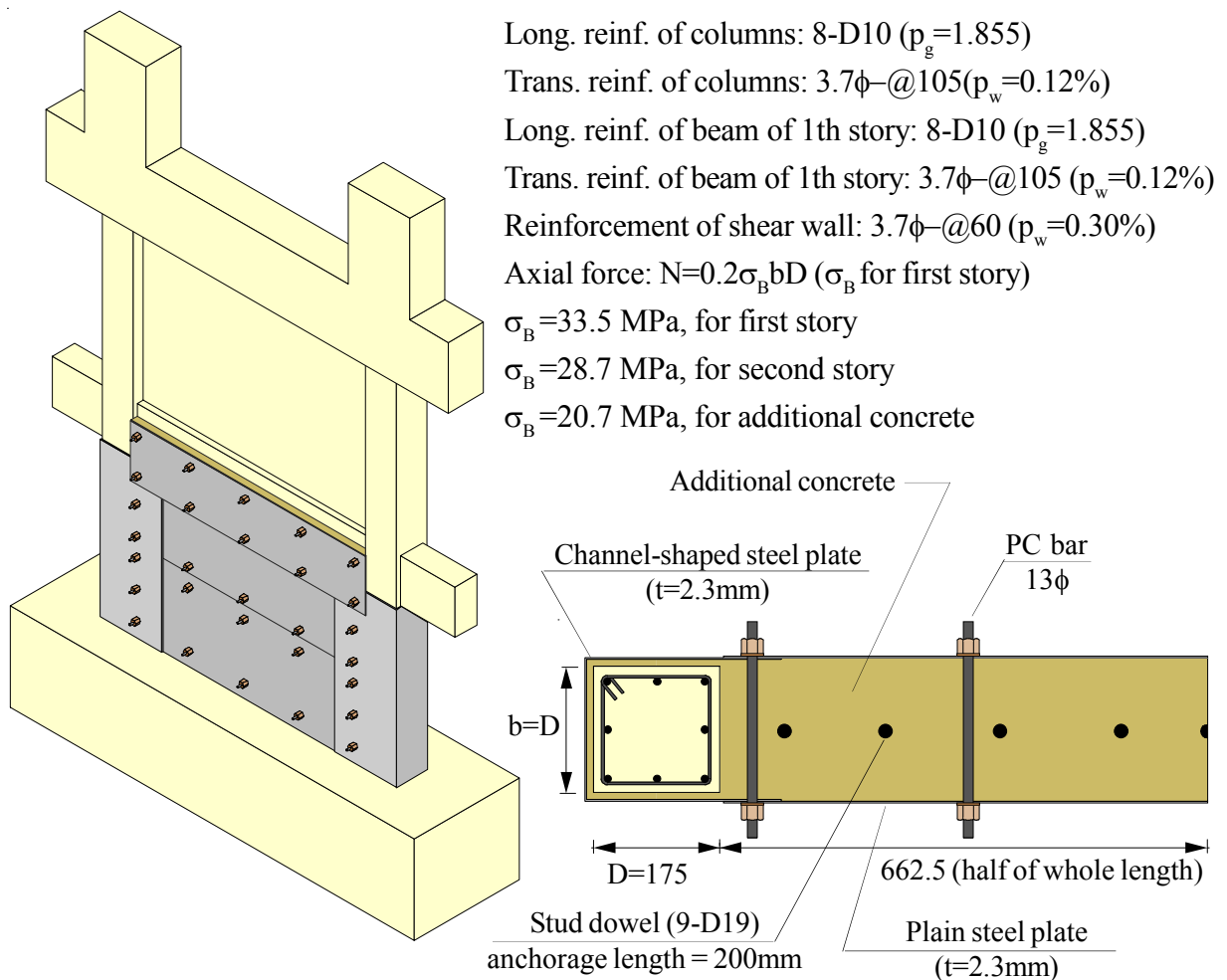
Fig. 2.8 Detail of retrofit scheme of specimen R06P-PS (unit:mm)

Specimen R06P-PS was retrofitted with panel-wall type thick hybrid technique. In the retrofitting procedure, channel-shaped steel plates jacketed the boundary columns. About 10 mm gap was considered between the jacketing steel plates and the faces of RC columns. Additional steel plates were arranged between the jacketing steel plates along the whole length of the bay of the frame. The pieces of steel plates were stitched together with the high strength steel bars (PC bars). Also, the steel plates were continued up to the middle-height of the top RC beam, and anchored to the beam to prevent the possible shear sliding at that zone. The stud dowels (were anchored at the base of the panel-wall to resist against the possible shear sliding. The steel plates were also used as a formwork for casting the additional concrete. After hardening the additional concrete, and before loading test, the PC bars were fastened with hand-force.

Table 2.1 Properties of steel materials

Steel material		a (cm²)	σ_y (MPa)	ε_y (%)	E_s (GPa)
Rebar or Dowel	D10	0.71	349	0.17	202
			355	0.18	201
	D13	1.27	359	0.20	179
			342	0.17	201
	M16	1.57	725	—	—
Hoop or Stirrup	3.7ϕ	0.11	650	0.31	208
			683	0.34	202
			617	0.33	188
	D6	0.32	432	0.25	175
			504	0.26	194
			449	0.29	153
PC bar	13ϕ	1.33	1220	0.61	200
Deck plate	t=1.2mm	—	268	0.13	203
Plain plate		—	348	0.16	212
			335	0.16	209
			358	0.16	218

Notes: a=cross sectional area; σ_y=yield strength of steel; ε_y=yield strain of steel; E_s=Young's modulus of elasticity; [1] for R06P; [2] for R07P; [3] for R08P.

2.3 Test setup and loading program

A schematic view of test setup and the position of the test specimen are illustrated in **Fig. 2.9**. The test specimen placed on a strong stub. The stub was anchored to the rigid concrete floor by the means of long anchors. A thin layer of gypsum is provided between the bottom of specimen and the stub to be sure that the specimen perfectly is in contact with the stub. The specimens were tested under constant axial force and horizontal cyclic loading. The horizontal force applied on each through two vertical strong girders at right and left of the specimen. The horizontal force was applied to the specimen by a double acting single hydraulic oil jack and it is distributed along the height of the spacemen by the girder. When the specimen was pushed from left to right, the hydraulic oil jack directly pushed the right-side girder, but when the specimen was pulled from right to left, long PC bars transferred the pulling force to the left-side girder. The weight of the girders were canceled by the counter balance systems. A load cell monitors the applied force in the path which hydraulic oil jack is placed. A series of Linear Variable Differential Transformers (LVDTs) detected the displacements of the specimen. The lateral displacements of the specimen

Pull (-) ◄──────► Push (+)

1. Servohydraulic actuator; 2. Horizontal loading reaction wall; 3. Hydraulic oil jack; 4. Load cell; 5. Counter balance; 6. Specimen; 7. Long PC bar; 8. Strong floor; 9. Vertical right-side strong girder; 10. Out-of-plane resistance devices
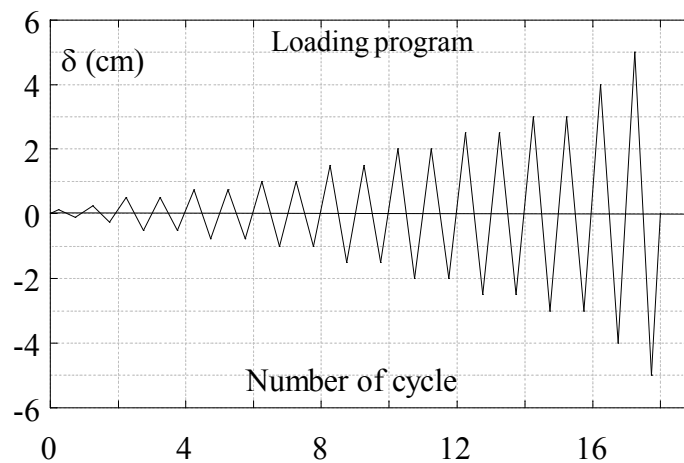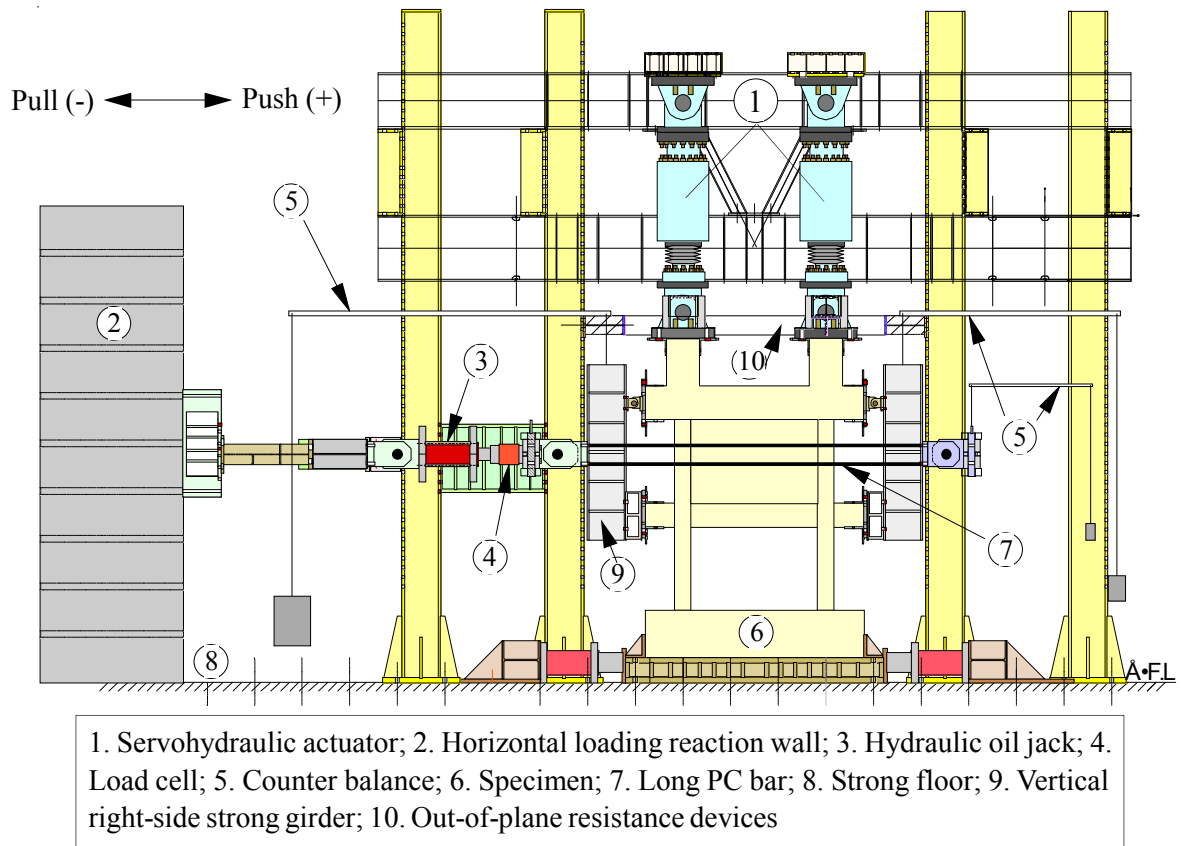
Fig. 2.9 Schematic view of test setup and loading program

were controlled during cyclic loading. On the other hand, the specimen was pushed or pulled to a pre-determinate values programmed to the controlling computer, for example the specimen push till the drift angle of first story reached to R=1.0%. A vertical rigid concrete wall reacts against the horizontal force. Vertical forces act on the specimen by two servohydraulic actuator. The actuators were maintained the axial force constantly even during large rotation of the specimen due to overturning moment. Four beams which are perpendicular to the specimen resist against possible

Fig. 2.10 Arrangement of Linear Variable Differential Transformers (LVDTs)
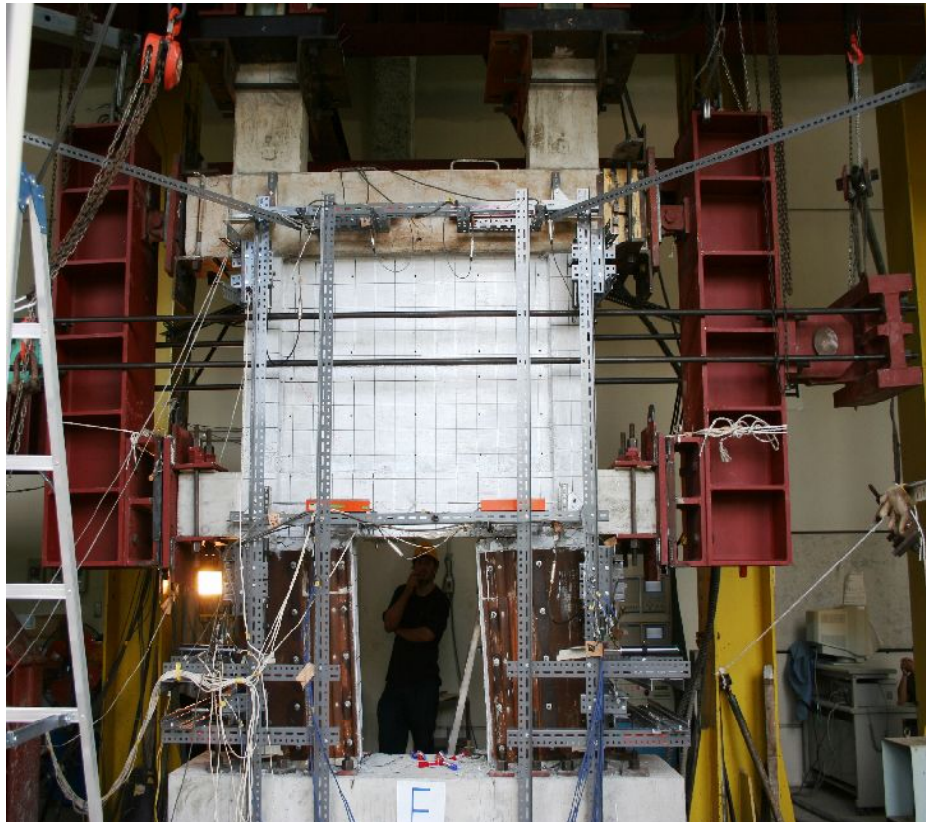
Fig. 2.11 Test setup of specimen R06P-WW
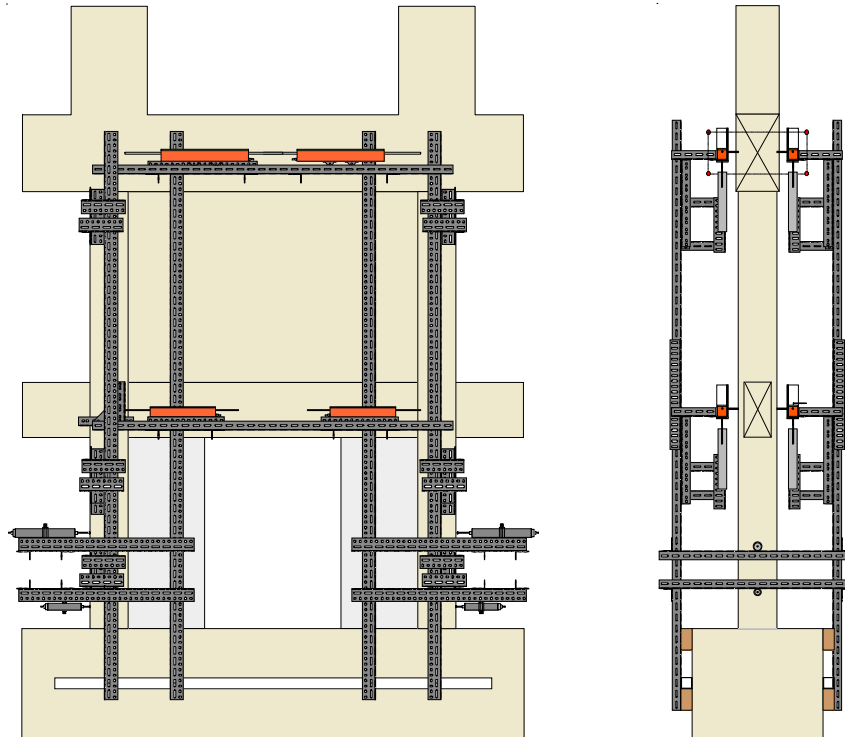
out-of-plane displacements of the specimen. It should be noted that the vertical girder connected to the specimen with pined-end condition. The displacement-controlled program of the first story of the specimen is shown in the **Fig. 2.9**. The cyclic loading test was carried out in the range of drift angle ±0.5%, ±1.0, ±1.5%, ±2.0%, ±2.5% and ±3.0% at two successive cycles, and ±0.125%, ±0.25%, ±4.0%, and ±5.0% at one cycle. As mentioned previously, a series of LVDTs were arranged to detect the displacements of the specimens. As an example the arrangement of LVDTs for specimen R06P-WW is given in **Fig. 2.10**. Also, the specimen R06P-WW is shown in **Fig. 2.11** during cyclic loading test.

2.4 Experimental results and discussions

In this section, the experimental results of the tests specimens will be discussed in detail. During the loading test, the crack pattern and the major phenomenon was marked and noted. The specimens were tested under constant axial force of ($N=0.2\sigma_B bD$) and cyclic horizontal loading. The observed behavior of the specimen will be explained one-by-one and their crack patterns and their V-R relationships are illustrated in **Fig. 2.12 to 2.21**.

Specimen **R07P-P0** is a non-retrofitted benchmark specimen to verify the effectiveness of the proposed technique in increasing the lateral strength and stiffness. In this specimen, the flexural cracks formed at the top of the columns at drift angle of R=0.5% as well as the shear cracks appeared at the same zones at drift angle of R=0.75%. By progressing the loading test, the number and width of the flexural and shear cracks increased. The lateral strength of the specimen was governed by formation of flexural plastic hinges at both ends of the first story columns, but the specimen finally collapsed due to shear failure of right side column at drift angle of R=1.64%.

In specimen **R06P-WW**, the resistant mechanisms of two ends of the column-wing-wall are different. When specimen subjected to push loading (from left to right), the acting section at the bottom of right column contains the column and the wing-wall, whereas the acting section of the top contains the column only. The detail discussion on section analysis of the retrofitted column is deferred to the next section. Because of long level arm between the tensile and compression regions of the section at bottom, the longitudinal rebars of the columns yielded early at drift angle of R=0.3%. The wing-walls of this specimen were jacketed by deck steel plates. Since the steel deck plates did not have sufficient resistance against the horizontal and transversal deformations, the confinement of the wing-wall was poor, and therefore diagonal shear crack occurred in wing-wall. Cracks appeared at top and bottom of the columns at drift angle of R=0.5 %. The lateral

force reached to the maximum value at drift angle of R=1.5%. Even though the shear yielding took place in the wing-walls, the lateral resisting force of the first story maintained larger than 0.8Vmax until drift angle of R=4.0%, and the specimen exhibited a ductile shear response. During the loading test, outer row of longitudinal rebars of the columns broken but because the lateral resisting force was governed by the shear resistance of the wing-walls, the broken of the longitudinal rebars did not affect the lateral resisting force. The wing-wall resisted against the lateral load by action of compression strut. Because of long-length arm between tension and compression zones at both ends of wing-wall-column, the longitudinal reinforcements prematurely yielded at drift angle of R=0.3%. After loading test finished, the jacketing deck steel plates were detached, and it was observed that a diagonal shear crack had formed in each wing-wall. The lateral displacement of the specimen was governed by flexural deformation of wing-wall-column and overall flexural behavior of the specimen (overturning resistance). Considering this combined mechanism, when the specimen was pushed from left to right, it is expected the compression force in the wing-wall at right-side column would be significantly greater than that at left-side column due to overturning resistance. This mechanism was confirmed through the direction of diagonal shear cracks in the wing-walls. In each direction, the wing-wall with higher compression force in its strut, diagonally cracked.

In specimen **R08P-WN**, due to long-length arm between tension and compression zones at wing-wall-columns, the longitudinal reinforcements of the boundary columns at bottoms yielded at drift angle of R=0.3%. The flexural cracks appeared at the bottom of the columns at drift angle of R=0.5%. At the top sections of the columns, the flexural tension and compression stresses, and shear-friction stress mainly acted. Since the tension actions of longitudinal reinforcements contribute in both flexural and shear-friction resistances, the exact evaluation of shear-punching at the top of columns become complex. In this specimen the sections of columns initially withstood against shear-punching through the shear-friction resistance, but by preceding the loading test, the longitudinal reinforcements gradually entered to the inelastic state due to flexural behavior, and consequently the shear-punching resistance considerably decreased. As the longitudinal reinforcements at the top of column yielded, the lateral resistance of the specimen suddenly dropped due to shear-punching failure. After that, the shear-sliding resistance at the compression zone maintained the lateral strength, and the V-R response exhibit a ductile response up to drift angle of R=5.0%.

In specimen **R08P-WA**, the longitudinal reinforcements of boundary columns at bottom yielded at drift angle of R=0.3%. The flexural cracks at the bottom of wing-wall-columns appeared at drift angle of R=0.5%. By preceding the loading test the width and number of crack increased. Moderate

strength degradation was obvious in the *V-R* relationship of specimen R08P-WA that results from crushing of concrete at compression zone and buckling of longitudinal reinforcements. The resisting force maintained greater than 0.8 Vmax up to drift angle of *R=5.0%*, and the overall response of the specimen shows a ductile behavior. To verify the shear sliding resistance carried by steel plates at top of wing-wall, shear strain-gauges were attached at that level. The produced shear force in the steel plates that resisted against shear-sliding was about 27% of overall lateral strength of the specimen. It should be emphasized the reduction of lateral strength in specimen R08P-WN due to shear-punching failure was about 18% of its overall lateral strength. Comparison between the behavior of specimens R08P-WN and R08P-WA exhibits the efficiency of steel plates in shear-sliding resistance at the top of wing-wall-column.

Specimen **R06P-PS** was retrofitted with non-opening-type thick hybrid wall. Since, in this specimen, the first story was completely filled with the additional concrete, the first story became so stiff. As mentioned previously, the stud dowels were installed at the base of panel-wall to prevent the possible shear-sliding. The fixed-base-rotation of the specimen led to premature yielding of longitudinal reinforcements of the boundary columns at drift angle of 0.2%. Cracks appeared at the base of the columns and the wing-wall at drift angle of R=0.5%. By progressing the loading test, the width of the cracks gradually increased. Shear cracks formed in the shear wall of the second story when the drift angle of first story was R=1.0%, but the shear wall did not fail until the end of the test. The lateral resisting force reached to the yielding value at drift angle of R=0.24% and its maximum value, about 4.8 times the lateral strength of the non-retrofitted specimen, was obtained at drift angle of R=0.94%. After drift angle of R=2%, the lateral resisting force sharply dropped due to the rapture of longitudinal reinforcements of the boundary columns. The breakage of the longitudinal reinforcements indicates a high concentrated tensile force in the boundary columns.
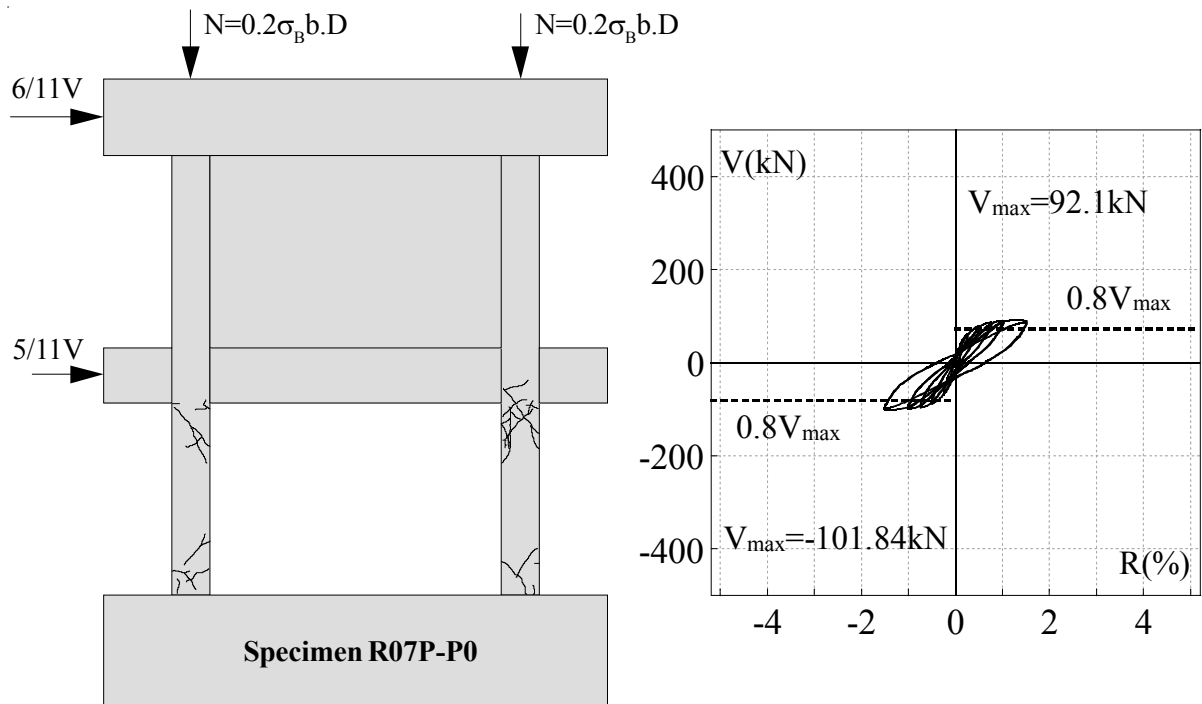
Fig. 2.12 Crack pattern and V-R relationship of the specimen R07P-P0
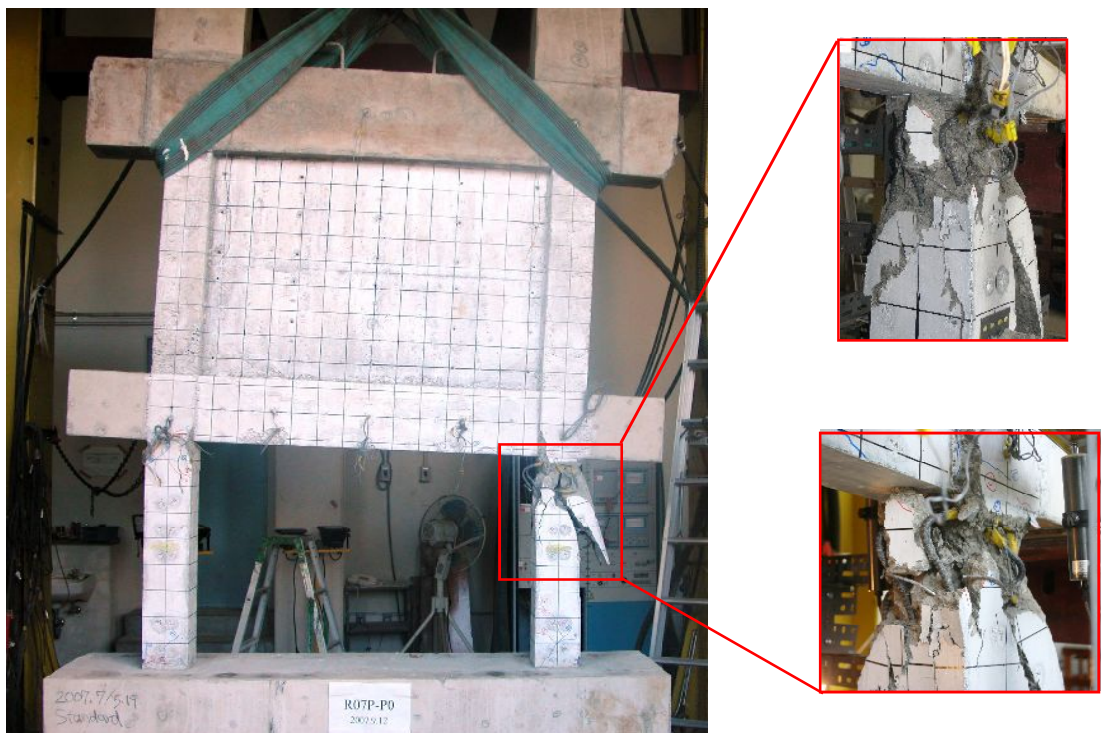
Fig. 2.13 Shear failure feature of column of the specimen R07P-P0

Fig. 2.14 Crack pattern and V-R relationship of the specimen R06P-WW

Fig. 2.15 Feature of the specimen R06P-WW after finishing loading test
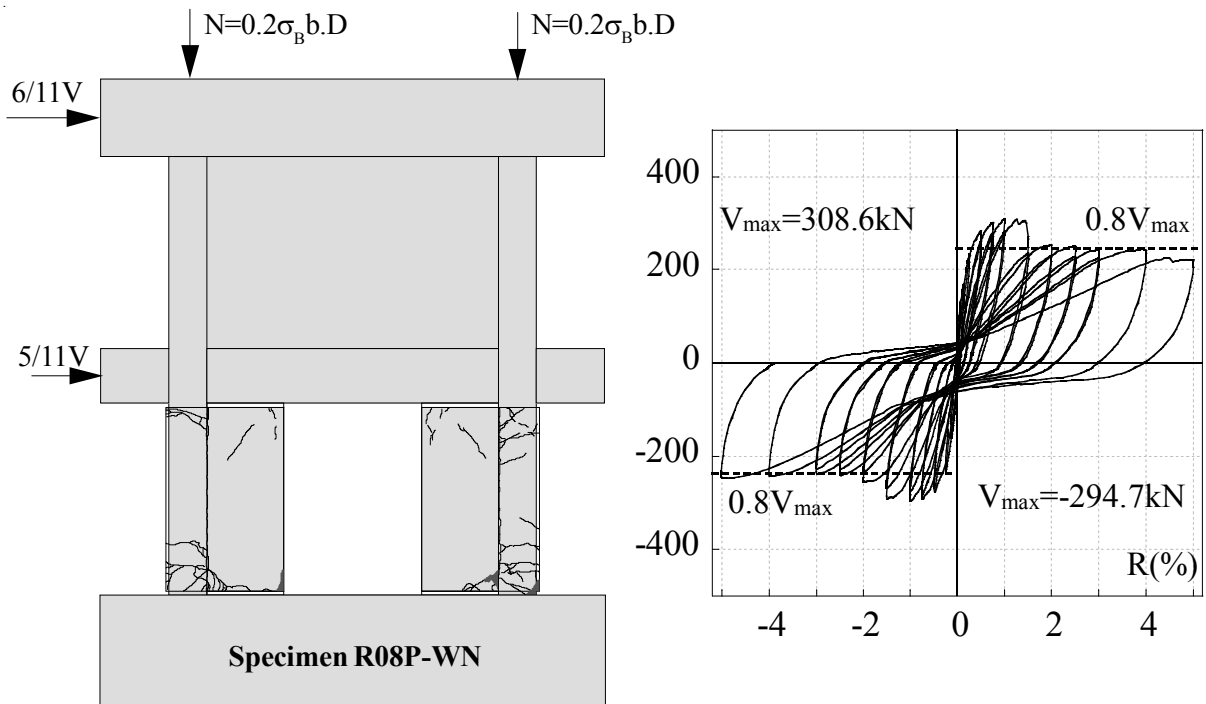
Fig. 2.16 Crack pattern and V-R relationship of the specimen R08P-WN
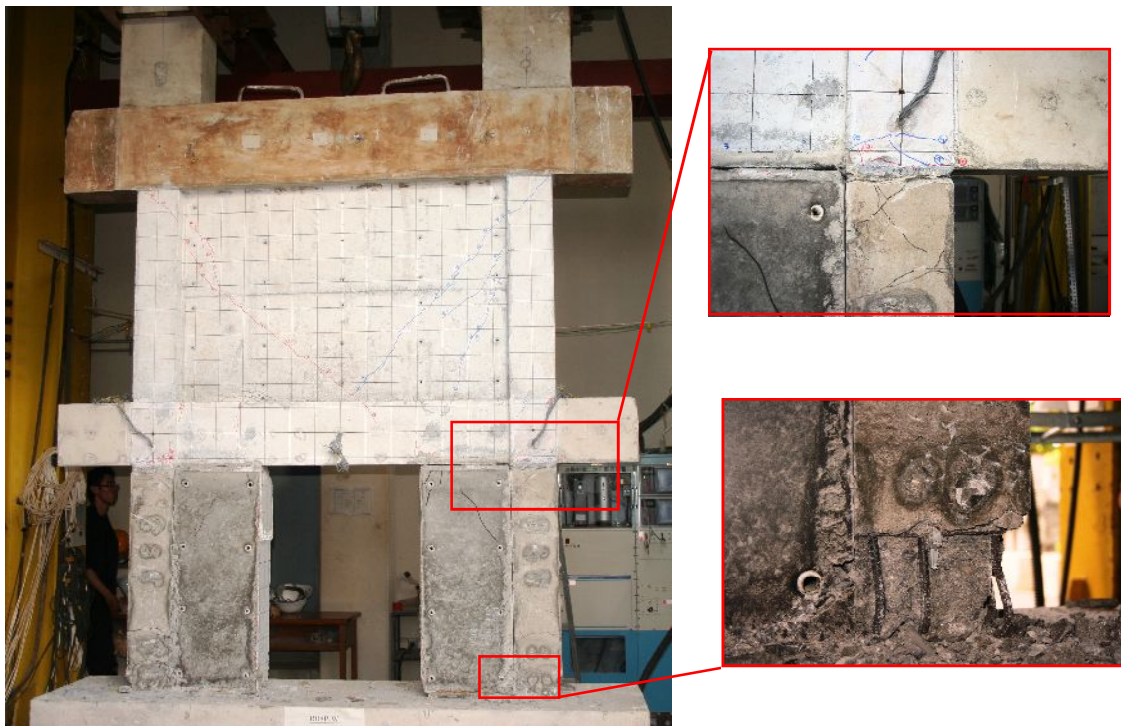
Fig. 2.17 Feature of the specimen R08P-WN after finishing loading test
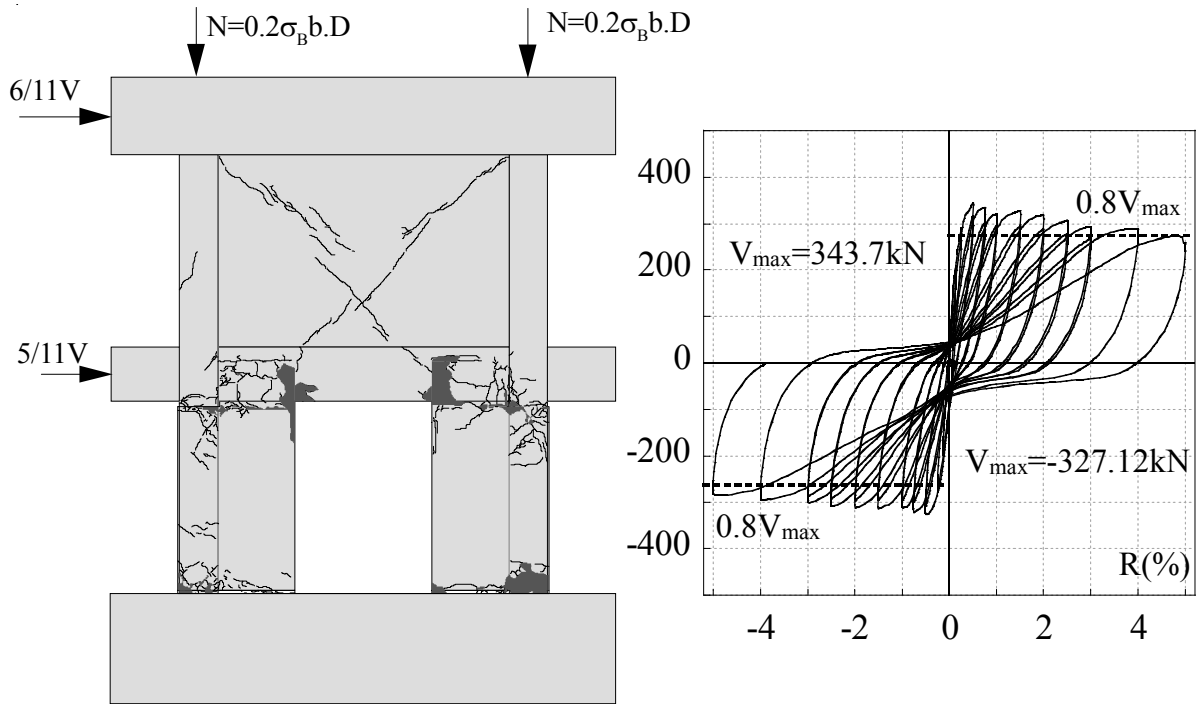
Fig. 2.18 Crack pattern and V-R relationship of the specimen R08P-WA
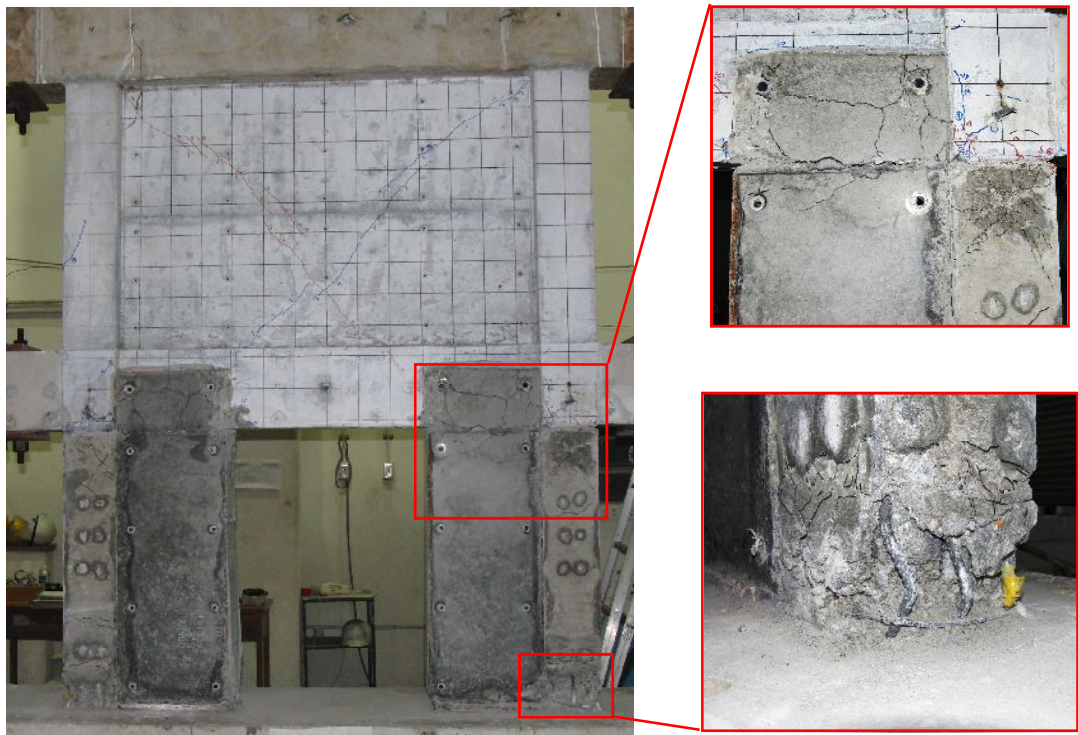
Fig. 2.19 Feature of the specimen R08P-WA after finishing loading test

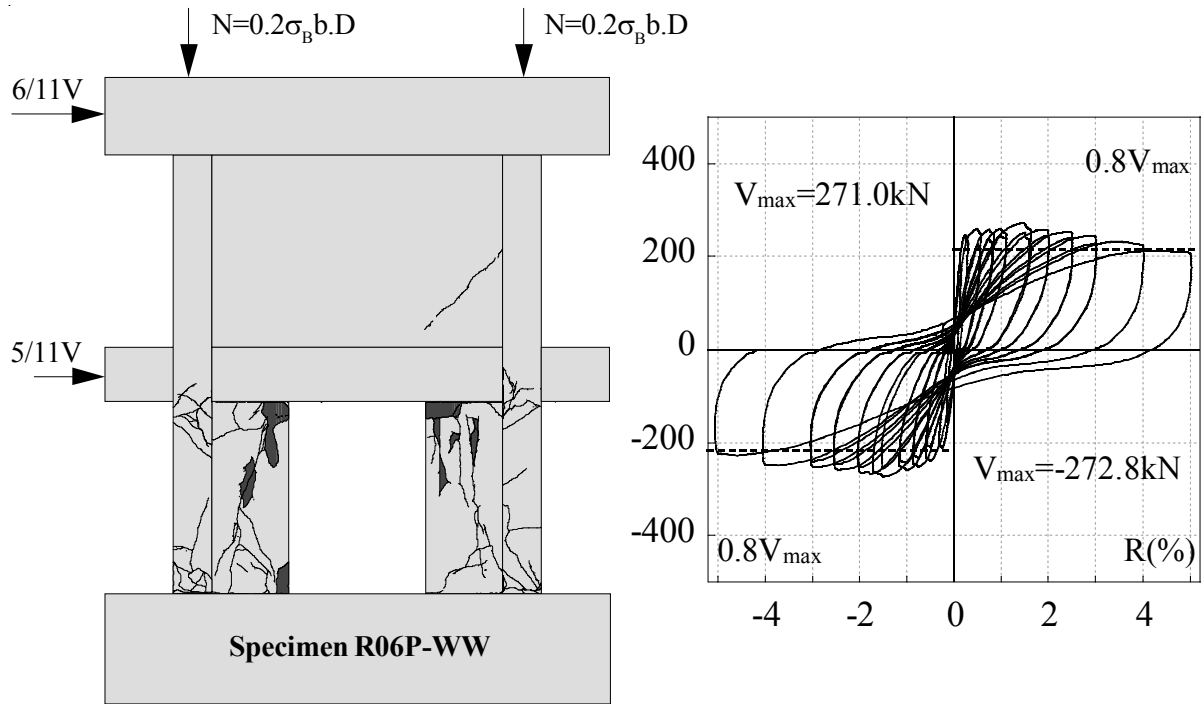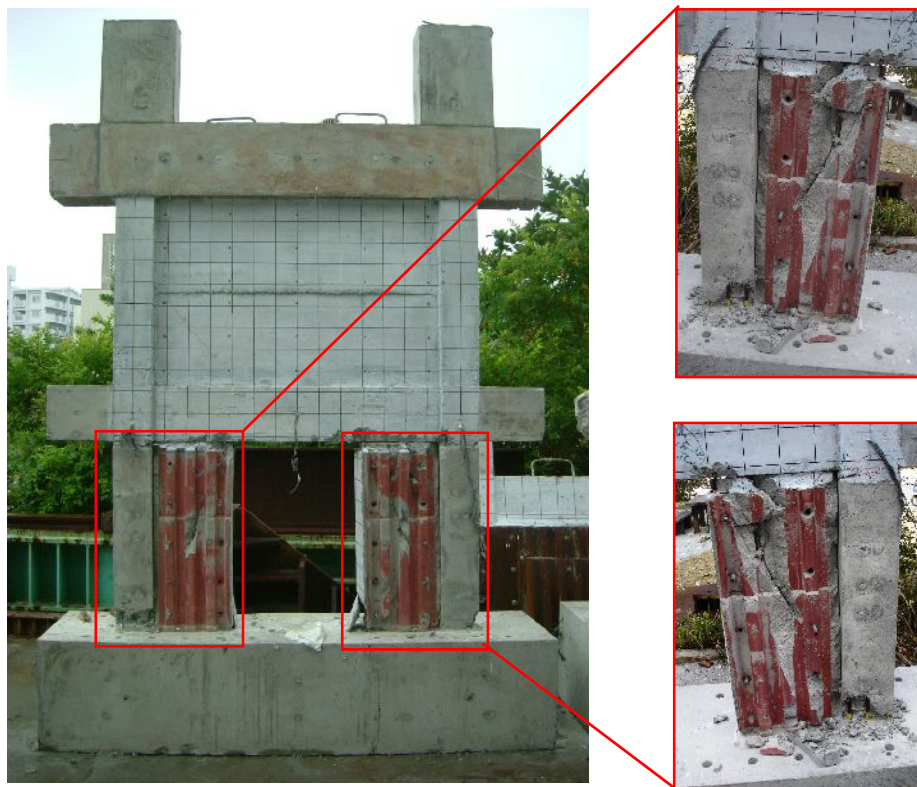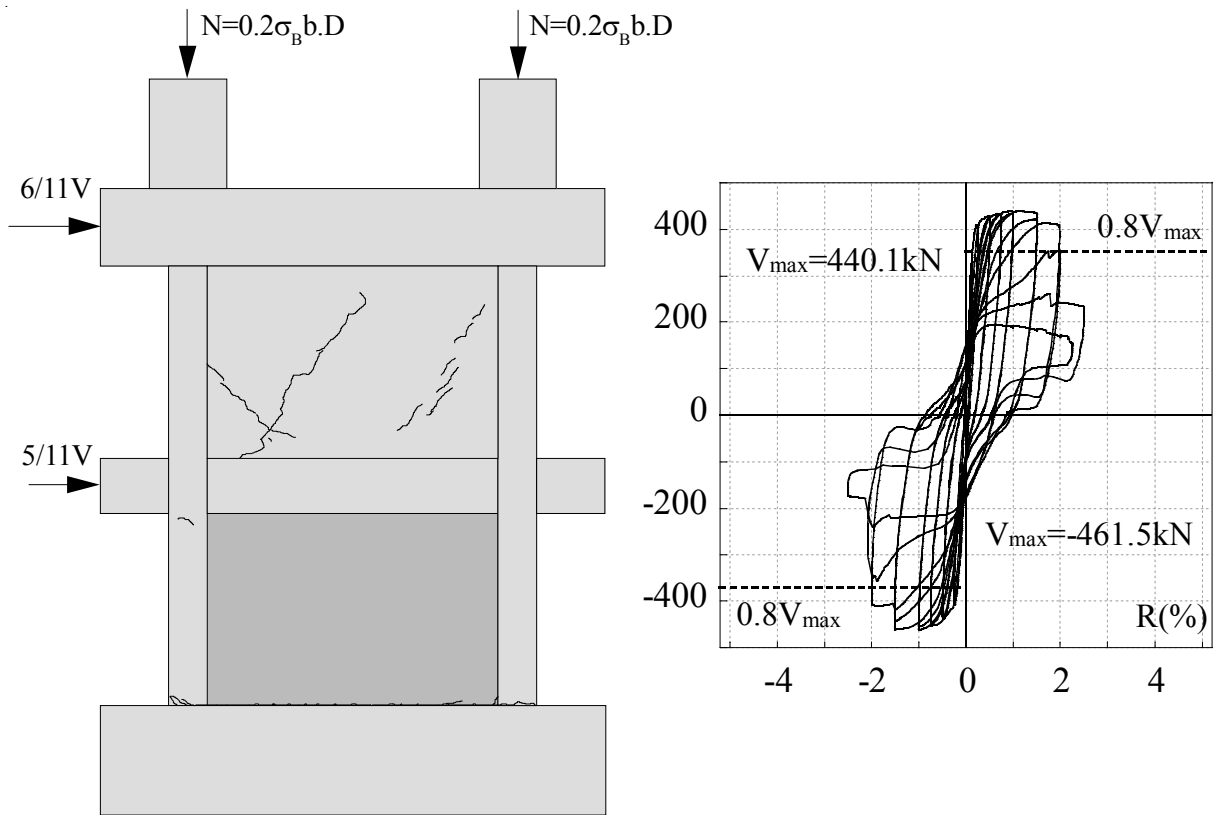**Fig. 2.20 Crack pattern and V-R relationship of the specimen R06P-PS**

Fig. 2.21 Feature of the specimen R06P-PS after finishing loading test

2.5 Calculation method for lateral strengths

2.5.1 General

Based on the experimental observed behavior and physical concepts of the possible failures of soft-story frames retrofitted by thick hybrid wall, different mechanisms are likely to happen. The main mechanisms include flexural mechanism with ductile behavior, shear mechanism with brittle behavior, and shear sliding mechanism with brittle or ductile behavior. Design procedure proposed for regulatory standards should be safe, correct in concept, and simple to understand, and should not necessarily add either design or construction costs. These procedures are most effective if they are based on relatively simple conceptual models rather than on complex empirical equations. This sub-section introduces design engineers to some approaches for the flexural, shear and sliding designs of one-bay two-story frame retrofitted with wing-wall technique. The suggested procedures provide a unified, rational, and safe design framework for structural concrete under combined actions, including the effects of axial load, bending. The methods of calculation of lateral strengths of each dominant mechanism will be explained in the following.

2.5.2 Flexural strength

Up to now, calculation of flexural strength for ordinary columns is the most simple, rational method in compared to other calculations such shear and sliding. The criteria of equivalent stress block in obtaining the compressive force of the concrete is adopted as a worldwide accepted method in calculation the flexural strength of the reinforced concrete section. In this type retrofit, since the wing-wall and column stitch together with channel-shaped steel plate and PC bars, it is expected that the column and additional wing-wall behave as a unified member with high rigidity. Typical mechanism of one-bay two-story frames retrofitted by thick hybrid wing-wall and panel-wall are illustrated in **Fig. 2.22**. In wing-wall type retrofit, when the specimen is pushed or pulled the resistance mechanism of the wing-wall-column is different. In fact, when the specimen push from left to right a diagonal strut forms in each wing-wall-column to resist against the lateral force. As shown in **Fig. 2.22**, in right-side column at top, the compression zone falls in the column section, and, at bottom, the compression zone acts on the wing-wall. At top, since in the wing-wall the longitudinal reinforcements do not resist in tension, the tension force also applied on the column, and in fact the additional wing-wall does not work. In the right-side column, the mechanism is reverse. On the other hand, at top section, the compression zone falls on the additional wing-wall, while at bottom the compression zone acts on the column.
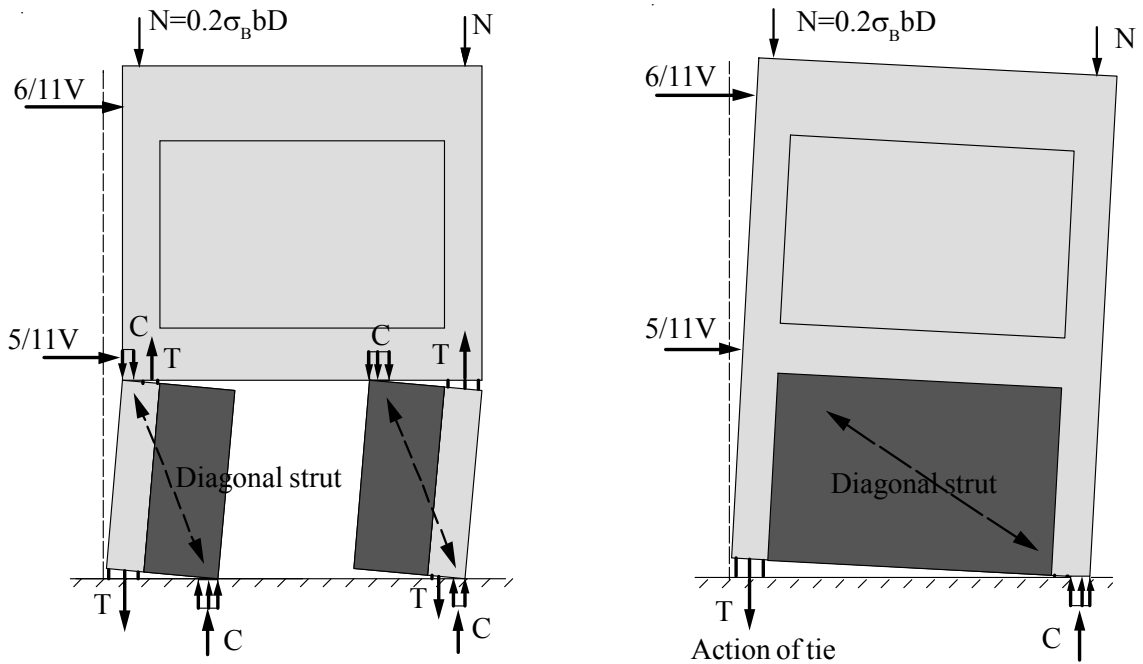
Fig. 2.22 Typical behaviors of the frames retrofitted with thick hybrid wall

Considering the described mechanisms, the flexural strength of the wing-wall-column can be calculated for two cases including when the column is in compression or when the wing-wall is in compression as follows:

When the compression stress acts on column:
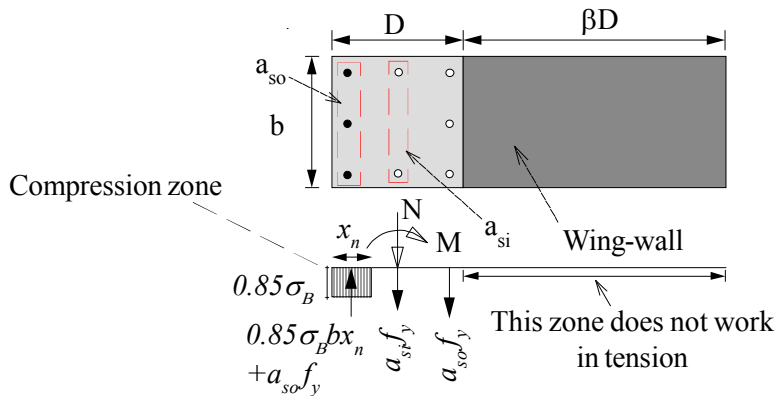
Fig. 2.23 Flexural resistance of wing-wall column when compression is in column

$$M = 0.8 D a_{so} f_y + (N + a_{si} f_y)\left(0.5D - \frac{N + a_{si} f_y}{1.7 b \sigma_B}\right) \quad \text{.. 2.1}$$

where M : ultimate moment capacity, N : axial load, σ_B : cylinder strength of concrete or additional mortar, D : depth of column, b : width of column, f_y : yield strength of rebar in column, a_{so} : total area of longitudinal rebars in column in one outer row, a_{si} : total area of longitudinal rebars in column in inner rows, and x_n : neutral axes depth.
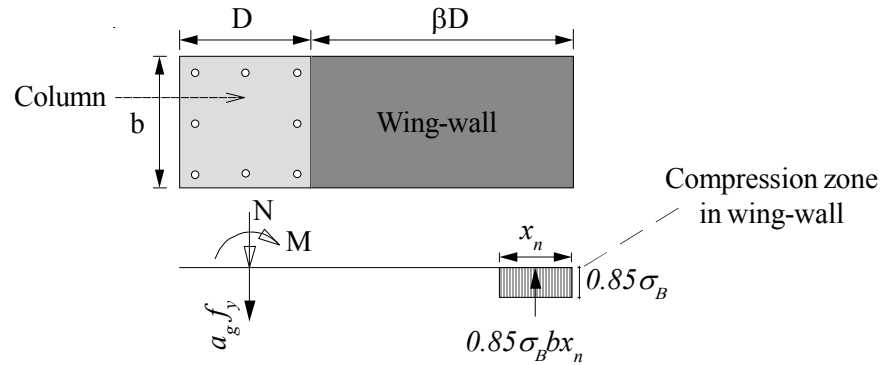
Fig. 2.24 Flexural resistance of wing-wall column when compression is in column

When the compression stress act on wing-wall [12]:

$$M = (N + a_g f_y) \left\{ (0.5 + \beta)D - \frac{N + a_g f_y}{1.7 b \sigma_B} \right\} \qquad \text{... 2.2}$$

where M : ultimate moment capacity, N : axial load, σ_B : cylinder strength of concrete or additional mortar, D : depth of column, b : width of column, a_g : total area of longitudinal rebars in column, f_y : yield strength of rebar in column, and x_n : neutral axes depth. It is worthy to note that in most of cases during the earthquake excitations, the provided overturning moment causes that the axial force in the boundary columns increased or decreased. Considering this fact, in calculation of flexural strength, the influence of variation of axial force due to overturning moment should be carefully taken into consideration.

In case of thick hybrid wall, since the additional concrete with the help of steel plates and PC bars is perfectly stitched to the boundary columns, the additional panel-wall and the boundary columns work together. So, when the specimen is pushed from left to right a tie provides in the left-side column, and a strut (arch) forms in the panel-wall. The compression side mainly falls on the right-side column. If the value of axial force is high, the compression zone will increase to the panel-wall. The overall flexural strength of thick hybrid panel-wall is calculated as follow;

$$M = 0.9 a_t f_y L + 0.4 a_w f_{wy} L + 0.5 N L (1 - \frac{N}{b L \sigma_B}) \qquad \text{... 2.3}$$

Where M: ultimate moment at base, a_t:total area of longitudinal rebars in one column, f_y: yield strength of rebars in column, L: total depth of the section (wall with both columns), a_w: total area of longitudinal rebars in wall. f_{wy}: yield strength of rebars in wall, N=total axial load in both of columns, b: width of the section, σ_B: cylinder strength of concrete.

2.5.3 Shear strength

Although current design provides for shear strength in the ACI 318 Building Code are simple in nature, they do not provide a consistent framework applicable to different types of reinforced concrete members [13]. Because the design equations for slender members neglect the effect of the shear span-to-depth ratio on shear strength, there is no smooth transition between squat (relatively short shear span-to-depth ratios) and slender (relatively large shear span-to-depth ratio) members. Additionally, recent studies have shown that the strength of members without transverse reinforcement tends to decrease with increasing effective depth [14~18], an effective which is not reflected by the design equations in the ACI code.

A more comprehensive model proposed by Watanabe and Ichinose [19], and Aoyama [20] accounts for the effects of the shear span-to-depth ratio and repeated load reversals on shear strength. This model, adopted in the design guidelines of the Architectural Institute of Japan [21], consists of separate contribution from arch and strut, which makes it applicable to both deep and slender members. More recent studies conducted in Japan have resulted in modifications to the AIJ design guidelines to make them applicable to members with axial load and high-strength concrete [22], [23]. In AIJ design guideline, the capacity of arch action in calculation of shear strength is calculated based on the rigid-plastic analysis. As long as the stress in a body of rigid-plastic material are below the yield point, no deformation occur. This idealization implies that we can not determine the stress field in such a body when the stress are below the yield point. When the loading increases to a point where it can be carried only by stresses at the yield point, unlimited deformations are possible without changing the load, if the strains (determined by the normality condition) correspond to a geometrically possible displacement field. The body is then said to be subjected to collapse by yielding. The terms yield load and failure load or the load-carrying capacity of the body. The terms yield load and failure load will also be used. The theory of collapse by yielding is termed limit analysis. For determination of the load-carrying capacity of rigid-plastic bodies the following principles are very useful [24].

- The lower bound theorem

Because of importance of the lower bound theorem, the main concept of this theorem will be explained. The theorem of lower bound solution was applied for calculation of shear strength of RC members by Nielsen [24]. First, it will be shown that if the load has such a magnitude that it is possible to find a stress distribution corresponding to stresses within yield surface and satisfying the equilibrium conditions and the statical boundary conditions for the actual load, then this load

will not be able to cause collapse of the body. A stress distribution such as this is denoted a safe and statically admissible stress distribution.

The proof is made indirectly. Let us assume that for the external load we can find a statically admissible stress distribution $\sigma = (Q_1, Q_2, ...)$ which in the body or part of the body corresponds to stresses on the yield surface, and that the stresses correspond to strain $\varepsilon = (q_1, q_2, ...)$ in accordance with a displacement field that is geometrically possible for the body. Thus the principle of virtual work reads,

$$\sum P_i u_i = \int_v \sigma.\varepsilon dv \qquad\text{..} \quad 2.4$$

where P_i and u_i are external forces and the corresponding displacements and d_v is a volume element, an area element, or a length element. Now, according to the assumption, we can find a safe, statically admissible stress distribution. If this is denoted $\sigma' = (Q1, ...)$, we have

$$\sum P_i u_i = \int_v \sigma'.\varepsilon dv \qquad\text{..} \quad 2.5$$

using P_i and Q_i as static quantities in the principle of virtual work, and u_i and ε' as deformation quantities. Now according the principle that the yield work should be less than the maximum work,

$$\sigma'.\varepsilon < \sigma.\varepsilon \qquad\text{..} \quad 2.6$$

leading to a contradiction. It is possible to, of course, that statically admission stress distributions corresponding to stresses above the yield point also exist, but we have shown that if only we can find one corresponding to stresses bellow the yield point, the load can not causes collapse. If the external load is determined by one parameter μ>0 in such a way that the individual loading components are proportional to μ, we have a proportional loading. The theorem we can then be used to find values of the load that are lower than the collapse load corresponding to μ=μ$_p$, whence the name the lower bound theorem. For all loads μ for which a safe and statically admissible stress distribution can be found, we have;

$$\mu = \mu_p \qquad\text{..} \quad 2.7$$

The above equation also applies if only part of the load is proportional to μ and the rest of the load is constant. In the following sections it is sometimes more convenient to define a safe stress field as a stress field on or within the yield surface.

- Maximum shear capacity, beams without shear reinforcement

It is first considered the case of a rectangular beam with concentrated loading. A lower bound solution can be derived for the idealized case shown in the **Fig. 2.25**. The loads and the tensile force in the reinforcement are transferred to the arch through regions *AEF* and *BCD*, which are in biaxial hydrostatic pressure. The anchoring force is transferred to the uniaxial stress, and both are assumed equal to the load is obtained when BC is as large as possible. Since *D* lies on a circle having *BE* as diameter, the maximum load is obtained when CD=h/2. Then it is only a matter of geometry to calculate;

$$BC = x_0 = 1/2(\sqrt{a^2 + h^2} - a)$$ 2.8

The lower bound solutions thus

$$P = bx_0 f_c$$ 2.9

which can be written

$$\frac{\tau}{f_c} = \frac{P}{bhf_c} = \frac{x_o}{h} = \frac{1}{2}\left[\sqrt{1 + (\frac{a}{h})^2} - \frac{a}{h}\right]$$ 2.10

For this solution to be valid for a real beam, we must require, of course, that the loads can be transferred along a length longer than x_o, and that the reinforcement can be fully anchored and placed in a position corresponding to the solution above.
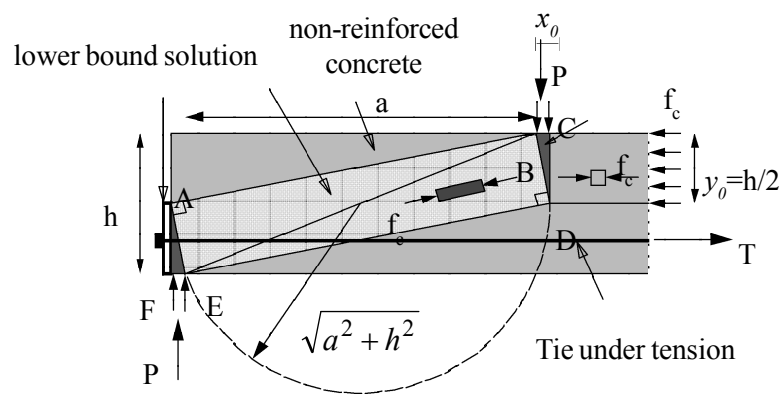
Fig. 2.25 Lower bound for a beam without shear reinforcement [24]

- Shear strength of wing-wall column

The shear strength of the column retrofitted by thick hybrid wing-wall consists of contribution of arch

Mechanism of arch action   **Mechanism of jacketing steel plate at wing-wall part**
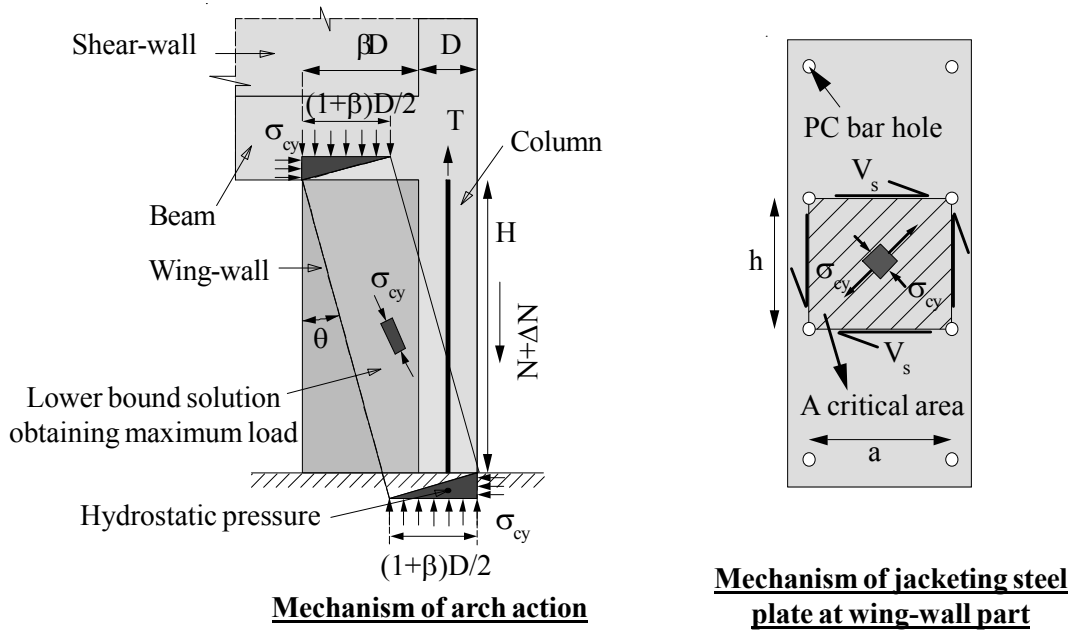
Fig. 2.26 Shear resistance of wing-wall-column

action and contribution of steel plates. Since there is not bond resistance between the steel plates and additional concrete, it can be assumed that each mechanism acts independently.

V=Va (arch) +Vs (steel plate) 2.11

The arch action is calculated according to lower bound solution for plastic analysis as described previously. In this calculation, it was considered the width of arch is half of the total width. According to this assumption which is based on the lower bound solution of plastic analysis the value of shear strength is estimated through the Eq. 2.11. When deck steel plate used instead of steel plate, the confining effect of deck plate is weak because it has not sufficient out-of-plane resistance. But the plain steel plate can increase the confinement by out-of-plane resistance. The confining coefficient in each case is calculated through the Eq. 2.13 or 2.14.

$$V_a = 0.5(1+\beta)bD\upsilon\sigma_B \tan\theta$$ 2.12

$$\tan\theta = \sqrt{1 + (\frac{H}{(1+\beta)D})^2} - \frac{H}{(1+\beta)D}$$ 2.13

$$\nu = 0.7 - \frac{\sigma_B}{200}$$ .... for deck plate 2.14

$$\nu = 1.0$$ 2.15

The shear resistance of steel plates is calculated based on the procedure which is an adaptation of procedures in the AISC Specifications for steel plate girders. For the background on these

equations, the reader is referred to SSRC Guide edited by Theodore V. Galambos. as reported by Astaneh-asl [25], as follows;

for compact steel plate when $h/t_w \leq 1.10\sqrt{k_v E / F_{ys}}$:

$$V_s = 0.6 A_w F_{ys}$$ 2.16

for non-compact and slender steel plate when $h/t_w > 1.10\sqrt{k_v E / F_{ys}}$:

$$V_s = 0.6 A_w F_{ys} \frac{1 - C_v}{1.15\sqrt{1 + (a/h)^2}}$$ 2.17

$$k_v = 5 + \frac{5}{(a/h)^2}$$ 2.18

The value of kv should be taken as 5.0 if a/h is greater than 3.0 or $[260/(h/tw)^2]$. The value of C_v is given as follows:

if $\quad 1.10\sqrt{\frac{k_v E}{F_{ys}}} \leq \frac{h}{t_w} \leq 1.37\sqrt{\frac{k_v E}{F_{ys}}} \quad$ then $\quad C_v = \frac{1.10\sqrt{k_v E / F_{ys}}}{h/t_w}$

if $\quad \frac{h}{t_w} > 1.37\sqrt{\frac{k_v E}{F_{ys}}} \quad$ then $\quad C_v = \frac{1.51 k_v E}{(h/t_w)^2 F_{ys}}$

where E and F_y are elasticity modulus and yield stress of steel plate, and the A_w is the cross-sectional area. In case of application of steel deck plate, the contribution of steel deck plate should be ignored due to low in-plane shear resistance.

- Shear strength of panel-wall with boundary columns

In case of non-opening type panel wall specimen, the shear strength is calculated based on the design guidelines for framed shear wall by AIJ with considering the arch mechanism only. Since the transverse reinforcements were not used in the panel-wall, the truss mechanism is not considered. As described for opening-type thick hybrid wall the contribution of steel plate can be added to the resistance obtained by arch action of the additional concrete. The related equation is presented in Eq. 2.18.

$$Va = 0.5 \sigma_B t_w l_w \tan\theta$$ 2.19

$$\tan\theta = \sqrt{(\frac{h_w}{l_w})^2 + 1} - (\frac{h_w}{l_w})$$ 2.20

Where V: ultimate shear strength; σ_B: cylinder strength of concrete; tw: thickness of panel wall; l_w: center to center distance between the columns; h_w: height between bottom of panel wall to top of beam.

2.5.4 Shear sliding

In general the shear sliding resistance at potential sliding plane consists of shear friction resistance of concrete, dowel action of longitudinal reinforcements, and shear resistance of sliding-resistance device. In this part the mechanism of each source of resistance will be explained one-by-one.

- Shear friction

The shear-friction approach, as it is known today, was first introduced by Birkeland and Birkeland [26]. It was originally developed to deal with force transfer across joints in precast concrete construction. **Fig. 2.27** illustrates the shear-friction hypothesis. Assuming sliding along the failure plane m-m, and simple Coulomb friction, the shear force V required to produced sliding is equal to μP, where μ is the coefficient of friction of friction between the two elements and P is the clamping force perpendicular to the sliding plane. The roughness of crack m-m will create a separation δ between the two halves. If reinforcement is placed across the interface, the separation will develop tension T in the reinforcement. The tension provides an external clamping force on the concrete resulting in compression across the interface of equal magnitude. The roughness may be visualized as a series of frictionless fine saw-tooth having a slop of tan ϕ. Comparing **Figs 2.27 a** and **b**, it is seen that T tan ϕ is equivalent to the frictional force μP. Test revealed that the separation δ is usually sufficient to yield the reinforcement crossing the crack. Thus,

$$V_n = \mu A_s f_y$$ 2.21

Where μ=1.4 for monolithic concrete, 1.0 for artificially roughened construction joints, and 0.8 to 1.0 for ordinary construction joints and for concrete or steel interfaces. To prevent crushing of the concrete in the crack (caused by clamping force from the steel), before yielding of the steel, the steel ratio across the crack was limited to 0.015 and the shearing stress was limited to not more than 5.5MPa for concrete with fc=27.6 MPa.

(a) Shear friction hypothesis [26]

(b) Idealized model
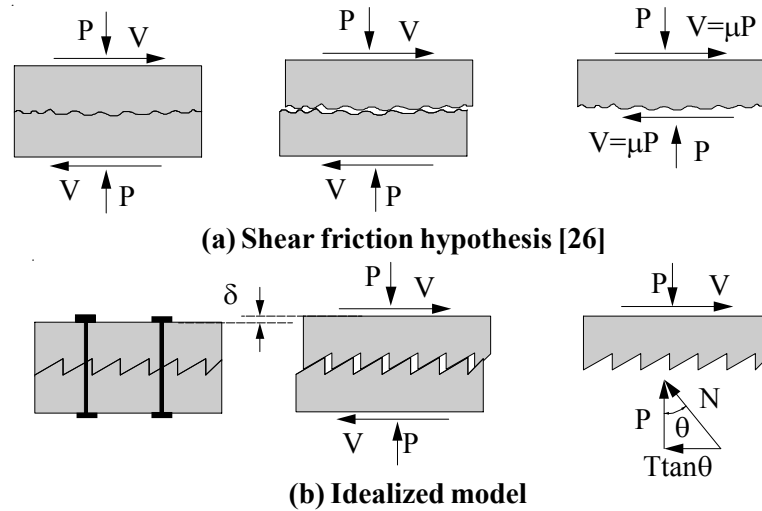
Fig. 2.27 Shear friction mechanism [26]

According to recent investigation by Valluvan et al. [27] on evaluation of ACI 318-95 shear-friction provisions, the provided shear sliding is modified as follows;

$$V_n = (A_s f_y + N)\mu \qquad \text{........ when } N \le 5.5\, Ac \qquad \text{...} \quad 2.22$$

$$V_n = N\mu \qquad \text{........................ when } N > 5.52\, Ac \qquad \text{.......................................} \quad 2.23$$

Where V_n shall not be taken greater than $0.25 f_c A_c$ in Eq. 2.21 and $0.6 f_c A_c$ in Eq. 2.22. The A_c is the area of concrete which is under net compression. In case of application of thick hybrid wall, two conditions happen. One condition is that when the compression zone falls in the column and another condition is that when the compression zone acts on the wing-wall in the additional part. Based on the compatibility between the experimental and analytical results it is suggested that the for the first aforementioned condition $\mu=1.4$ and for the second condition $\mu=0.6$.

– Dowel action resistance (V_d)

The opening of the crack can be controlled by reinforcements that normally crosses the shear plane at right angles. Such bars will also be subjected to shear displacement, hence a certain amount of additional shear can be transmitted by dowel action. Dowel strength across a shear plane can be developed by three mechanisms: the flexural of the reinforcing bars, the shear strength across the bars, and the kinking of the reinforcements. It is to be noted,, however, that the yield strength of a bar in flexure and shear can not fully utilized for dowel action if the same bar is provide a clamping force, as well [28]. As mentioned by Park and Paulay [28], tests by Phillips indicated that kinking is likely to be the major source of dowel strength, particularly when small size bars are used.

$$V_d = \frac{4d_b}{3\pi} \frac{A_s f_y}{l} \qquad .... \text{ Flexure mechanism } .... 2.24$$

$$V_d = \frac{A_s f_y}{\sqrt{3}} \qquad .... \text{ Shear mechanism } .... 2.25$$

$$V_d = A_s f_y \cos\alpha = 0.25 A_s f_y \qquad .... \text{ Kinking mechanism } .... 2.26$$

where d_b: the diameter of the bar; A_s: the sectional area of bar; f_y: the yield strength; l: the possible flexural length.

By referring to **Fig. 2.27**, the shear sliding of the longitudinal reinforcements can be explained. The longitudinal reinforcements of the wing-wall-column considerably resist in shear sliding when the compression stresses act on the wing-wall. Also, in case of retrofitting with panel-wall, the longitudinal reinforcements of boundary column in tension resist by dowel action.

2.6 Dominant mechanism of test specimens

According to experimentally observed mechanism and based on the physical concept which explained in the previous part, the lateral strength of possible mechanisms will be compare with the experimental results to exhibit the compatibility between calculated lateral strength and the dominant mechanism. The dominant mechanism of the test specimens are shown in **Fig. 2.28**.

In specimen **R07P-P0**, at first flexural plastic hinges formed at both ends of the first story columns. At drift angle of R=1.64%, shear failure happened at the top of right-side column.

In specimen **R06P-WW**, the shear force induced in the wing-wall-column reached to the shear strength, and consequently a diagonal shear crack occurs in the wing-wall. But since deck plate and bolts prevent the crushing of concrete, the lateral strength maintained greater than 0.8Vmax up to drift angle of R=0.5%.

In specimen **R08P-WN**, at first, flexural plastic hinges formed at the first story columns. After significant yielding of longitudinal reinforcements, the shear-friction of the columns reduced and then suddenly punching failure happened at the top column.

In specimen **R08P-WA**, flexural plastic hinges generated at both ends of the wing-wall-columns. A moderate strength degradation appears in the response due to buckling of longitudinal reinforcements.

In specimen **R06P-PS**, overall flexural behavior appears during the experimental test. The first and second stories relatively behaved as rigid member and the lateral displacements mainly generated by rotation at base.

Dominant mechanisms:

R07P-P0: Flexural yielding followed by shear failure.

R06P-WW: Flexural yielding accompanied by strut failure of wing-wall.

R08P-WN: Flexural yielding accompanied by punching failure at top of wing-wall-column

R08P-WA: Flexural yielding at ends of wing-wall-column.

R06P-PS: Flexural behavior at base.
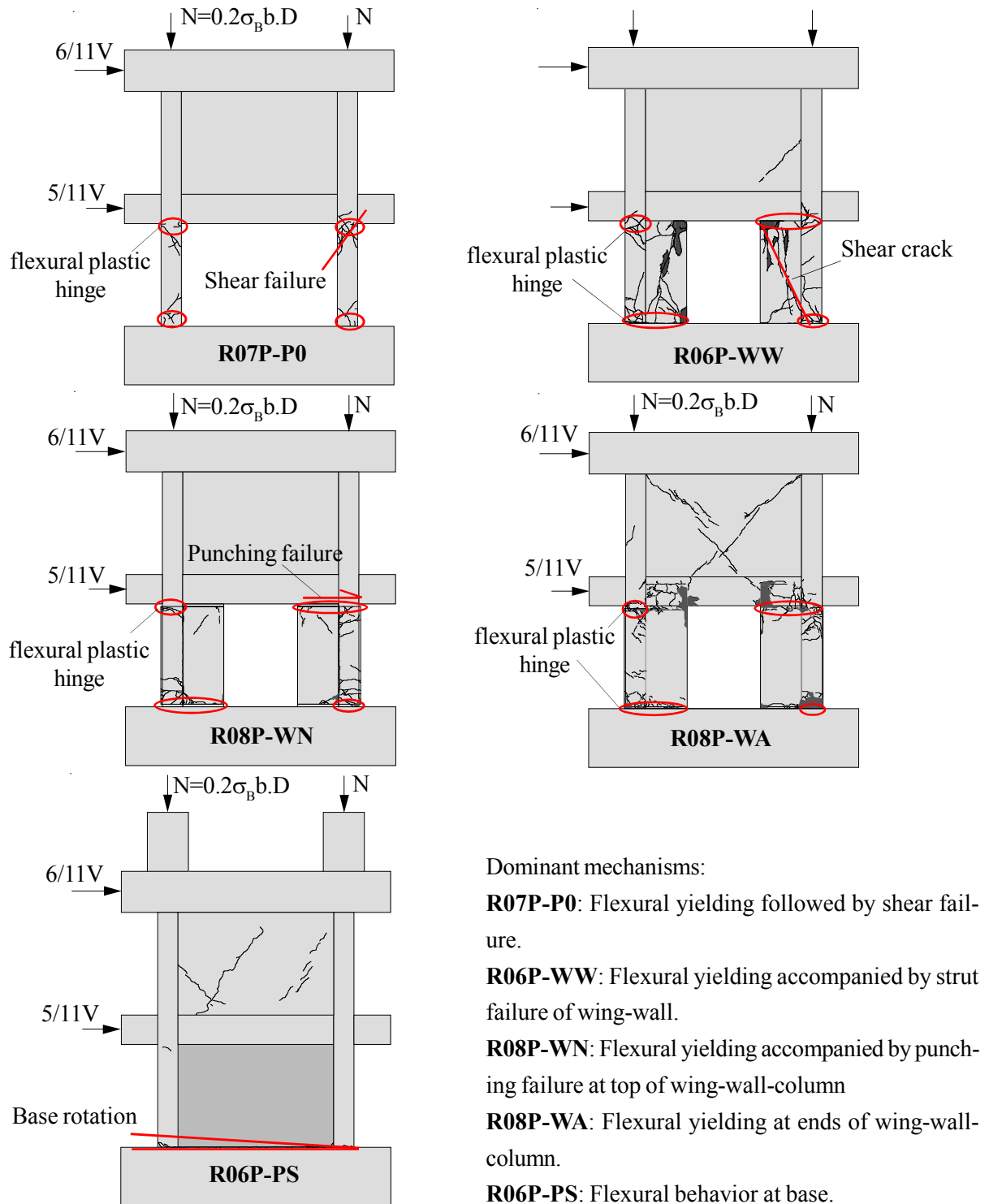
Fig. 2.28 Dominant mechanisms of one-bay two-story frames retrofitted by thick hybrid wall

■ Experimental result

▨ Flexural strength

▨ Shear strength

☐ Shear sliding resistance at top

▨ Shear sliding resistance at bottom
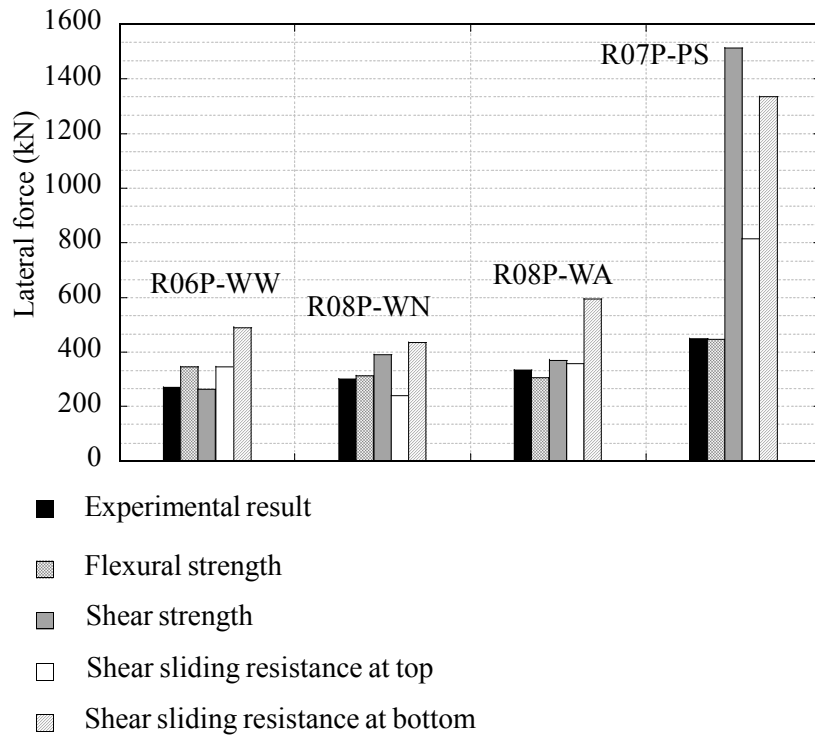
Fig. 2.29 Summary of calculated lateral strengths
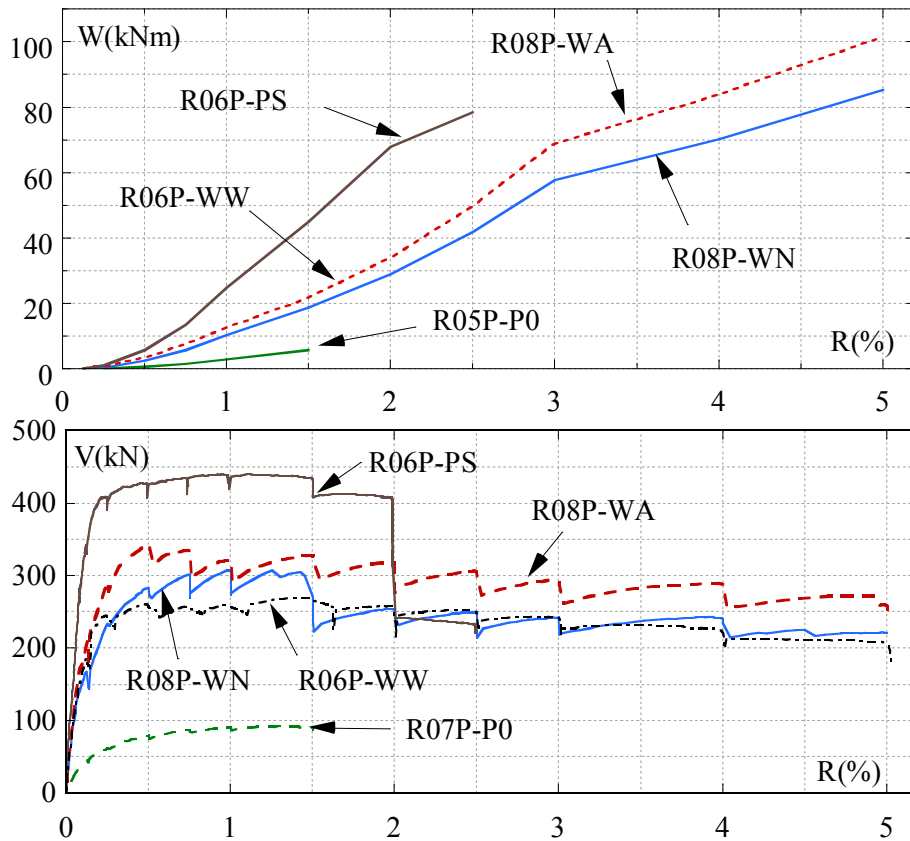
Fig. 2.30 Accumulative absorbed energy of the test specimens

Accumulative absorbed energy and skeleton curves of the test specimens are shown in **Fig. 2.30**. It is obvious that after retrofitting the test specimens with thick hybrid wall the lateral strength and ductility of the test specimens significantly increased. Also, the comparison of accumulative absorbed energy exhibits the huge amounts of energy dissipations through the application of thick hybrid walls.

3. CALIBRATION OF HYSTERETIC RESPONSES OF RETROFITTED MEMBERS

3.1. General

When numerical methods were made easily available to experimental investigators in the late 1960's, many realistic hysteresis models were claiming the best of a kind, without understanding which hysteretic properties have a significant influence on the earthquake response [29]. The properties of a hysteresis model were studied by those who developed the model. The effect of some hysteretic characteristics on the response of single-degree-of-freedom systems was discussed by Umemura [30] and Tani et al. [31].

In some structures designed according to the present state of earthquake resistance design the forces induced in the structure during a major earthquake will exceed the yield capacity of some members and cause large inelastic deformations. These deformations resulting from the combined effect of gravity and lateral loads are concentrated in areas of maximum internal forces which are called critical regions. Critical regions can be classified into different types depending on the internal forces which are induced in them and control their hysteretic behavior [32]. These types are: regions subjected to flexure, regions subjected to flexure combined with high shear and axial forces. Beam-column joints are critical regions which are subjected to large shear and axial forces. The forces induced in different critical regions depend on the structural system, the type of excitation of the structure, the location of the critical region, and the span to depth ratio of the given member [7].

Since the seismic response of the entire structure depends on the hysteretic behavior of these regions, accurate models of such behavior need to be developed. Ideally these models should be based on the fundamental principles of mechanics using the material properties of concrete and reinforcing steel with due account for crushing and spalling of concrete, bond slip of reinforcement and shear sliding. The discrete nature of flexural and shear cracks should also be taken into

consideration. Not only is such a degree of refinement difficult to achieve, but the detailed information obtained from such refined nonlinear analysis is unnecessary in the response description of entire structures [30]. Moreover, the implementation of such models in dynamic response analysis of large structural systems is prohibitively expensive.

In determining the seismic response of multistory buildings point hinge models have been used extensively because of their simplicity (Umemura and Takizawa 1982). In these models the inelastic behavior of reinforced concrete elements is represented by concentrated springs at the ends of the member. Since it is computationally convenient to use a single spring to describe the inelastic behavior of any type of critical region, several parameters need to be defined for describing the behavior of the springs. These parameters depend on the actions that control the inelastic behavior of the member and are established empirically.

3.2 Hysteretic models for reinforced concrete members

A hysteretic model must be able to provide the stiffness and resistance under any displacement history. Many hysteresis have been developed. Some hysteresis models are elaborate, and include many hysteretic rules. Others are simple. The complicatedness of a hysteretic model indicates a large memory to store the hysteretic rule program, but does not necessarily lead to a longer computation time because the complicatedness of a hysteretic model requires simply many branchings in a computer program, and only a few branches are referred to for a step of response computation.

Different hysteresis models representing dominantly flexural behavior of the reinforced concrete members are briefly described in this section. The following definition are used to simplify the description of the hysteretic conditions:

- Loading : the amplitude (in positive or negative) of resistance increases without change in sign;
- Unloading: the amplitude (in positive or negative) of resistance decreases without change in sign;
- Load reversal: the sign of resistance changes, and the response point crosses the displacement axis;
- Primary curve: a resistance-displacement relation curve under monotonically increasing load;
- Unloading point: a resistance-displacement point from which unloading has started.

3.3 Calibration of column retrofitted with thick hybrid wing-wall

As mentioned in chapter 2, application of thick hybrid wing-wall is a method in increasing the lateral strength and ductility of non-ductile RC columns. The main objectives in application of this technique are that the brittle shear failure of RC column changes to a ductile flexural one and consequently increasing the lateral strength. To obtain the seismic response of the column retrofitted with this retrofit type, it is necessary to model its hysteretic behavior. Since in modeling a frame different elements have contribution in the lateral resisting force-lateral displacement response, it provides some complexity to find the exact behavior of a element (retrofitted column) from a global response. Considering this rational reason, the calibration of hysteretic model for this retrofit type was carried out for a wing-wall-column retrofitted with thick hybrid wall. Even though, the feature of wing-wall-column is different from a column, after retrofitting, it is expected that their behavior would be almost same. The calibration procedure was implemented for specimen R03WO-S [33] which is retrofitted with opening type thick hybrid wall. This specimen is a shear critical one. In the retrofitting procedure, a channel-shaped steel plate jacketed the column. Steel plates were also encased the wing-wall with a length equal to the column depth. After that PC bars were crossed the wing-wall and imposed that the original wing-wall, additional concrete part , and the jacketing steel plates act as unified member with high flexural and shear rigidity. The column of specimen R03WO-S has the shear span to depth ratio of $M/(VD)=2.0$. In additional part, high-strength mortar ($\sigma_B=68.5$) was used. The schematic view of the specimen R03WO-S is illustrated in **Fig. 3.1**. As shown in Fig. 3.1, the body of the retrofitted wing-wall-column remained without considerable damage, and most damages were concentrated at both ends of the wing-wall-column. The critical zones have the flexural behavior.
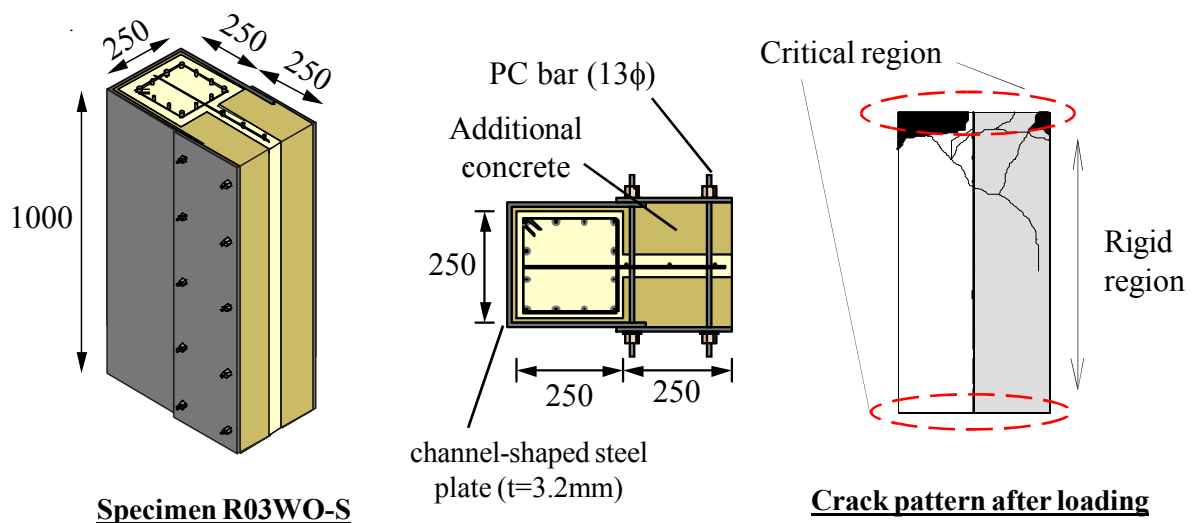

Specimen R03WO-S **Crack pattern after loading**

Fig. 3.1 Properties of specimen R03WO-S

The major mechanisms that controlled the hysteretic response of the test specimen included deformation of flexural plastic hinges at the both ends of the wing-wall-column and shear sliding along open full-depth cracks at interface sections. There are different hystereses such as Clough, Degrading Trilinear, Takeda, Bilinear, Ramberg-Osgood and Sina which can be used for modeling the reinforced concrete members. Among different types of hystereses, the Sina hysteresis rule was found appropriate to model the hysteretic behavior. The Sina hysteretic rule is a trilinear hysteretic model used to describe the stiffness degradation of reinforced concrete members in flexure as well as account for the pinching effect due to interface shear sliding and bond deterioration [34]. In this study, new parameters were defined for modification of the hysteretic rules to obtain an acceptable agreement between the observed hysteretic response and applied hysteretic rule. In experimental V-δ relationship, it was found out that increasing the residual deformation δ_0 in unloading phase led to increasing the displacement coordinate δ_p of the pinching point in next reloading with a approximately constant value of $C_p = \delta_p/\delta_0$. Considering this behavior, in modeling the pinching phenomenon, the break point P was defined as function of residual deformation δ_0 and maximum load experienced in the direction of loading V_y^+. Definition of the punching point as a function of maximum permanent deformation of δ_0 and the maximum load experienced in the direction of loading V_y^+ was also defined by Ibarrab et al. for reinforced concrete members. The rule of unloading branches was also modified according to Emori unloading formula with a variable exponent factor α to obtain an appropriate unloading stiffness. In this modeling, based on the experimental results, the exponent factor of Emori formula α, pinching factors $C_p = \delta_p/\delta_0$ and $\eta = V_p^+/V_y^+$ were defined 0, 0.2 and 0.2, respectively. As illustrated in **Fig. 3.2**, the wing-wall-column retrofitted with thick hybrid wing-wall was modeled by two springs to represent the
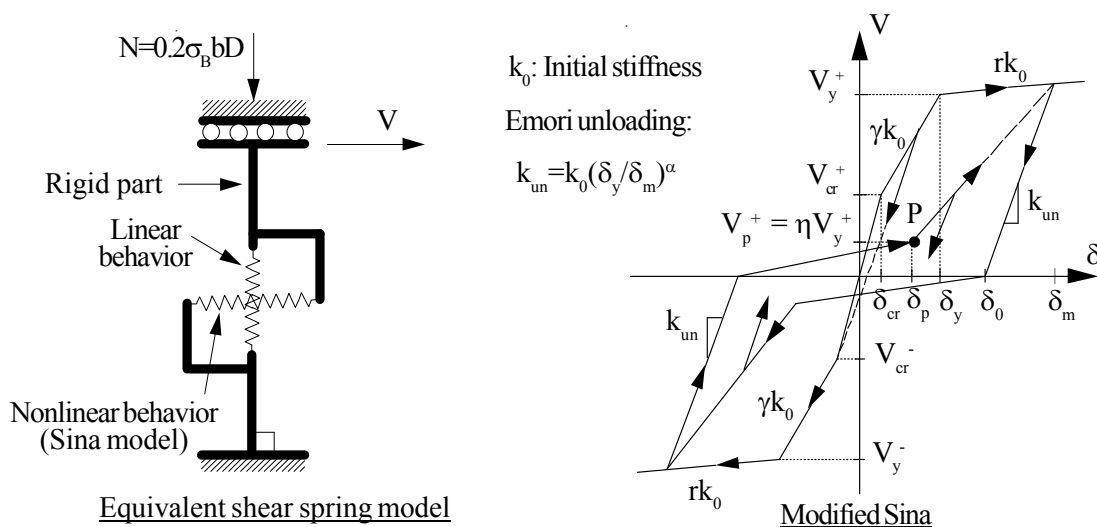

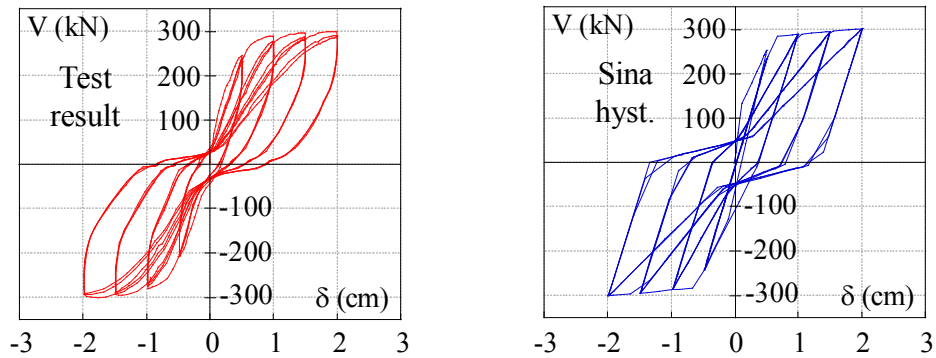**Fig. 3.2 Model of specimen R03WO-S [35] and modified Sina hysteresis**

Fig. 3.3 Exprimenatl and analytical results of specimen R03WO-S

behavior of the member in axial and transverse directions. The numerical analysis of the model was implemented in RUAUMOKO computer program [35]. In modeling the specimen, the axial spring was assigned with nonlinear behavior described with the modified Sina hysteretic rule. The analytical results and experimental data are shown in **Fig. 3.3**. The comparison between the analytical and experimental results exhibited an acceptable correlation.

3.4 Calibration of frame retrofitted by thick hybrid panel-wall

In modeling the non-opening type thick hybrid panel-wall, the test specimen R06P-PS (see **Fig. 2.21**) was used to assess and calibrate the hysteretic behavior of this type retrofit. In the experimental observation, it was evident that the basic mechanism of this specimen contained the flexural rotation concentrated at the base of the boundary columns and panel-wall. The body of the panel-wall and the second story relatively behaved as a rigid member. Based on the experimental hysteretic response of the specimen, the modified Sina hysteretic rule was used to describe its hysteretic behavior. As previously
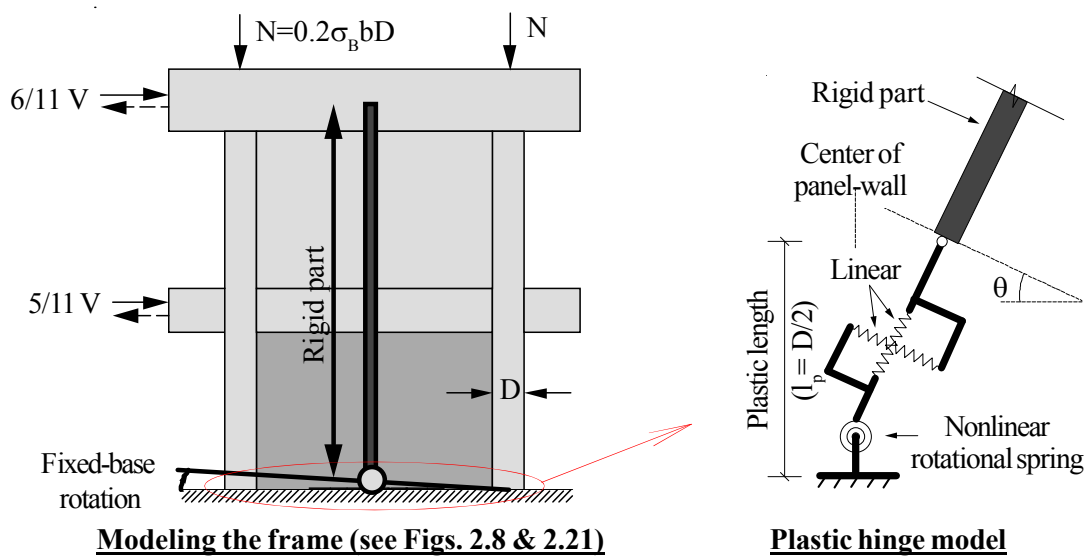

Modeling the frame (see Figs. 2.8 & 2.21)　　**Plastic hinge model**

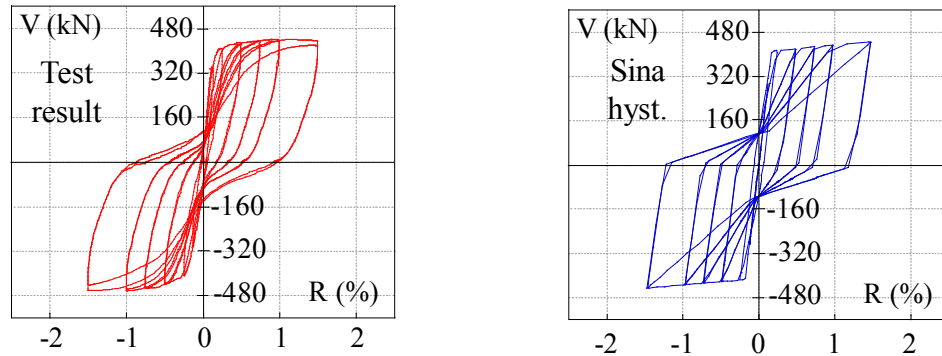**Fig. 3.4 Modeling the specimen R06P-PS**

Fig. 3.5 Exprimenatl and analytical results of specimen R03WO-S

explained, the jacketing steel plates make the boundary columns and panel-wall behave as a rigid member. In modeling one-bay two-story test specimen, the specimen was separated vertically into two individual regions including the plastic hinge zone at base and rigid body part. As shown in **Fig. 3.4,** the plastic hinge zone in the assumed length of *D/2* (half of the depth of the column) was modeled by two linear springs representing the axial and transverse behaviors of this critical region as well as one rotational nonlinear spring describing the flexural behavior through the modified Sina hysteresis. Curvature ϕ was postulated to be constant along the considered plastic hinge length $l_p=D/2$, and, hence, a concentrated rotational spring was used to describe the rotation in this zone $(\theta_p=l_p\phi)$. In construction of hysteresis rules, based on the experimental data, the exponent factor of Emori formula α, pinching factors $C_p=\delta_p/\delta_0$ and $\eta=V_p^+/V_y^+$ were defined 0.1, 0.1 and 0.3, respectively. In **Fig. 3.5**, the comparison between the experimental data and analytical results shows an acceptable agreement at small to moderate drift angles.

3.5 Calibration of column retrofitted by PC bar prestressing

Application of PC bar (high strength steel bar) as an external transverse reinforcing device was first proposed by Yamakawa et al. [36,37,38]. By utilizing this method, brittle shear failure mode of the columns with poor ratio of transverse reinforcements successfully converted to ductile flexural behavior through the enhancement of transverse confinement induced by PC bar prestressing. To find out the dynamic response of the columns retrofitted by the PC bar prestressing, specimen R98M-P65 was used to assess and calibrate the hysteretic response of this retrofit type. Specimen R98M-P65 is a shear critical column due to poor ratio of transverse reinforcements. After installation of PC bar prestressing, it was observed that shear failure of column was prevented and the retrofitted column exhibited a ductile flexural response. In simulating the behavior of retrofitted column, it was modeled by beam-column element with plastic hinge length of *lp=D/2*. Moment-curvature relationship *M-ϕ* at plastic hinge length was defined by Takeda hys-
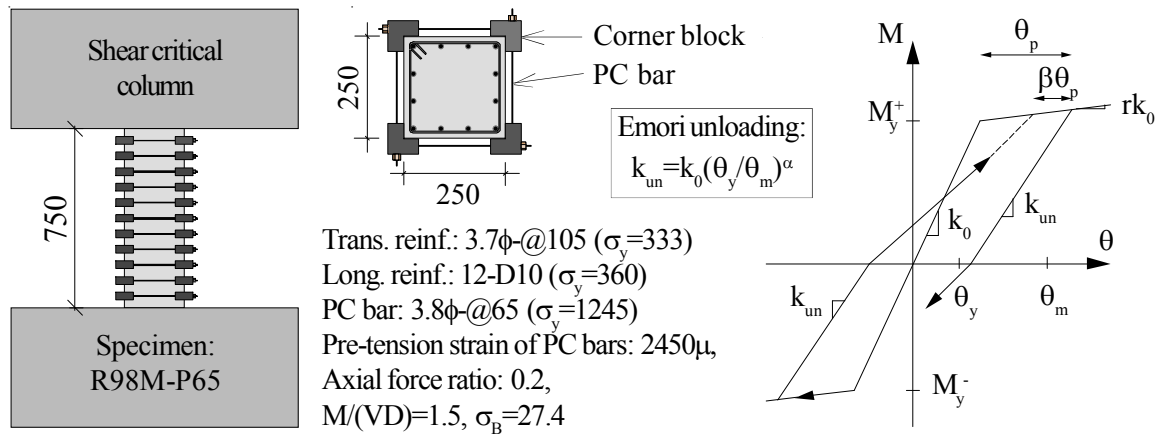
Fig. 3.6 Column retrofitted by PC bars and Takeda hysteresis

teretic rule [39]. Takeda hysteresis is a refined model was proposed by Takeda et al. for RC members. In this model monotonic behavior is described by a bilinear skeleton curve which accounts for yielding of reinforcing steel or bilinear skeleton curve neglecting the cracking stage. The hysteretic behavior is described through a number of rules for unloading and reloading and is based on the data obtained from specimens tested in an earthquake simulator. Even though Takeda's hysteretic model was originally proposed for simulating the load-displacement relation of RC members, it has been widely used since in the description of the hysteretic moment-curvature or moment-rotation relations of RC members. In order to obtain a hysteretic behavior compatible with experimental data, the parameters α and β were considered 0.5 and 0, respectively. Comparison between the test results and Takeda hysteresis rules shows an acceptable agreement between them (see **Fig. 3.7**).

Fig. 3.7 Experimental and analytical results of specimen R98M-P65 [36]

3.6 Cumulative absorbed energy of experimental results and models

In calibration of hysteretic behavior of the test specimens, the applied hysteretic models were se-

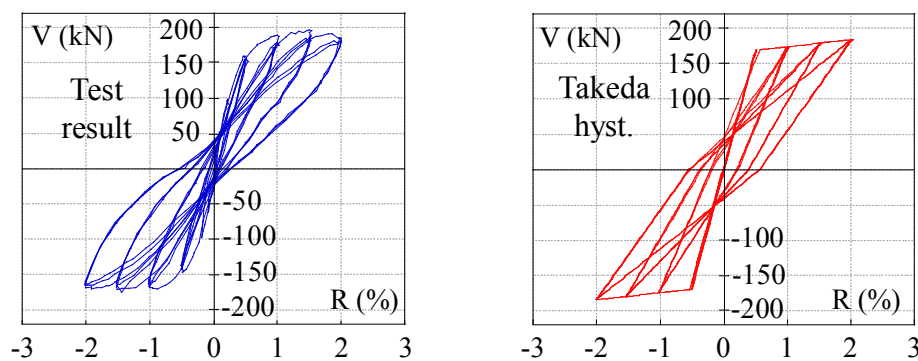lected based on the observed major mechanisms. In order to show the capability of models to represent the energy dissipation in the excursion loops, cumulative absorbed energy was compared between experimental data and analytical results.

In specimen R03WO-S, cumulative absorbed energy by model is less than that by experimental data. This bias is mainly generated by discrepancy of experimental response curve and linear approximation of model in loading path after crack closing and in unloading path after peak point. Since the applied model exhibits lower absorbed energy in comparison with experimental data, it can be adopted as a conservative estimation in representing cumulative absorbed energy of this type retrofit. In specimen R06P-PS and R98M-P65, the cumulative absorbed energy by analytical result are close to experimental results at small drift angle, but by increasing the drift angle the bias appears between two curves. However, it is expected the dynamic response of members retrofitted by thick hybrid wall R06P-PS and by PC bar prestressing R98M-P65 will be restricted to drift angle of $R=1\%$ and $R=2\%$, respectively, at which the cumulative absorbed energy between analytical results and experimental data does not show marked difference. It should be noted the number of cycles in loading program of the test specimens are not identical, and for this reason, the cumulative absorbed energy can not be compared between the specimens.
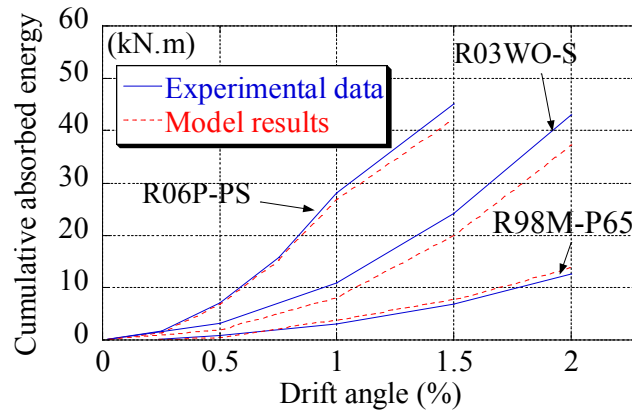

Fig. 3.8 Comparison of cumulative absorbed energy

4. SEISMIC EVALUATION OF AN EXISTING SOFT-FIRST-STORY BUILDING

4.1 General

In this section, it is aimed to evaluate the seismic performance of an existing soft-first-story building before and after retrofitting with thick hybrid wall technique. Seismic evaluations are conducted in cases of dynamic response analyses during earthquake excitations and seismic vulnerability assessment based on the seismic retrofit guidelines provided by Japan Building Disaster Provision Association (JBDPA). Dynamic Response Analyses were carried out in RUAUMOKO software programmed by J. A. Carr [40]. The physical and mathematical approach in numerical analyses will be explained regarding the methods used in RUAUMOKO computer program. After modeling the buildings retrofitted by different retrofit types and carrying out the dynamic response analyses, the seismic performance of the building will be evaluated through the approach used in seismic retrofit guideline by JBDPA. Different retrofitting schemes for the existing soft-first-story building are verified to propose a desired one. The responses of dynamic response analyses and retrofit procedure of JBDPA will be compared.

4.2 Physical and mathematical principles in dynamic response analysis

4.2.1 Mass matrix

The mass of the structure is input in the form of weight and internally converted by the program to mass units by dividing the weights by the acceleration of gravity. The mass may be provided by both specified nodal weights or by member weight/unit length or element material density. Nodal weights will contribute to only the diagonal terms of the mass matrix where the terms associated with the rotational degrees of freedom are usually taken as zero. There is a lumped mass representation where contribution are made to the diagonal terms to the diagonal terms associated with the three translational degrees of freedom at each end of the member or to

all four nodes for quadrilateral or panel elements with no contribution to the rotational degree of freedom. The diagonal mass representation is the same as the lumped model described previously except that the contribution to the rotational degrees of freedom is equal to the diagonal term of the appropriate consistent mass matrix of the member concerned for beam, beam-column and wall elements [41].

The third option is the consistent mass representation using the kinematically equivalent mass matrix [42] where inertia forces are associated with all degrees of freedom. This will result in a mass matrix with the same banded skyline form as that of the stiffness matrix. The consistent mass model requires a greater computational effort in the multiplication by the nodal accelerations to get the inertia forces at each time step in the analysis. It also bounds all natural frequencies and consequently gives a slight bias to the frequency content of the structure. If the only masses are those from the input nodal masses there is no difference in the actual mass matrices for the structure through the consistent mass option would involve the extra cost of multiplying all the zero terms within the matrix skyline of the associated stiffness matrix when computing the inertia forces. The mass matrix used for the mode shape and frequency analysis is a diagonal mass matrix. As the computed free-vibration frequencies are only used for checking purposes and for computing the damping matrix this is of little consequence. To use the consistent matrix would require a double eigenvalue solution or the Cholesky decomposition of the mass matrix. The first approach is computationally expense and the second is not possible if there are any degree of freedom without mass as the matrix would then be singular. If a Rayleigh damping matrix is being specified, the frequencies are used to compute the contributions of both the mass and stiffness matrices to the damping matrix. In all of the modeling of the building the consistent mass matrix were used.

4.2.2 Damping matrix

There are several damping model options available. The traditional approach has been to use a Rayleigh or Proportional damping model where the structures damping matrix is given by

$$C=\alpha M+\beta K \qquad\text{.. 4.1}$$

where M and K are the mass and stiffness matrices for the structure. The coefficient α and β are computed to give the required levels of viscous damping at two different frequencies, most commonly those of the first and second modes of free vibration. Reyleigh damping may be modeled proportional to tangent stiffness matrix or the initial stiffness matrix. Work by Crisp [43]

showed that high levels of viscous damping in the high modes of free vibration of a structure has a marked effect on the response of an inelastic structure. The use of the tangent stiffness may be criticized from the philosophical point of view that when the structure goes inelastic one does not expect the damping to reduce. However, it appears that this reduction of the damping partially compensates for the excessive higher mode damping associated with the Rayleigh damping model. With tangent stiffness damping the fractions of critical damping in the structures tend to remain more constant as the stiffness of the structures reduces whereas the constant mass and initial stiffness damping contributions imply increasing fractions of critical damping as the stiffness of the structure reduces with inelastic response.

In the response of inelastic structures to earthquake excitation a step-by-step integration of the equation of dynamic equilibrium is required as the non-linearity of the structures precludes the use of super-position and hence any modal methods such as the use of response spectra techniques. This makes it difficult for the engineer in that the structure must be analyzed for all the load cases simultaneously as the separate gravity and seismic excitation response can not be obtained and combined for alternate excitation directions as is traditionally used in seismic design.

In inelastic structures various hysteresis rules are used to represent the inelastic behavior of the member actions, such as the moment-curvature relationships in beam members. These non-linear rules allow for the energy dissipation due to the non-linearity of the members and although these members do not go through many complete hysteresis loops within a single earthquake excitation the large forces associated with these member hysteresis loop means that a considerable amount of energy is removed from the structural response. However, these hysteresis models do not, in general, account properly for the energy removed from the system by small cycle oscillations within the structure. Even structures that remain elastic show a damped response and the effect of this low level damping in the structure has marked effect of the response of the structure. An examination of any earthquake response spectrum will show that even small amounts, i.e., 2 to 5%, of critical damping will significantly reduce the response of the structure. Some suitable damping model is required in the analysis to represent this decay. Whether the damping in the structure is actually viscouser hysteretic is something that has yet to be determined, but in the meaning it is generally assumed to be a viscous damping mechanism. This is usually justified in that as the damping forces are assumed to small any error due to this mathematically convenient assumption is not very significant in the response. This appears to be reasonably well justified in terms of an elastic response. Most analysts assumed that if they specified say 5% of critical damping at two modes then their structure had effectively 5% of critical damping.

- Caughey Damping

A means of matching the required amount of damping at a greater number of modes is provided by a damping model proposed by Caughey [44] where the damping matrix may be expressed as follow;

$$C = M \sum_{b=0}^{N-1+q} a_b [M^{-1}K]^b \qquad \dots\dots\dots\dots\dots\dots\dots\dots\dots\dots\dots\dots\dots\dots\dots \text{4.2}$$

where q is any integer and N is number of nodes at which damping is specified. This equation enables the fraction of critical damping to be expressed at all, or any, of the natural frequencies of free vibration. The difficulty is the large powers of ω required in the expressions to evaluate the coefficients of a_b and the computationally awkward matrix products involved. Wilson and Penzien [45] proposed a much simpler way of obtaining the same damping model using the N mode shapes of free-vibration. The disadvantage of this approach is the large eigenvalue problem to be solved for all N natural frequencies and mode shapes of free vibration before commencing the time-history analysis as well as the other disadvantage of the Caughey damping model in that the damping matrix C is fully populated, i.e. it is no longer a banded matrix. The method suggested by Wilson and Penzien makes use of the properties of orthogonality of the mode shapes with respect to the mass, damping and stiffness matrices. Given the ith mode shape of free-vibration ϕ_i such that:

$$m_i = \phi_i^T M \phi_i \qquad \dots\dots\dots\dots\dots\dots\dots\dots\dots\dots\dots\dots\dots\dots\dots\dots\dots \text{4.3}$$

where m_i is the generalized mass for the ith mode. In a similar manner the generalized damping can be computed from:

$$c_i = 2\lambda_i \omega_i m_i = \phi_i^T C \phi_i \qquad \dots\dots\dots\dots\dots\dots\dots\dots\dots\dots\dots\dots\dots \text{4.4}$$
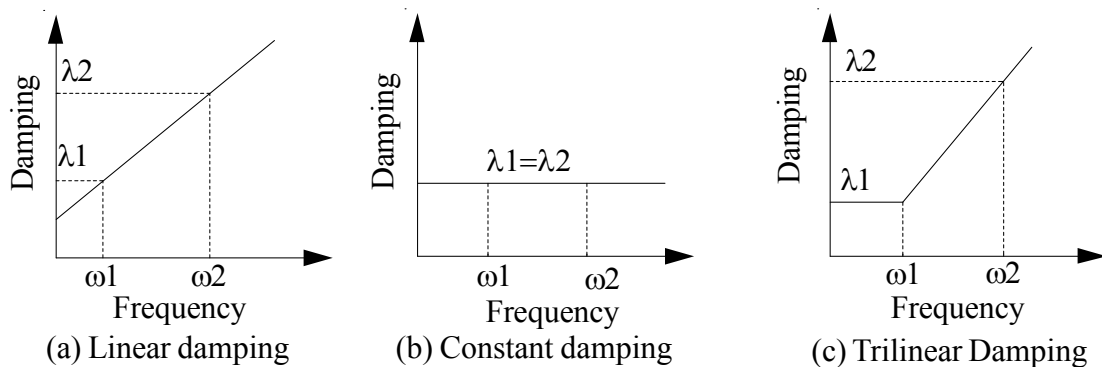

Fig. 4.1 Different damping models

if the fraction of critical damping λ is specified for each mode the damping matrix C can be obtained using the inverse of the model matrix to transform back from the generalized damping matrix. The actual operation may be simplified and the reader is referred to the original paper of Wilson and Penzien for further details.

4.2.3 Structural members

In this study for modeling buildings, two element types including beam-column and spring elements are mainly used (see **Fig. 4.2**). A beam member may also have a bi-linear axial load-axial displacement hysteresis. However, there is no interaction between the axial yield states and those associated with the moment-curvature yield states. A beam-column member differs from a beam member in that the axial force in the member affects the current yield moments at each end of the member. The inelastic behavior of a beam and beam-column member, in general, follows the concept of the Giberson one-component model [45] which has a plastic hinge possible at one or both ends of the elastic central length of the member. Rigid end-block may be incorporated within the length of any of the frame members. If there are joint flexibility or shear deformations, the member stiffness is inverted to get the member flexibility, the joint and shear flexibility are added and the resulting matrix is again inverted to get the final stiffness of the beam member. The stiffness of the hinge is controlled by the tangent stiffness of the current point on the appropriate hysteresis rule. The stiffness of the hinges is such that the rotation of the hinge together with the rotation associated with the elastic curvature of the beam over the hinge length is the same as the rotation associated with the curvature over the hinges length with inelastic properties in the hinge zone.

Spring members may be used to model special effects in the structure. In two-dimensional structural analyses they can be used to represent members acting out of the plane of a frame but representing forces that act in the plane of the frame. An example of the latter is a rotational
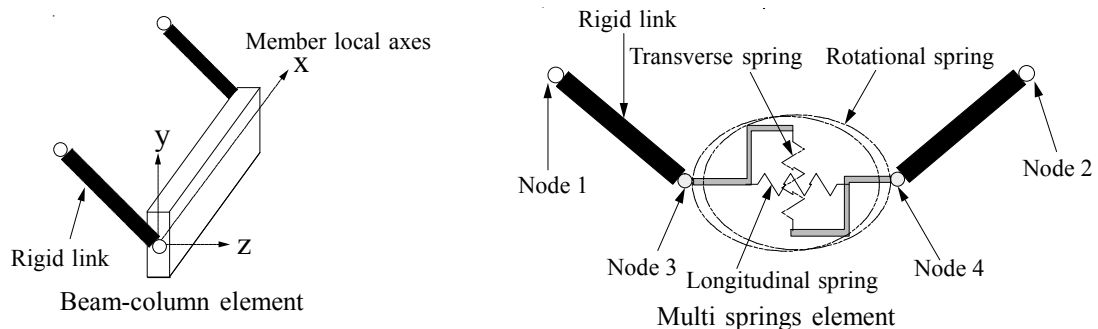

Fig. 4.2 Beam-column and multi springs element

spring representing the torsional spring representing the torsional behavior of a beam oriented perpendicular to the plane of the frame and connecting it to an adjacent parallel frame. The spring member orientation is given by the axial orientation of the member but if the two end nodes coincide resulting in a zero length member then the longitudinal and transverse directions coincide with structure, or global X, Y and Z axes, respectively.

4.2.4 Stiffness and strength degradation

Many different hysteresis rule have been proposed up to now to represent the inelastic behavior of frame and spring members. They range from the simple elasto-plastic and bi-linear rules, the computationally more expensive Ramberg-Osgood rule [45] to rules such as those developed by Wayne Stewart [46] which requires over thirty parameters to keep track of the current stiffness. The required parameters for definition of a hysteresis include the yielding point, if necessary, the crack point, and the stiffness of loading and unloading branches. In this study three hysteresis rules are used. The Takeda hysteresis rule are applied for modeling the ordinary nonretrofitted columns (see **Fig. 4.3**). Also, the strength degradation is assigned to consider the moderate or sharp degradations of lateral resisting force. For instance, it is expected that the ordinary column yield in flexure but by increasing the lateral displacement and consequently by forming the flexural crack at plastic hinge zone, the shear strength of that zone gradually decrease [47]. The degradation in shear resistance at plastic hinge zones leads to a sharp reduction in lateral strength. For considering this effect the strength degradation in the lateral strength due to shear failure is defined based on the equation proposed by AIJ [47] for calculation of shear
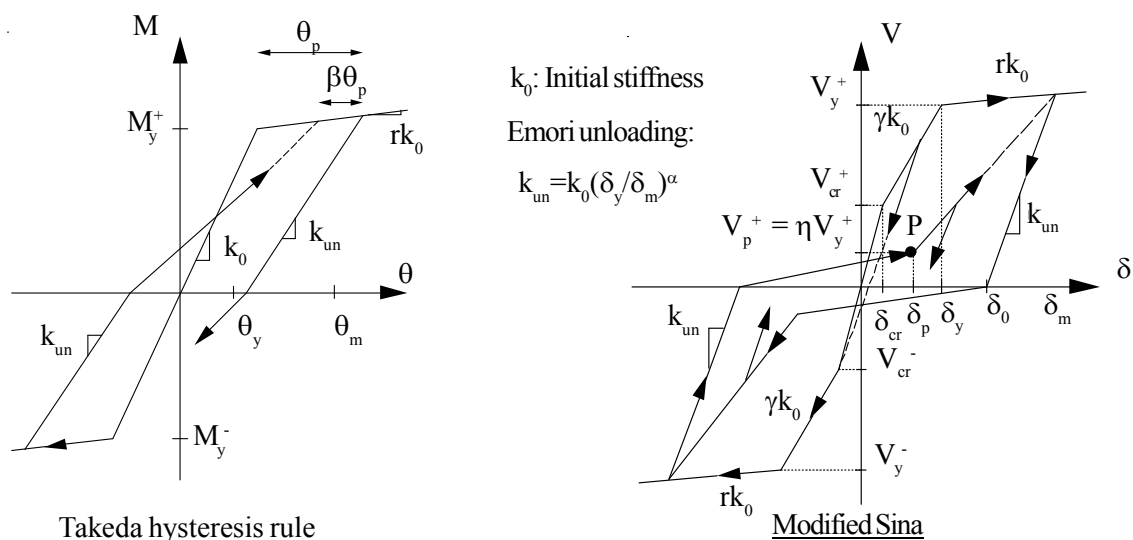

Fig. 4.3 Takeda and Modified Sina hysteresis rule

Origin centred hysteresis   Strength reduction variation
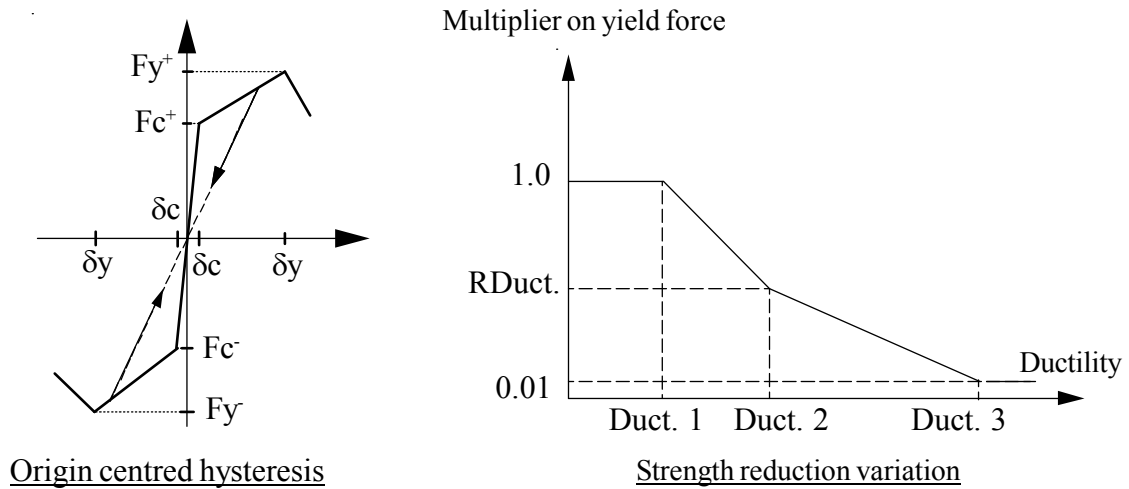
Fig. 4.4 Origin centred hysteresis and strength reduction variation

strength. As shown in **Fig. 4.4**, in this study the shear wall was modeled by the Origin-centred hysteresis rule. Since the origin-centred hysteresis rule represents a minimum energy absorption, it is suitable for modeling the shear-dominant shear wall. Also, as explained in **Section 3-3**, the column retrofitted by thick hybrid wall can be modeled by Sina hysteresis rule.

4.2.5 Modal analysis

In this study, modal analyses are carried out even though the results are not generally used during the dynamic analyses. A modal analysis does provide a check on the structural data in that designer can check that the natural frequencies and mode shapes are what would be expected for such a structure. In some cases a modal analysis is necessary as the natural frequencies of free vibration, and in some cases the mode shapes, are used to generate the appropriate damping matrix for the structure. Taking the equation of undamped free vibration, where no loads are assumed to act upon the structure, the N degree-of-freedom equation of equilibrium becomes;

$$[M]\{\ddot{u}\}+[K]\{u\}=\{0\} \quad\text{..}\quad 4.5$$

and assuming simple harmonic motion $\quad\{u\}=\{\phi\}_i\,Y_i\sin\omega_i t\quad$ then the equation of free-vibration is simplified to:

$$\{u(t)\}=[\phi]\{Y(t)\} \quad\text{..}\quad 4.6$$

where $\{\phi\}_i$ and ω_i are the ith mode and frequency of free vibration, respectively. The N vectors from a basis set of vectors in that any vector in the N dimensional space may be represented as a combination of the mode shapes:

$$-\omega_i^2[M]\{\phi\}_i+[K]\{\phi\}_i=\{0\} \quad\text{..}\quad 4.7$$

where {Y} are the modal amplitudes and [ϕ] is the modal matrix in which each column is a mode shape. Substituting this into the equation of equilibrium and pre-multiplying by [ϕ]^T gives

$$[M^*]\{\ddot{Y}\}+[C^*]\{\dot{Y}\}=-\{L^*\}\ddot{u}_g(t)$$ 4.8

$$[\phi]^T[M][\phi]=[M^*]$$ 4.9

$$[\phi]^T[C][\phi]=[C^*]$$ 4.10

$$[\phi]^T[K][\phi]=[K^*]$$ 4.11

$$[\phi]^T[M][r]=[L^*]$$ 4.12

From the properties of orthogonality of the mode shapes it can be shown that [M*], [C*] and [K*] are diagonal matrices with;

$$M_i^*=\{\phi\}_i^T[M]\{\phi\}_i$$ 4.13

$$C_i^*=\{\phi\}_i^T[C]\{\phi\}_i=2\lambda_i\omega_iM_i^*$$ 4.14

$$K_i^*=\{\phi\}_i^T[K]\{\phi\}_i=\omega_i^2M_i^*$$ 4.15

$$L_i^*=\{\phi\}_i^T[M]\{r\}$$ 4.16

Thus for each modes:

$$M_i^*\ddot{Y}_i+C_i^*\dot{Y}_i+K_i^*Y_i=-L_i^*\ddot{u}_g(t)\qquad i=1,2,...,N$$ 4.17

The system is now represented as N uncoupled single degree-of-freedom systems. Dividing through by M_i^* the second order differential equation is obtained for each mode i as

$$\ddot{Y}_i+2\lambda_i\omega_i\dot{Y}_i+\omega_i^2Y_i=\frac{-L_i}{M_i^*}\ddot{u}_g(t)=-\frac{\{\phi\}_i^T[M]\{r\}}{\{\phi\}_i^T[M]\{\phi\}_i}\ddot{u}_g(t)=-PF_i\ddot{u}_g(t)$$ 4.18

The term PF$_i$ is called the participation factor for the ith mode and it is an indicator of how much the ith mode is excited by the ground acceleration in the direction of the earthquake and indicates the importance of the contribution of the ith mode to the displacements of the structure. It should be noted that the numerical magnitude of the participation factors depend on the type of normalization used for the mode shapes. Once the Y$_i$ are found then relative structural displacements are found from:

$$\{u\}=[\phi]\{Y\}$$ 4.19

and the effects of the choice of normalization of the mode shapes is cancelled out. In a modal Response Spectrum analysis the base shear V$_i$ in the mode of a structure can be obtained from the

spectral acceleration S_A [48] using the following equation:

$$V_{i\max} = \frac{(L_i^*)^2}{M_i^*} g\{\frac{S_A}{g}\}_i = (effective\, weight)_i\{\frac{S_A}{g}\}_i \quad \text{..} \quad 4.20$$

The effective weight of the **i**th mode indicates the importance of the contribution of the **i**th mode to the total base shear acting on the structure in the same way that participation factor shows the condition of the **i**th mode to the displacement of the structure. The number of modes required in a modal analysis is specified in many codes to be such that the sum of the effective weights of the modes used must be at least of the order of 90% of the total weight of the structure. In the applied software, the modal analysis is normally performed after carrying out the static analysis as this allows, in P-Δ and large displacement analyses, for the adjustment of the member stiffness of frame members that have axial loads in them. Compressive forces will lead to a geometric stiffness terms that reduce the stiffness of the members. This means that in multistory frames the lateral stiffness of the structure more accurately represents the real of the structure with gravity acting upon it. In case of soft-first-story frames, since, usually, the contribution of first mode including concentration of lateral displacement in the first story is considerably higher than modes, application of equation 4.17 has high accuracy in prediction of lateral force.

4.2.6 Time history integration (Newmark Constant Average Acceleration Method)

The dynamic equation of equilibrium is integrated by the unconditionally stable implicit Newmark constant average acceleration (Newmark β=0.25) method [49]. The time step should be less than 0.1 of the period of the highest mode of free vibration that contributes significantly to the response of the structure. In general for multi-story frames buildings, experience has shown that 0.01 second is satisfactorily but for most digitized earthquake accelerograms the time step should never exceed 0.02 seconds. The Newmark scheme has been modified from the original incremental equilibrium at each time-step. As a further option, the Newton-Raphson iteration scheme can be employed to converge to a true solution at each time-step. Any residual force error is carried forward to the next time-step in a self-correcting procedure. The constant average acceleration method has the advantage of being unconditionally stable but also the advantage that not all degree of freedom need to have an associated mass. During the time step from time t to time t+Δt the acceleration is assumed to be constant:

$$\ddot{u} = \frac{\ddot{u}(t) + \ddot{u}(t+\Delta t)}{2} \quad \text{..} \quad 4.21$$

Integration with respect to time over the time-step Δt to get the velocity and displacement and rearranging to use the increment in the displacement Δu as the variable gives the increment in the acceleration:

$$\Delta \ddot{u} = \ddot{u}(t + \Delta t) - \ddot{u}(t) = \frac{4\Delta u}{(\Delta t)^2} - \frac{4\dot{u}(t)}{\Delta t} - 2\ddot{u}(t) \qquad \text{............................ 4.22}$$

and the increment in the velocity as

$$\Delta \dot{u} = \dot{u}(t + \Delta t) - \dot{u}(t) = \frac{2\Delta u}{\Delta t} - 2\dot{u}(t) \qquad \text{............................ 4.23}$$

substituting into the equation of equilibrium at time t+Δt gives

$$[M]\{\ddot{u}(t) + \Delta \ddot{u}\} + [C]\{\dot{u} + \Delta \dot{u}\} + [K]\{u(t) + \Delta u\} = \{P(t + \Delta t)\} \qquad \text{........................ 4.24}$$

Noting that the stiffness term mat be rewritten as

$$[K(t + \Delta t)]\{u(t) + \Delta u\} = [K(t)]\{u(t)\} + [K_T]\{u(t) + \Delta u\} = \{F_{elastic}(t)\} + [K_T]\{\Delta u\} \ \ 4.25$$

where [K(t)] represents the secant stiffness matrix at time t and the elastic forces are the nodal equivalent of the member forces at time t and the matrix [K_T] is the current tangent stiffness matrix. Similarly the damping term may be rewritten in terms of the nodal damping forces and the current tangent damping matrix and the increment of the velocities.

$$[C(t + \Delta t)]\{\dot{u}(t) + \Delta \dot{u}\} = [C(t)]\{\dot{u}(t)\} + [C_T]\{\Delta \dot{u}\} = \{F_{Damping}(t)\} + [C_T]\{\Delta \dot{u}\} \ \text{.... 4.26}$$

where the damping forces are those at time t and the matrix [C_T] is the current tangent damping matrix. This means that the equation of equilibrium may be written in the form:

$$[M]\{\Delta \ddot{u}\} + [C_T]\{\Delta \dot{u}\} + [K_T]\{\Delta u\} = \{P(t + \Delta t)\} - [M]\{\ddot{u}(t)\}...$$

$$- \{F_{damping}(t)\} - \{F_{elastic}(t)\} \qquad \text{............................ 4.27}$$

Substituting for the increments of acceleration and increments velocity in terms of the increments of velocity in terms of the increments of displacement leads to the equation:

$$[\frac{4}{(\Delta t)^2}[M] + \frac{2}{\Delta t}[C_T] + [K_T]]\{\Delta u\} = ...$$

$$\{P(t + \Delta t)\} + [M]\{\ddot{u}(t) + \frac{4}{\Delta t}\dot{u}(t)\} + 2[C_T]\{\dot{u}(t)\} - \{F_{damping}\} - \{F_{elastic}\} \qquad 4.28$$

If the damping matrix is consist, i.e. does not change with time, this equation may be simplified to give the following equation;

$$[\frac{4}{(\Delta t)^2}[M]+\frac{2}{\Delta t}[C_T]+[K_T]]\{\Delta u\}=...$$

$$\{P(t+\Delta t)\}+[M]\{\ddot{u}(t)+\frac{4}{\Delta t}\dot{u}(t)\}+\{F_{damping}\}-\{F_{elastic}\} \quad............ \quad 4.29$$

This equation can be solved for the incremental displacements. The displacement, velocity and acceleration vectors can be updated and the member forces at time t+Δt computed giving the elastic force vector and the damping force vector at the new time-step can also be updated. After updating the damping and stiffness matrices the above sequence is repeated for the next time-step.

As mentioned above, this integration scheme is unconditionally stable but that does not imply that it is unconditionally accurate. Error will be caused by modes that have too small a natural period of free vibration to be accurately integrated with the chosen time-step and yet have a significant contribution to the response. Error will also be caused in system where there are very large changes to the stiffness of the structure within the time-step, by using Newton-Raphson iteration within each time, or by a combination of these approaches. If there are noticeable differences in the response then this indicates that the time-step is not small enough and further investigation to find a time-step that is small enough to maintain accuracy needs to be made.

4.2.7 Small and large displacement

Small displacement analyses are appropriate for must dynamic analyses. In this case the members' stiffness are not affected by the deformations of the structure and the nodal coordinate remain unchanged during the analysis. In large displacement analyses the coordinate are updates at every time-step and the stiffness, allowing for changes in the axial forces in the beam or wall members and the changes in geometry in the members, are recomputed at every time-step. This procedure is computationally expensive, but it is important if the frame undergoing large displacements. An example would be when the interstory drifts are significantly greater than 1% of the story height or where the axial forces in frame members are large. The P-Δ option, where the displacements are assumed to be small and the coordinate are uncharged but the beam and column member stiffness are adjusted for the axial forces from the static analysis. This allows for the lateral softening of the columns due to the gravity loads. The P−Δ effect is assumed to be constant as the increase in stiffness on one side of the structure due to overturning moment is offset
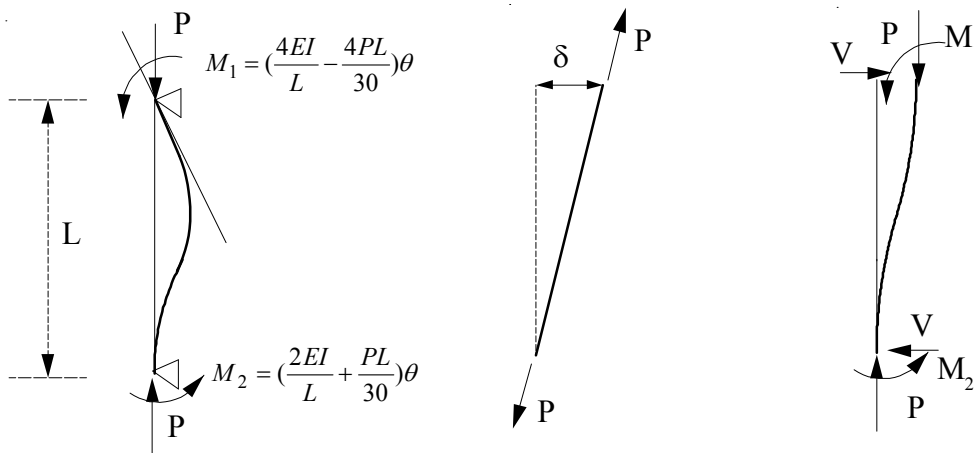
$$M_1 = (\frac{4EI}{L} - \frac{4PL}{30})\theta$$

$$M_2 = (\frac{2EI}{L} + \frac{PL}{30})\theta$$

Fig. 4.5 Geometric stiffness effects

by the decrease in stiffness on the other side of the structure. This approach has a minimal effect on the cost of the analysis. In the analysis of soft story frame, since the overturning moment considerably works, the large displacement analysis is selected.

The effect of the axial force on frame and wall member is shown **Fig. 4.5**. There are two components, the first is the softening of the flexural stiffness of the member and the second is the string stiffness reduction of the lateral stiffness of the member. The net effect is the same as substracting the geometric stiffness from the member stiffness but is computationally more efficient. The first part also accounts for the effects of the axial forces on the member moment-rotation properties.

4.3 Screening procedure according to JBDPA

In this study the seismic performance of an existing RC building by JBDPA (Japan Building Disaster Prevention Association) will be discussed. So, in this part, the method of evaluation will be briefly explained. In general, the seismic evaluation includes three procedures, namely, first, second and third levels of screening procedure. The standard uses three-level screening procedures. A simple screening procedure is intended to identify majority of earthquake resistance buildings by examining story shear strength provided by columns and structural walls. Those buildings,, identified by as questionable by the simple procedure, must be analyzed by more sophisticated second-level procedure considering deformation capacity of vertical members. The third level procedure is a general and detail procedure and requires the nonlinear static or dynamic analysis of the entire structure. In this study, the seismic evaluations are conducted only for second level screening procedure, and therefore this procedure is explained.

The second level screening procedure is to be applied if any building is found vulnerable or questionable by the first-level screening procedure. In this procedure again, the girder is assumed to be infinity stiff and strong. The ductility capacity of columns and walls is estimated crudely for their failure modes (shear or flexure) and on the basis of shear-flexural strength ratios. The combination of different ductility levels and shear resistance of vertical members were considered in estimating the earthquake resistance of a structure.

The shear resistance of vertical members (column and walls) must be calculated at the formation of flexural yielding at the member ends and at shear failure on the basis of the geometry, the amount of longitudinal and lateral reinforcement, and strength of concrete and reinforcement. Failure mode, either flexure or shear, is determined by comparing the shear strength and flexural strength, where the flexural strength is defined as shear force acting at the flexural yielding at member ends.

In general, the flexural strength of a structural wall becomes unrealistically high if the lateral resistance is evaluated for flexural yielding at the top and bottom of a story. Therefore, an inflection point of bending moment distribution can be assumed to locate at mid-height from the story concerned and the top of the wall. The flexural strength of a wall is calculated as a shear force acting at the flexural strength at the base of the story. The flexural strength of a column and a wall may be calculated for the axial force acting under the gravity load condition.

Vertical members are classified into one of the five groups depending on the failure mode; i. e.
(a) Flexural column (flexural strength lower than shear strength),
(b) Flexural wall (flexural strength lower than shear strength),
(c) Shear column (shear strength lower than flexural strength),
(d) Shear wall (shear strength lower than flexural strength), and
(e) Short column (shear column with clear height to depth ratio less than 2.0).
"Strength index" C_i of each group members is calculated by summing the story shear carried by the group divided by the total weight of the structure above the story. Value of "ductility index F" is assigned to each type of members as shown in **Table 4.1**.

Table 4.1 Ductility index for the second level screening procedure

Memeber type	Ductility index
Flexural columns	1.27-3.2
Flexural walls	1.0-2.0
Shear columns	1.0-1.27
Shear columns	1.0
Extremely short shear columns	0.8

"Ductility index F_{FC}" of flexural columns is estimated by the following expression, taken into consideration the story drift R_{mu} at flexural failure of columns:

$$F_{FC} = 1.0 + 0.27 \frac{R_{mu} - R_{250}}{R_y - R_{250}} \quad for \ R_{mu} < R_y \qquad \text{.............................} \quad 4.30$$

$$F_{FC} = \frac{\sqrt{2 \dfrac{R_{mu}}{R_y} - 1}}{0.75(1.0 + 0.05 \dfrac{R_{mu}}{R_y})} \quad but \ F_{FC} \leq 3.2 \ \ for \ R_{mu} \geq R_y \qquad \text{.........................} \quad 4.31$$

where, R_y: standard story drift angle at yielding (=1/150) and R_{250}=1/250. Stroy drift angle R_{mu}(inter-story deflection divided by story height) at the failure columns is estimated by the following

$$R_{mu} = \frac{h_o}{H_o} {}_c R_{my} \{1 + 1.0(\frac{{}_c V_{su}}{{}_c V_{mu}} - q)\} \qquad \text{.........................} \quad 4.32$$

$$_c R_{my} = \frac{1}{150} \qquad for \ \frac{h_o}{D} \geq 3.0 \qquad \text{.........................} \quad 4.33$$

$$_c R_{my} = \frac{1}{250} \qquad for \ \frac{h_o}{D} \leq 2.0 \qquad \text{.........................} \quad 4.33$$

where, $_c R_{my}$: member rotational angle of columns at flexural failure, $_c V_{su}$ and $_c V_{mu}$: shear strength and flexural strength of flexural columns, q=1.0 for columns with tie spacing less than 100 mm and 1.1 otherwise, h_o: clear height of a column, H_o: story height, and D: overall depth of a column. "Ductility index F_{FW}" of flexural walls is 1.0 when the flexural strength is equal to the shear strength, and is 2.0 (or 1.5 for walls without boundary columns) when the shear strength is more than 1.3 times the flexural strength; the value is linearly interpolated in-between.

"Ductility index F_{SC}" of shear columns is determinated by the following expression;

$$F_{FC} = 1.0 + 0.27 \frac{R_{su} - R_{250}}{R_y - R_{250}} \qquad \text{.........................} \quad 4.34$$

where, R_y: standard story drift angle at yielding (=1/150) and R_{250}=1/250. Story drift R_{su} at the failure shear columns is estimated by the following expression;

$$R_{su} = \frac{\dfrac{{_c}V_{su}}{{_c}V_{mu}} - 0.3}{0.7} R_{my} \quad but \geq R_{250} \quad if \quad {_c}V_{su} > {_c}\alpha \, {_c}V_{mu} \quad \dotfill \quad 4.35$$

$$R_{su} = R_{250} \quad \dotfill \quad 4.36$$

$$_c\alpha = 0.3 + 0.7 \frac{R_{250}}{R_{my}} \quad \dotfill \quad 4.37$$

$$R_{my} = \frac{h_o}{H_o} {_c}R_{my} \quad but \quad R_{my} \geq R_{250} \quad \dotfill \quad 4.38$$

where symbols are the same as in **Eqs 4.28~4.30**. The vertical members (columns and walls) are classified into three groups; each group is represented by the smallest ductility index of grouped member. Three groups are number from the smallest to the largest ductility indices (*F1*, *F2*, and *F3*), and corresponding strength indices *C1*, *C2*, and *C3* of the groups are evaluated. "Structural index E_{oi}" of story i is first calculated by **Eq. 4.36**.; any three groups of members can be selected to maximize the structural index;

$$E_{oi} = \frac{n+1}{n+i} \sqrt{E_{1i}^2 + E_{2i}^2 + E_{3i}^2} \quad \dotfill \quad 4.39$$

$$E_{1i} = C_1.F_1 \quad \dotfill \quad 4.40$$

$$E_{2i} = C_2.F_2$$

$$E_{3i} = C_3.F_3$$

The structural index E_{oi} is then evaluated at the failure of a group. The failing group is called group 1, and contribution of remaining member groups can be considered as

$$E_{oi} = \frac{n+1}{n+2}(C_1 + \sum_j \alpha_j C_j).F_1 \quad \dotfill \quad 4.41$$

where, α's are the ratio of story shear of each remaining group at the failure of group 1 members to the shear capacity of the group members.

4.4 An existing soft-first-story RC building

In order to verify the seismic performance of soft-first-story RC buildings, an existing soft-first-story RC building (See **Fig. 4.6**) is selected. The building is located in the Ryukyu Islands,
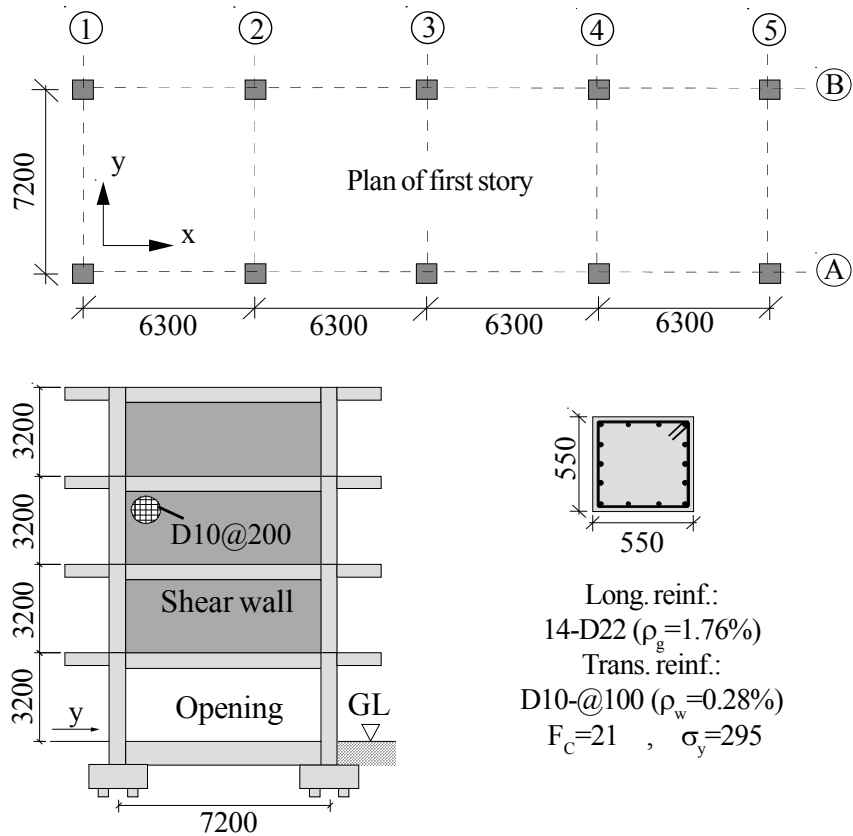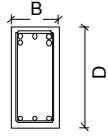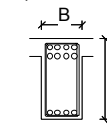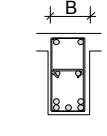
Fig. 4.6 An existing soft-first-story building
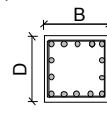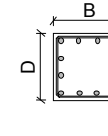
Fig. 4.7 Plan of first story and elevation of the building

Table 4.2 Details of the columns and beams

Details					
Level	footing (beam)	all stories (beam)	all stories (beam)	story 1, 2 (column)	story 3, 4 (column)
Position	all sections	end section	mid section	-	-
BxD	400x850	350x700	370x700	550x550	500x500
Rebar	8-D22	12-D22	9-D22	14-D22	12-D22
Hoop	D10-@150	D13-@100	D13-@100	D10-@100	D10-@100
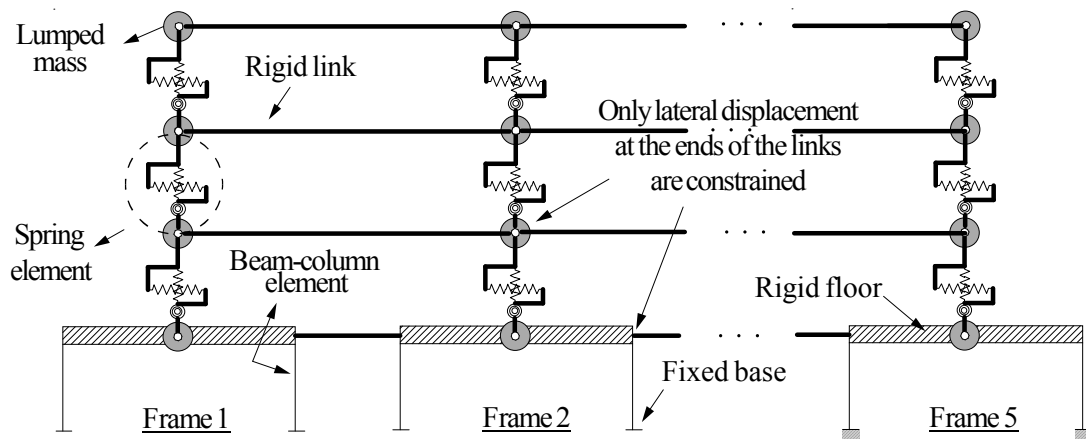
Fig. 4.8 Two-dimension model of building

Okinawa, Japan, where soft-first-story buildings are commonly built. The building was designed according the Building Standard Law of Japan revised in 1981, but, the irregularity of the lateral stiffness in the height of the building was not properly taken into consideration by the building designer. The building has four stories with one bay by four bays plan. In y-direction, the lateral resisting systems of the building include columns in the first story and framed shear walls in the upper stories. Since in y-direction, there is significant difference between the lateral strength and stiffness of the first story and second story, this direction was selected to analyze and assess. As shown in **Fig. 4.7** and **Table 4.2** , the columns have dimensions of 500X500mm. The ratio of longitudinal and transverse reinforcement ρ_g=1.76% and ρ_w=0.28%.

To obtain the exact behavior of the building due to moderate to strong earthquake excitations, nonlinear dynamic analyses of the building were implemented in RUAUMOKO-2D com-

puter program. Since the lateral stiffness distribution in the plan of building is symmetric, the rotation will not produce at the floors, so for simplicity the building was modeled as five two-dimension (2-D) frames that were laid in series and connected to each other with rigid links at the story level (see **Fig. 4.8**). Mass of each floor lumped at its story level. In simulating the building, the first story columns were modeled by beam-column elements considering their moment-axial force interaction. The moment-curvature of the beam-column elements were defined by modified Takeda hysteretic rule with the standard parameters of α=0.4 and β=0.0 (see **Fig. 4.3**). The framed shear walls of the upper stories were modeled by the spring elements consist of vertical, horizontal and rotational components. The horizontal spring was assigned by trilinear Origin-centered hysteresis model. The bases of the columns were considered to be fixed and, hence, the flexibility of foundation beam and the rotation of foundation were not taken into account.

4.5 Level of input earthquakes

As observed in the 1995 Kobe earthquake, buildings experienced a ground motion that its intensity was higher than the value considered for design level at life safety limit state. The same phenomenon was reported for the 2007 Niigata-ken Chuetsu-oki earthquake[19]. During this earthquake, in Kariwa village, the nuclear facilities suffered damage due to strong motion with peak ground acceleration (PGA) of 6.8 m/s² which was higher than two times of the designed value of 2.7 m/s² [50].

Three well-known ground motions, namely the 1940 El Centro (NS), the 1995 Kobe (NS) and the 1952 Taft (NS), were used to analyze the building. According to Standard for Structural Design of Buildings [51], the aforementioned earthquakes excitations were scaled to 35 cm/sec (50 cm/sec x Z, where Z is the seismic zone factor) for design basis earthquakes at life safety limit state considered in Building Standard Law of Japan. Furthermore, to exhibit the collapse prevention performance of the proposed method (application of thick hybrid wall), the retrofitted building were analyzed under an extreme level of seismic intensity of 70 cm/sec (100 cm/sec x Z) [52]

Table 4.3 Characteristics of ground motions

Earthquake	Date	Station	Component	M	PGA (g)	PGV (cm/s)
Imperial Valley	1940	El Centro	180° (NS)	7.0	0.318	29.8
Kern County	1952	Taft	021°	7.4	0.156	15.3
Kobe	1995	KJMA	000° (SN)	6.9	0.821	81.3

obtained on the base of recorded strong earthquake excitations. In this paper, for simplicity in expressing the level of input motions, the first and second levels of earthquake excitation are called design basis earthquake (DBE) and maximum capable earthquake (MCE), respectively. It should be noted that the maximum capable earthquake (MCE) has not established in the Building Standard Law of Japan. The MCE level earthquake was only used as a case study to verify the collapse prevention performance of the building retrofitted by the thick hybrid technique during extremely strong excitation.

4.6 Seismic evaluation of the building before retrofitting

Before conducting dynamic response analysis, modal analysis is carried out on the building to observe the distribution of lateral strength and also the contribution of effective modes. As shown in **Fig. 4.9**, the lateral displacement of the building is concentrated at its first story. It is expected the dynamic response analyses have a lateral displacement such that observed in the fundamental mode. The effective modal mass of the first story is about $M^*=100\%$.
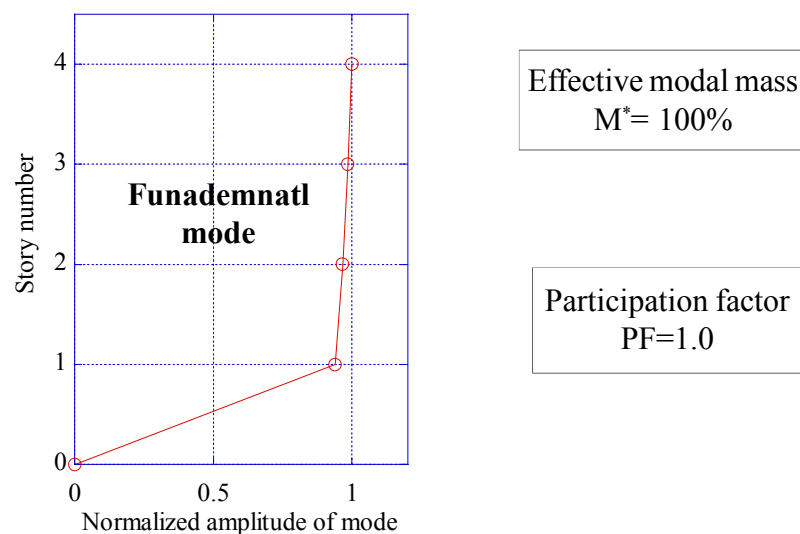

Fig. 4.9 Fundamental mode of the soft-first-story building

After analyzing the building due to three aforementioned earthquakes scaled to DBE level, it was observed that after formation of plastic hinges at the ends of the first story columns, the first story tended to have a large sway mechanism. According to AIJ design guideline, increasing the inelastic hinge rotation of the columns reduces the shear strength of the hinged regions, and, hence, led to shear failure of columns at drift angle of $R=1.7\%$ (see **Fig. 4.10**). As it appears in **Fig. 4.10**, the column of first story due to three aforementioned earthquakes scaled to 35kine
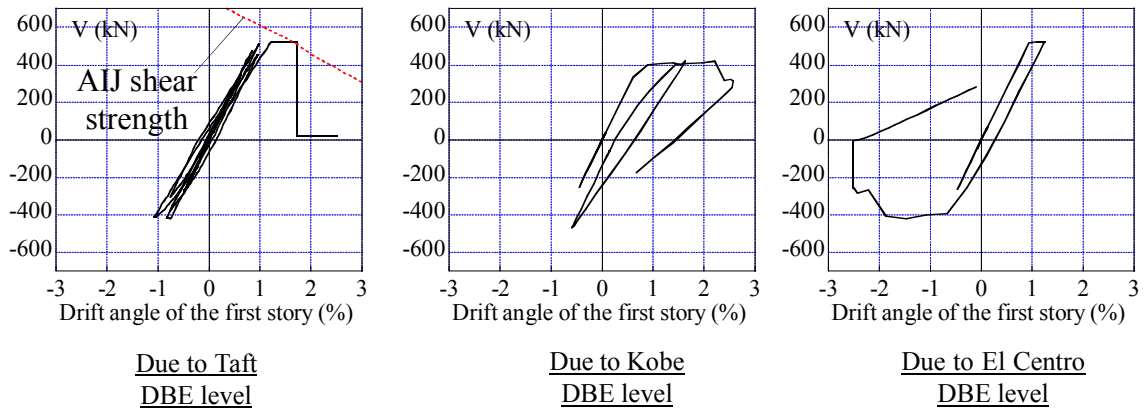
Due to Taft
DBE level

Due to Kobe
DBE level

Due to El Centro
DBE level

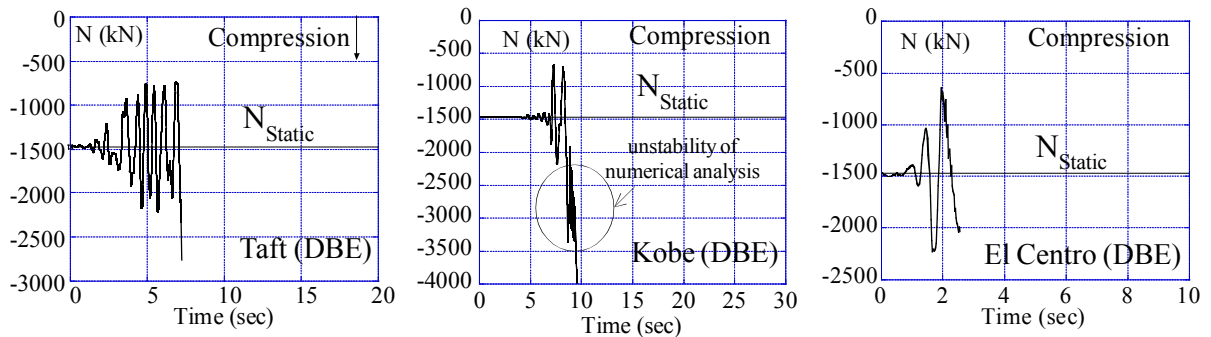**Fig. 4.10 Shear force- drift angle of first story of column B-1 (see Fig. 4.7)**

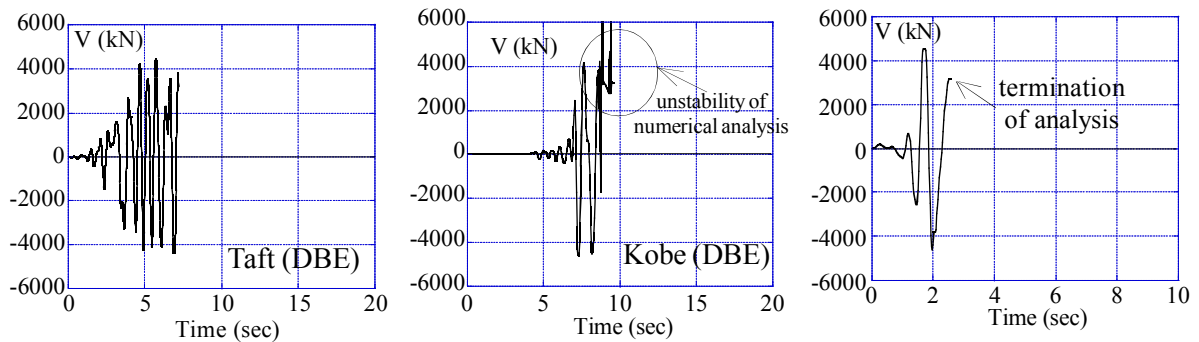**Fig. 4.11 Variation of axial force of column B-1 before retrofit (see Fig. 4.7)**

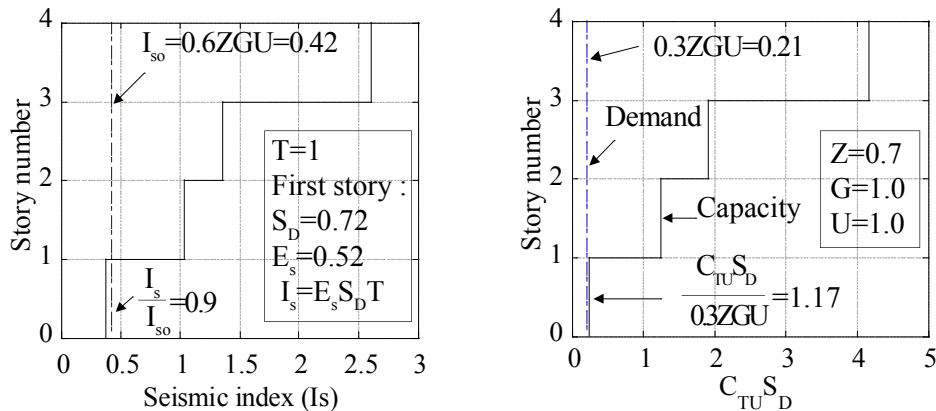**Fig. 4.12 Base shear response of the building before retrofit**

Fig. 4.13 Vulnerability assessment of the building before retrofit

(DBE) level, initially flexural behavior is observed, but by increasing the drift angle, finally the columns failed in shear. The variations of axial force of one of the columns (B-1, see **Fig. 4.6**) are shown in **Fig. 4.11**. It is obvious that the axial forces change during earthquake, but they do not enter in net tension. The base shear response of the building shows relatively low value of lateral strength that it can be later compared with the lateral strength after retrofitting.

Also, the seismic vulnerability assessment of the building was verified through the second level screening procedure provided by the Japan Building Disaster Prevention Association. As shown in **Fig. 4.13**, seismic index of the first story I_S is slightly less than demand value I_{SO}. The multiplied value of cumulative strength index C_{TU} by irregularity index S_D was calculated for each story, and they were found larger than required values. Here, it should be focused attention on the key parameters I_{SO} and $C_{TU}S_D$ derived from seismic vulnerability assessment of the building which did not satisfy the demand values (see **Fig. 4.13**), while the exact evaluation through nonlinear dynamic analyses confirmed the vulnerability of the building due to design basis earthquakes at life safety limit state (see **Fig. 4.10**). During dynamic analyses the shear forces of shear walls of the upper stories were checked, and the shear walls remained in the elastic domain observed, but by increasing the drift angle, finally the columns failed in shear. The variations of axial force of one of the columns (B-1, see **Fig. 4.7**) are shown in **Fig. 4.11**. It is obvious that the axial forces change during earthquake, but they do not enter in net tension. The base shear response of the building shows relatively low value of lateral strength that it can be later compared with the lateral strength after retrofitting.

4.7 Seismic evaluation of the building retrofitted by conventional method

Installation of reinforced shear wall inside soft-story frames is one of the conventional methods to increase the lateral strength and stiffness of the frames. In the first retrofitting strategy, it was decided to strengthen the existing soft-first-story building by conventional method (installation of shear wall). The details of the retrofitted building and its modeling are shown in **Figs. 4.14, 4.15 & 4.16**. The building was first assumed to be retrofitted by shear walls installed at the exterior frames (strategy A1). Two-dimension model of the retrofitted frames and their details are illustrated in **Figs. 4.15, 4.16**, respectively. The building was modeled as five two-dimension frames that were laid in series and connected to each other with rigid links at each story level. The seismic vulnerability assessment of the building after retrofitting by the conventional method was conducted based on the JBDPA guideline. As shown in **Fig. 4.17**, it was obtained that the cumulative strength index C_{TU} of the first story after retrofitting by strategy A1 increased significantly,

but due to low ductility index F of the installed shear wall, the seismic index I_S of the first story did not increase as well. In view point of seismic vulnerability assessment, the selected retrofit strategy satisfied the required seismic index $I_S/I_{SO}=1.2$ and cumulative strength index $C_{TU}S_D/(0.3ZGU)=2.4$ for the first story.

In another retrofitting strategy, strategy A2, to provide the notably safe margin for seismic index of the first story, it was supposed that, in addition to exterior frames, the middle frame was retrofitted by the reinforced shear wall. After retrofitting the first story by strategy A2, the ratio of seismic index and cumulative strength index of the first story reached to $I_S/I_{SO}=1.7$ and $C_{TU}S_D/(0.3ZGU)=3.4$, respectively.
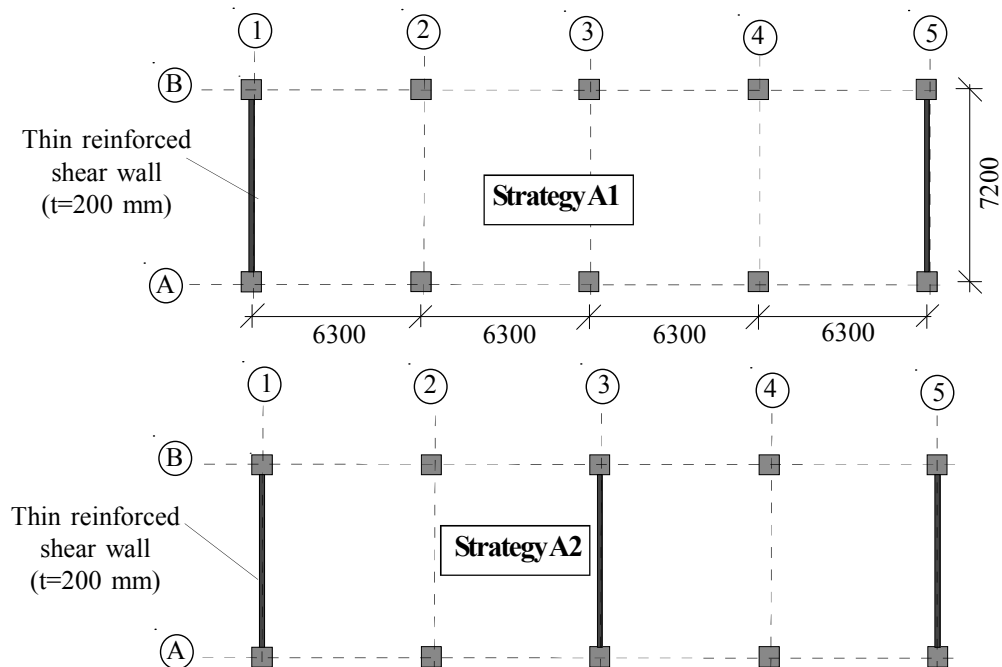
Fig. 4.14 Plan of retrofitting by strategies A1 and A2

Even though the seismic vulnerability assessment of the building retrofitted by shear walls exhibited a successful performance, its seismic evaluation was conducted through nonlinear dynamic analysis to find out the behavior of the building during earthquake excitations. In modeling the retrofitted building, the hysteretic behavior of the shear walls were defined by Origin-centered hysteresis considering cracking shear strength and ultimate shear strength (see **Fig. 4.16**). The initial elastic shear stiffness and cracking shear strength of the shear walls were calculated based on the suggested values by Kabeyasawa et al. [53] for hysteretic modeling of shear walls.
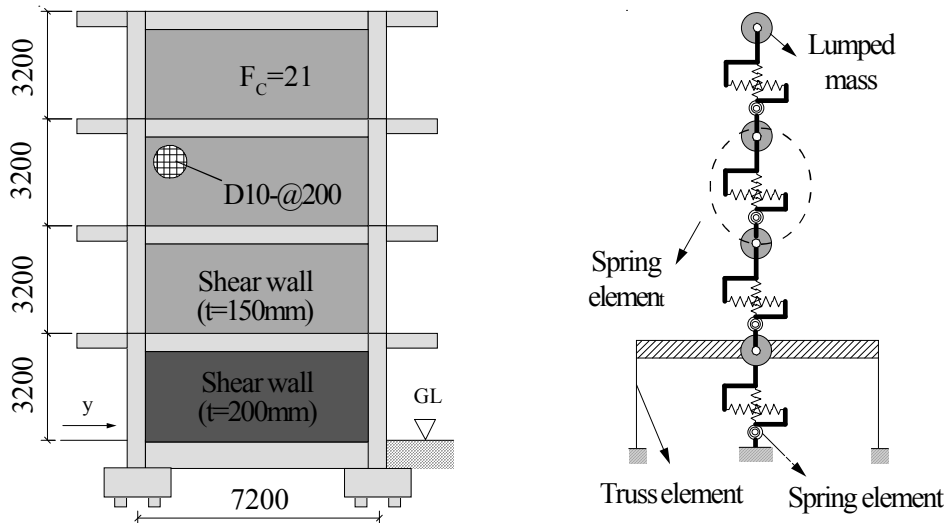
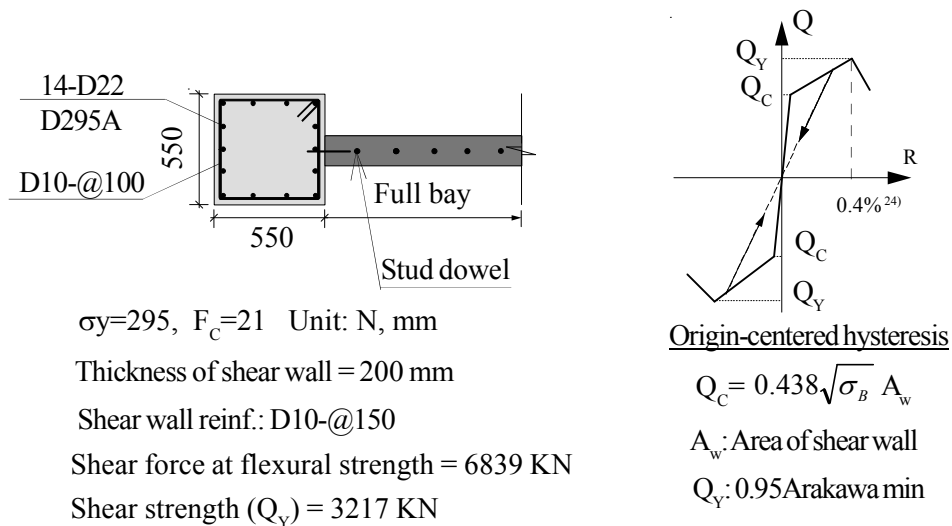**Fig. 4.15 Elevation and model of retrofitted frames by conventional method**

$\sigma y = 295$, $F_C = 21$ Unit: N, mm

Thickness of shear wall = 200 mm

Shear wall reinf.: D10-@150

Shear force at flexural strength = 6839 KN

Shear strength (Q_Y) = 3217 KN

Origin-centered hysteresis

$Q_C = 0.438\sqrt{\sigma_B}\ A_w$

A_w: Area of shear wall

Q_Y: 0.95 Arakawa min

Fig. 4.16 Installed shear wall and its hysteresis model (strategy A1 & A2)
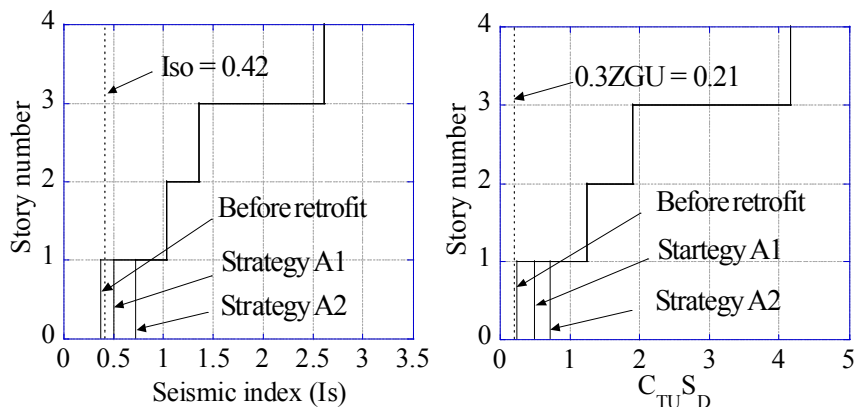
Fig. 4.17 Vulnerability assessment of the retrofitted building
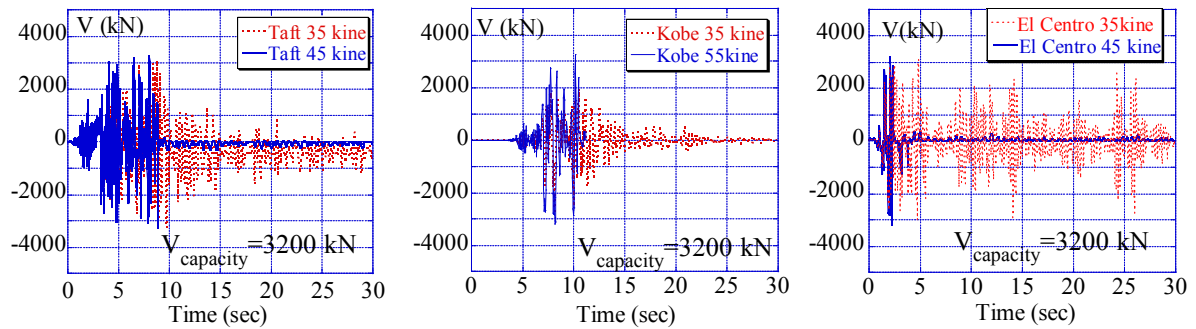
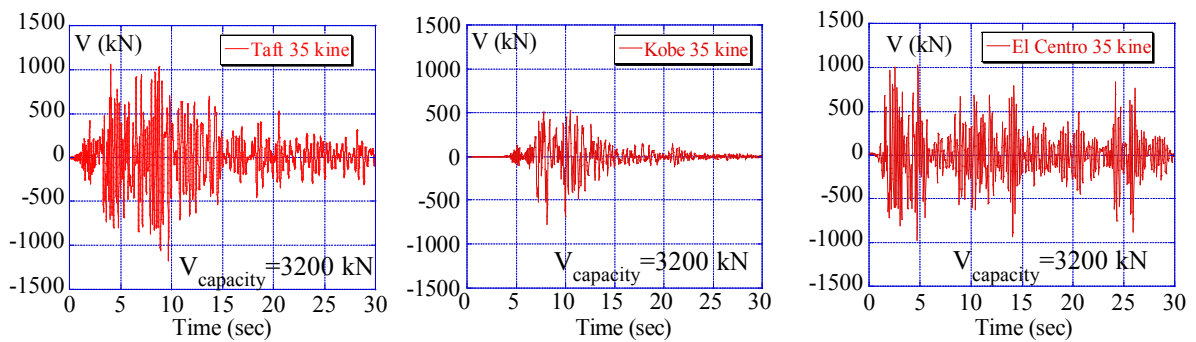**Fig. 4.18 Shear force response of installed shear wall in strategy A1**

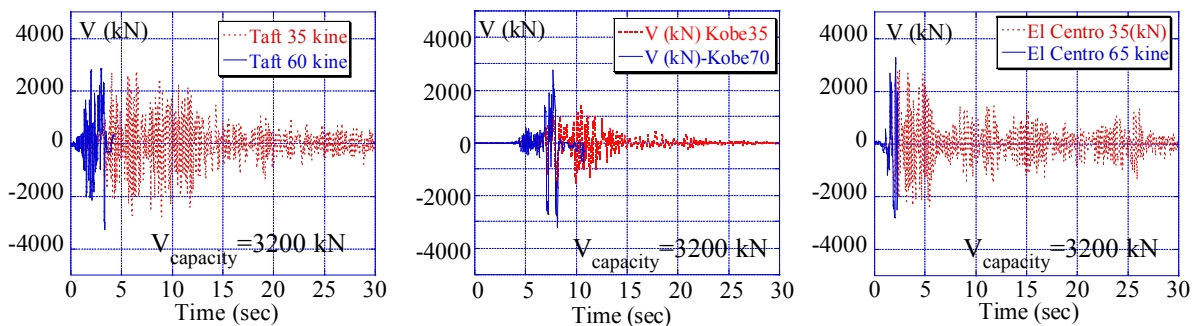**Fig. 4.19 Shear force response of shear wall at second story in strategy A1**

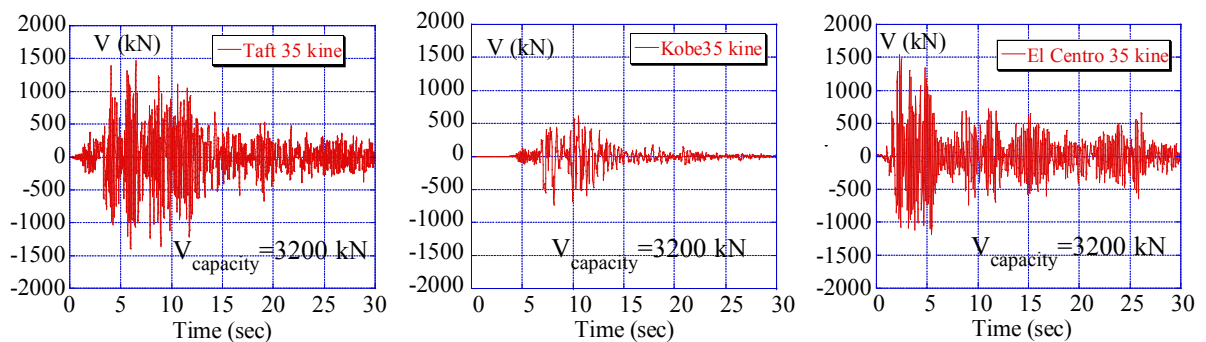**Fig. 4.20 Shear force response of installed shear wall in strategy A2**

Fig. 4.21 Shear force response of shear wall at second story in strategy A2
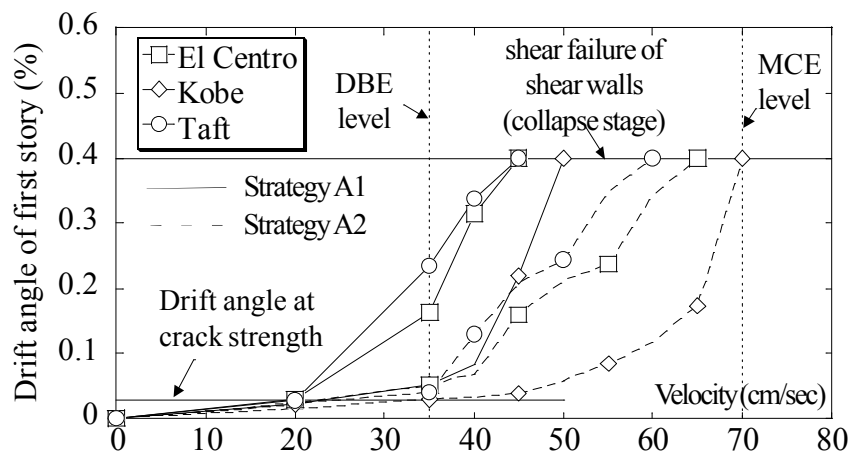
Fig. 4.22 Incremental dynamic analysis of the retrofitted building

According to vast investigation on shear walls by Tomii et al. [54], it was assumed that shear walls fail in shear at drift angle of $R=0.4\%$.

Nonlinear dynamic analyses were conducted for three aforementioned earthquakes, when the earthquake excitations scaled to 35 kine, the installed shear wall can suffered the induced shear forces. But there is not significant safe margin between design bases earthquakes and the intensities at which the shear failed (see **Figs. 4.18, 4.20**). The shear forces at the shear wall in the second story were checked during nonlinear analyses, but the induced shear forces did not exceed their capacities (see **Fig. 4.19 & 4.21**).

As shown in **Fig. 4.22**, in order to obtain the collapse stage of the building retrofitted by conventional method, incremental dynamic analyses were conducted due to three aforementioned earthquakes. Incremental dynamic analyses were implemented by using a series of nonlinear dynamic analyses under a multiply scaled suite of ground motion records to observe the ground intensity at which the shear walls fail, and, therefore, the building collapses. In **Fig. 4.22**, the responses of the building retrofitted by two shear walls (strategy A1) show that the building exhibit a rational performance for earthquake excitations scaled to DBE level (35 cm/s), but, by increasing the intensity of the ground motions, the building collapse due to shear failure of shear walls at ground motion intensities which are somewhat higher than considered DBE level (35 cm/s). In case of three installed shear walls (strategy A2), the lateral strength and stiffness of the first story considerably increase, and, for this reason, the incremental dynamic analysis shows the collapse of the first story occurred at the ground intensity that is markedly higher than the DBE level.

4.8 Seismic evaluation of the building retrofitted by proposed methods

In order to obtain a reasonable performance under strong earthquake excitation, the building was supposed to be retrofitted by proposed retrofitting strategies. As shown in **Fig. 4.23**, three retrofitting strategies B1, B2 and B3 were proposed for the vulnerable soft-first-story building. In strategy B1, all the columns of the first story were retrofitted by thick hybrid wing-walls to increase the lateral strength and stiffness as well as ductility. In strategy B2, the columns of frames 1, 3 and 5 were retrofitted by thick hybrid wing-walls to enhance the strength, stiffness and ductility, and the columns of frames 2 and 4 were retrofitted by PC bars to prevent the possible shear failure at large drift angle during strong earthquake excitations. In strategy B3, only two exterior frames 1 and 5 were retrofitted by thick hybrid panel-wall to provide sufficient lateral strength and stiffness.

As shown in **Fig. 4.24**, in modeling the building, the columns retrofitted by wing-walls were defined by the spring element contains vertical and horizontal components. The details of modeling were same as those used in calibration of specimen R03WO-S in Section 3.3. The columns retrofitted by PC bar prestressing (see **Fig. 4.26**) were assigned by beam-column element considering the moment-axial force interaction. The hysteretic behavior was defined based on the calibration explained in Section 3.5. In case of frame retrofitted by thick hybrid panel-wall, as discussed in Section 3.4, since the body of the retrofitted frame behaves as a rigid member, it can be modeled by a rigid element with a concentrated plastic hinge at the panel wall base to represent the concentrated deformations at this zone. In case of real building, same procedure was followed for modeling the frame retrofitted by panel-wall (see **Fig. 4.27**). The columns retrofitted by PC bars were model by beam-column elements assigned by Takeda hysteresis rule. Their details are same as those explained in Section 3.5. As shown in **Table 4.3**, the lateral strengths of retrofitted columns are calculated based on the formulations by Yamakawa et al. [9] and Rahman et al. [12] for application of thick hybrid wall and by Shinjo et al. [38] for utilizing PC bar prestressing.

In wing-wall type thick hybrid wall technique, the depth of the wing wall βD (see **Fig. 4.25**) can readily be designed to provide the required lateral strength and stiffness. The shear strength and flexural strength of the columns retrofitted by thick hybrid walls were calculated based on the formulations proposed by Yamakawa et al. [9]. To find out the dynamic responses of the building retrofitted by the wing-wall type method, analyses were performed due to three earthquake excitations, namely, El Centro (NS), Kobe (NS) and Taft (NS) scaled to both design basis earthquake (DBE) and maximum capable earthquake (MCE) as described in **Section 4.4**. In **Fig. 4.29**, the

maximum drift angle responses of the building retrofitted by strategies B1 and B2 due to three aforementioned earthquakes were obtained for different wing-wall depth ratio β. The maximum value computed from analyses due to three earthquakes was the basis of selecting the desired depth of the wing-wall. In strategy B1, the appropriate value of wing-wall depth ratio was obtained as β=1.5 that can provide reasonable performance for both DBE and MCE levels.

The desired performance assumed in this study is that the drift angle of the first story does not exceed one percent for DBE level, and the first story does not collapse for MCE level. As shown in **Fig. 4.29**, in case of strategy B2, the wing-wall depth ratio of β=2.0 provides a safe margin between the design basis earthquake and maximum capable earthquake. The results of nonlinear dynamic analysis of the existing building in **Section 4.5** showed that the columns of the non-retrofitted building failed in shear at drift angle of R=1.7% (see **Fig. 4.10**). By referring to experimental investigations of one-bay two-story test specimens in **Fig. 2.12**, it can be recognized that the non-retrofitted specimen R07P-P0 failed in shear at drift angle of R=1.64% (almost same as that happened for the existing building before retrofitting), but after installation of thick hybrid wing-wall for specimen R06P-WW, the brittle shear failure of the columns were prevented, and a ductile response was obtained up to drift angle of R=5.0%.

According to experimentally observed mechanisms, by applying thick hybrid wall technique shear failure of the columns of the existing building will be prevented and the building can maintain its stability under large lateral displacements. In **Fig. 4.29**, in case of strategy B2, the response of the building during extremely strong earthquakes (MCE level) exceed the drift angle at which it is expected ordinary columns fail in shear. Considering this behavior, utilizing PC bars for the columns which are not retrofitted by thick hybrid wall can guarantee the columns against possible shear failure at large drift angle. In case of strategy B3, the retrofitted building exhibit small relative displacement due to three earthquakes for both MCE and DBE levels. As an example, time history response of the retrofitted first story due to Taft earthquake is shown in **Fig. 4.30**. The induced lateral deformations are within the rational range. So, according to nonlinear dynamic response analyses, it can be concluded that retrofitting strategies B1, B2 and B3 satisfy the considered target performance including life safety for design basis earthquakes and collapse prevention for maximum capable earthquakes. It should be emphasized that the lengths of additional wing-walls (βD) are the values (β=1.5 and β=2.0) which were previously investigated through the experimental studies·

In **Fig. 4.31**, the global seismic assessment of the building was calculated for three retrofitting strategies based on the second level screening procedure of JBDPA. The results represent

the considerable improvements on the seismic index and cumulative strength index after installation of thick hybrid walls. According to this evaluation, significant improvements in the seismic performance of the retrofitted building are evident.

In **Figs. 4.32** & **4.33**, the global dynamic responses of the building retrofitted by thick hybrid wing-walls show that even though the concentrated displacement appeared in the first story, the obtained drift angle responses of the first story for both DBE level and, especially, for MCE level are within the rational range considering the capacities of the applied retrofitting systems. As shown in **Fig. 4.34**, the global responses of the building retrofitted by thick hybrid panel-wall exhibit cantilever-shape displacement due to the flexural rotation at the base of the panel-wall and boundary columns. In this type retrofit, the most part of the lateral displacement response was generated by the flexural rotation at the base of the panel-wall, and, hence, the relative displacements between the stories were small. The obtained results for both thick hybrid wing-wall and thick hybrid panel-wall demonstrated a reasonable performance, especially under strong ground motions. In comparing the proposed retrofit strategy and conventional method, it is clear that application of conventional method (in case of strategy A2) causes more architectural limitations in comparison with the proposed retrofitting strategies B1, B2 and B3. It should be noted there is hesitancy to employ conventional wall with a width equal to that of column, because delivering high shear force from floor beam to the wall through a localized connection is a challenging problem, but in the proposed method this concern is perfectly solved by anchoring the steel plates to the floor beam. In modeling the column retrofitted by wing-wall, the influence of the axial force on lateral strength was taken into account. **Fig. 4.35(a)** shows the variation of the lateral force of column B-1 due to the change of the axial force. As illustrated in **Fig. 4.35(b)**, the variation of the axial force resulted in changing of the lateral strength of the columns and, hence, fluctuation of the global lateral strength of the first story appeared in the response. The lateral strength of the first story after utilizing the proposed strategies (strategies B1, B2 and B3) significantly increase (see **Figs. 4.35(b), 4.36**), and the shear force-lateral displacement exhibit stable response during strong earthquake excitation (MCE level). The shear force induced in the first story in three retrofitting strategies due to three aforementioned earthquakes for both DBE and MCE levels were checked and they were obtained smaller than their shear strengths.

In retrofit design procedure, the shear strength of thick hybrid walls were calculated based on the formulation by Yamakawa et al. [9] and Rahman et al. [12]. In general the shear strength of the column retrofitted by thick hybrid wall is higher than its flexural strength. As an example the shear force response of the thick hybrid panel wall is illustrated in **Fig. 4.37**, the shear strength of the panel wall is markedly higher than its shear force at flexural strength.

As previously explained, it was assumed that the bases of the columns were fixed, and hence the uplift of the foundation was not taken into account. Since in the design procedure, the uplift of the foundation can be critical, the axial force variation of a column (column B-1) was monitored under earthquake excitations. As shown in **Fig. 4.38**, the compressive axial force of the column B-1 retrofitted by wing-wall, in case of strategies B1 and B2, decrease moderately under the DBE level earthquake, but due to MCE level earthquake it enters to net tension instantly. Although the columns experienced net tension for instant during extremely strong earthquake excitation (MCE level), this instant uplift could not cause instability in the building. In strategy B3, the variation of axial force of the boundary columns of the frames retrofitted with panel-wall
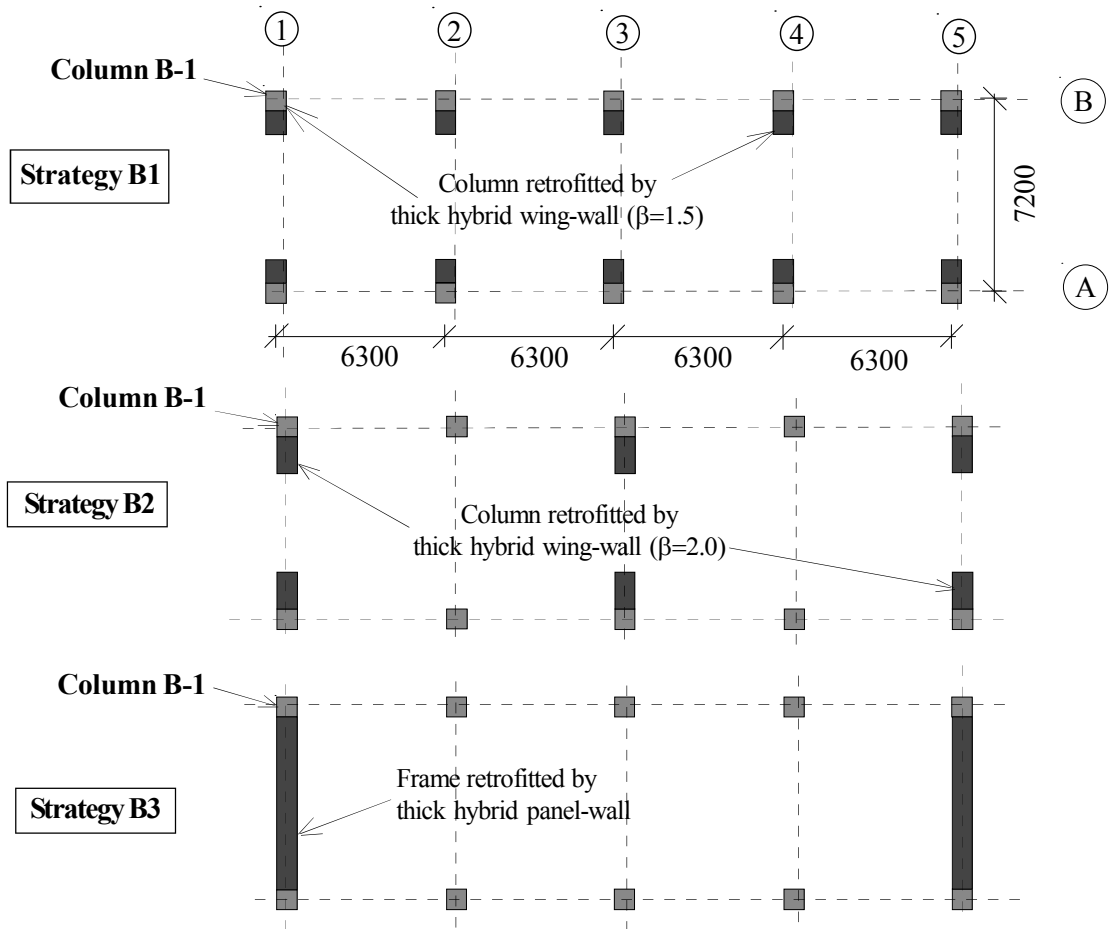
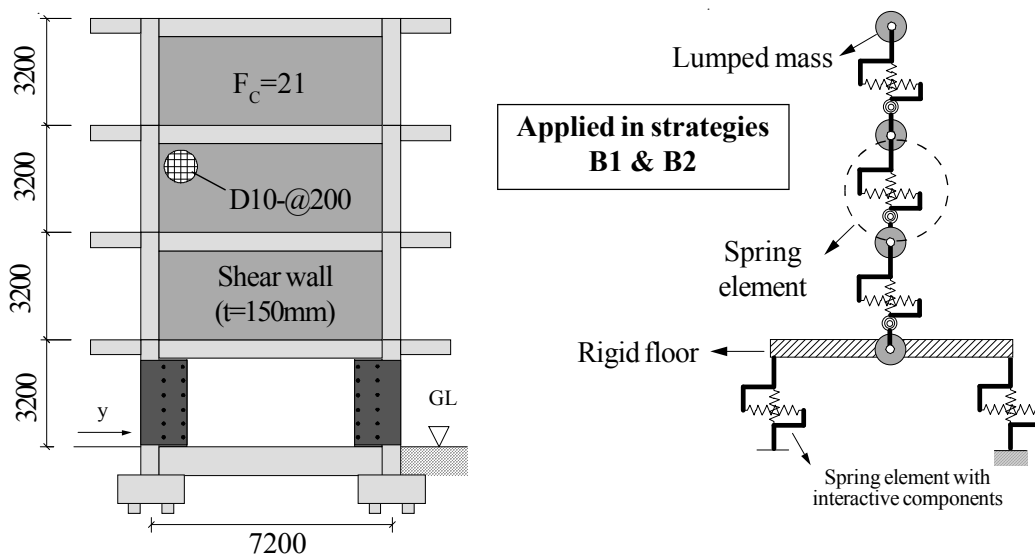**Fig. 4.23 Plans of first story after retrofitting by strategies B1, B2, B3**

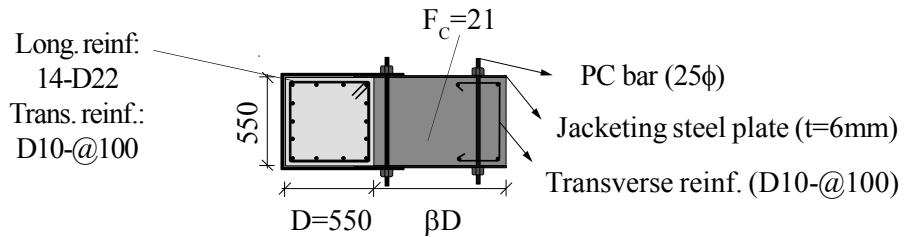**Fig. 4.24 Elevation and model of frame retrofitted by thick hybrid wing-wall (unit: mm)**

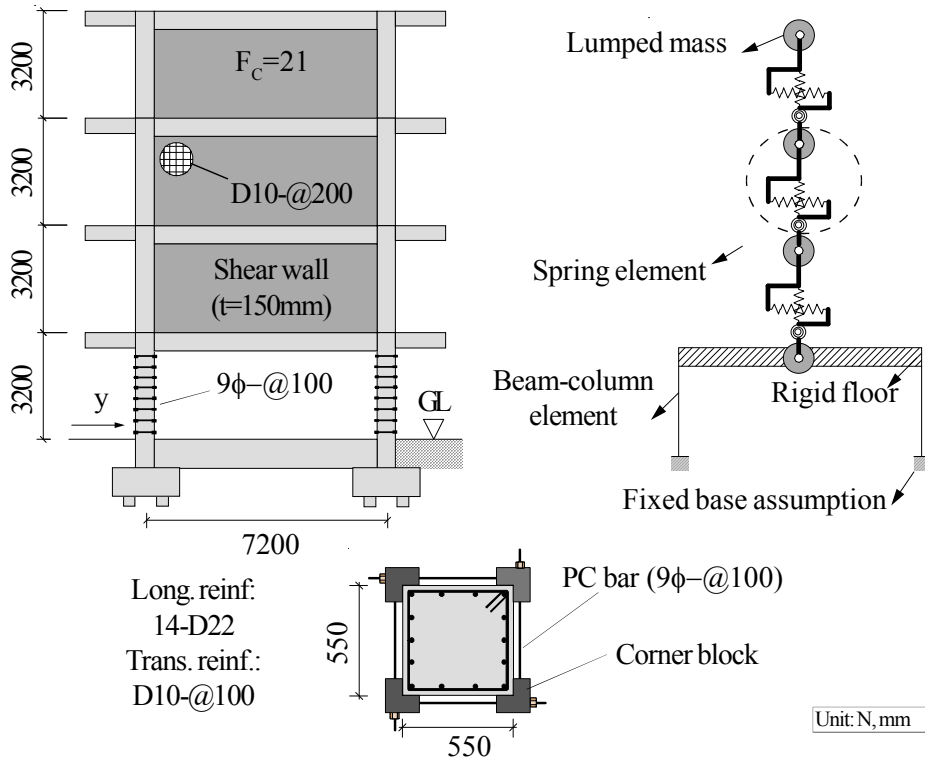**Fig. 4.25 Details of column retrofitted by thick hybrid wing-wall**

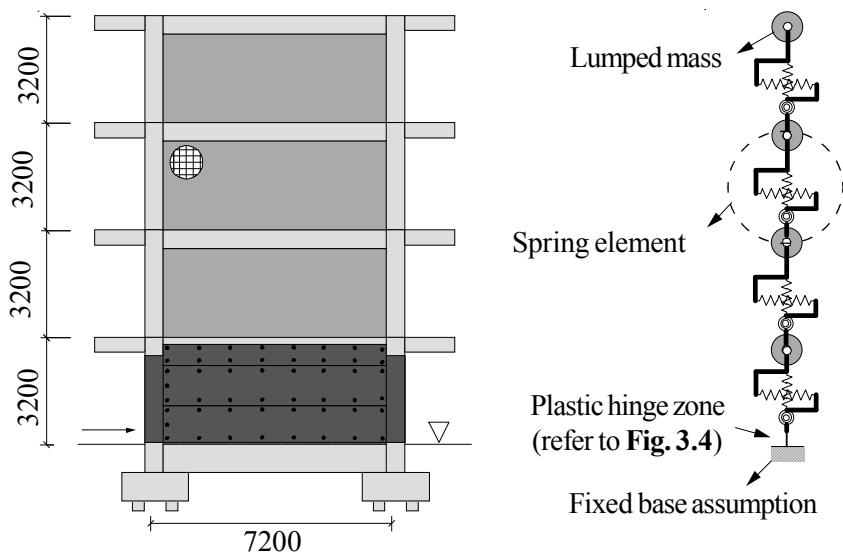**Fig. 4.26 Elevation and model of frame retrofitted by PC bars**

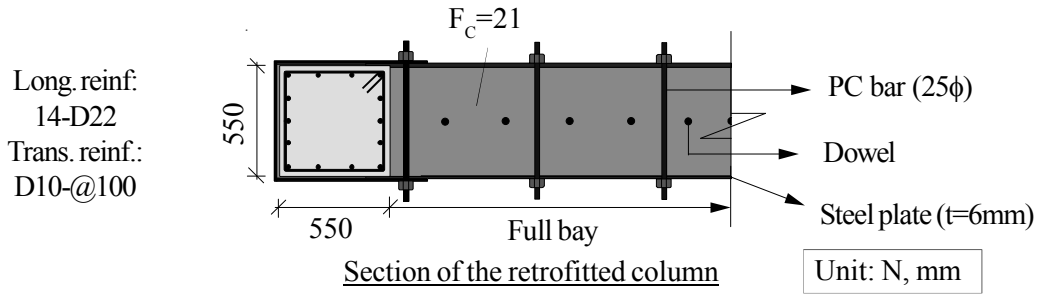**Fig. 4.27 Elevation and model of frame retrofitted by thick hybrid wing-wall (unit: mm)**

-81-

Fig. 4.28 Column retrofitted with thick hybrid panel wall

Table 4.4 Lateral strengths of the retrofitted columns (unit: kN)

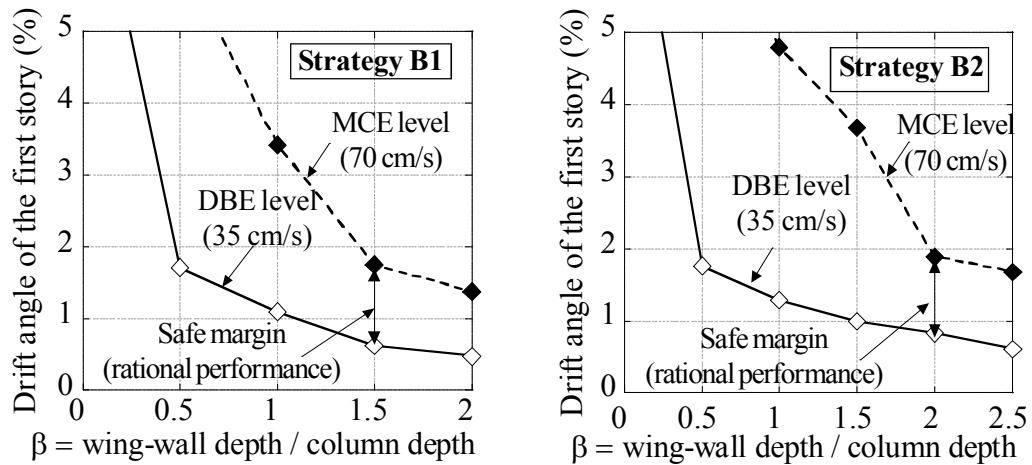| Retrofitted by	Wing-wall (β=1.5) (Strategy B1)	Wing-wall (β=2.0) (Strategy B2)	Panel-wall (Strategy B3)	PC bars (Strategy B2)
Shear force at flexural strength	1376	1708	6985	506
Shear strength	1568	1882	24033	1119

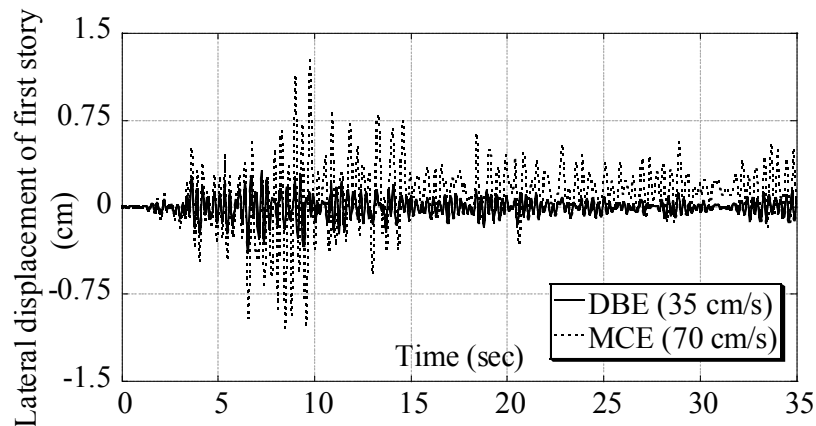**Fig. 4.29 Maximum response of first story due to El Centro, Kobe and Taft**

Fig. 4.30 Maximum response of first story obtained due to Taft earthquake
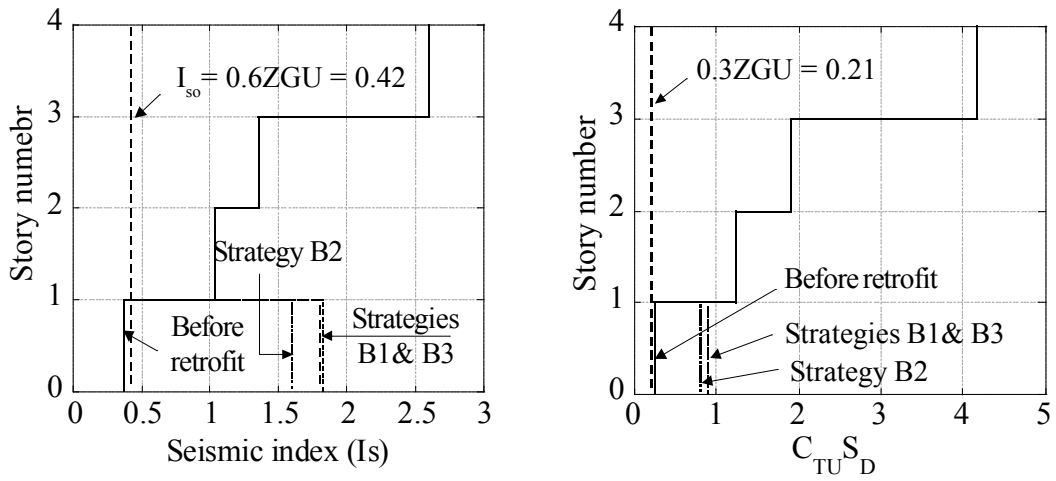
Fig. 4.31 Seismic vulnerability assessment of the proposed strategies

Fig. 4.32 Responses of the stories after retrofitting by the strategy B1
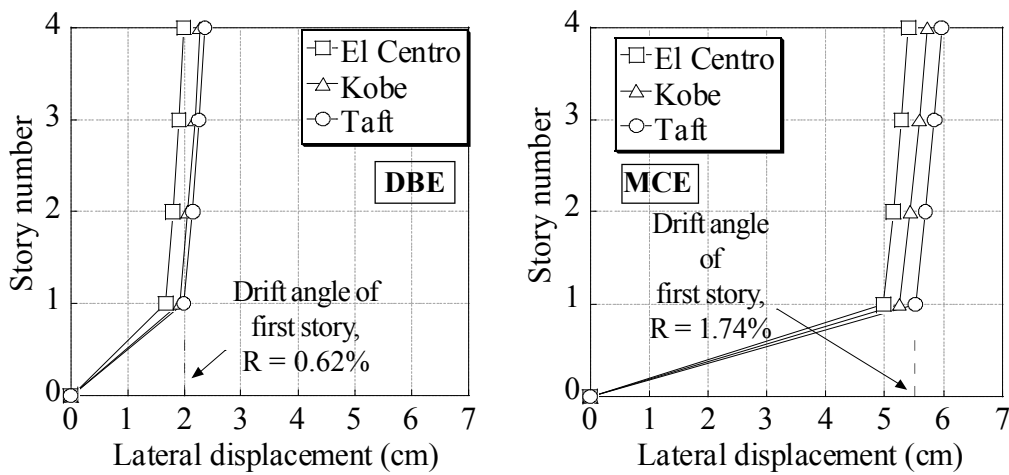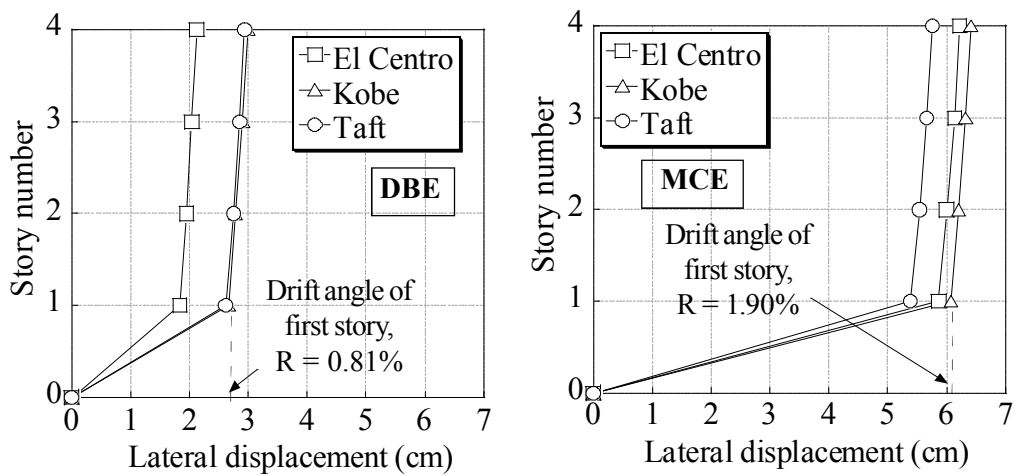

Fig. 4.33 Responses of the stories after retrofitting by the strategy B2

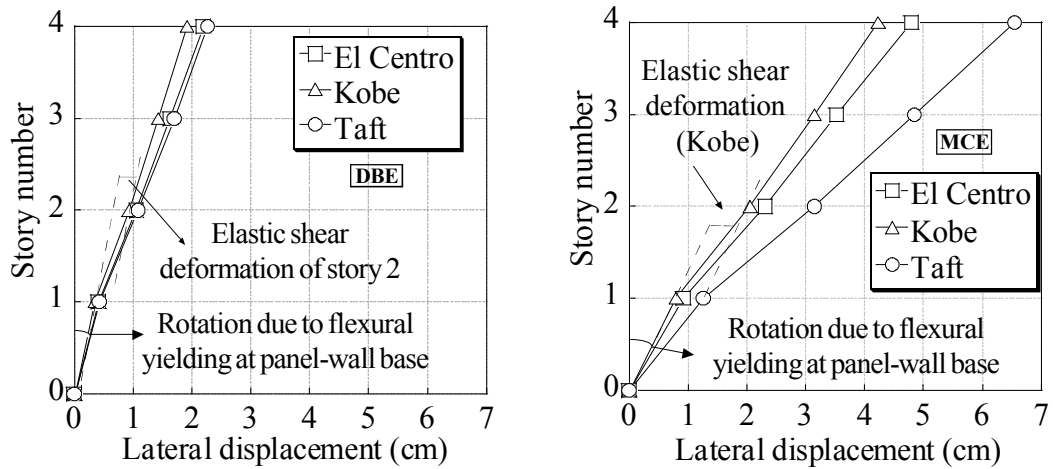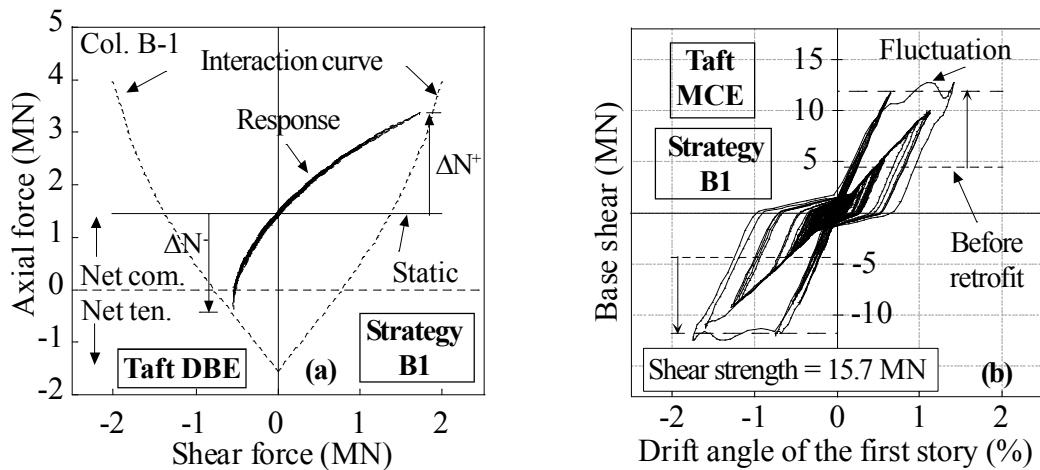**Fig. 4.34 Responses of the stories after retrofitting by the strategy B3**

Fig. 4.35 (a) Axial force-shear force response of the column B-1 (Fig. 18)
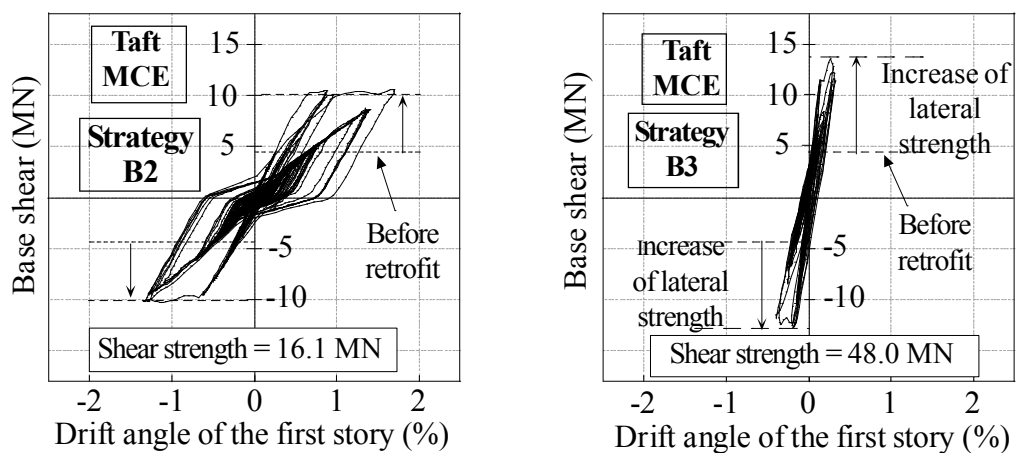**(b) Base shear versus drift angle of first story due to Taft**

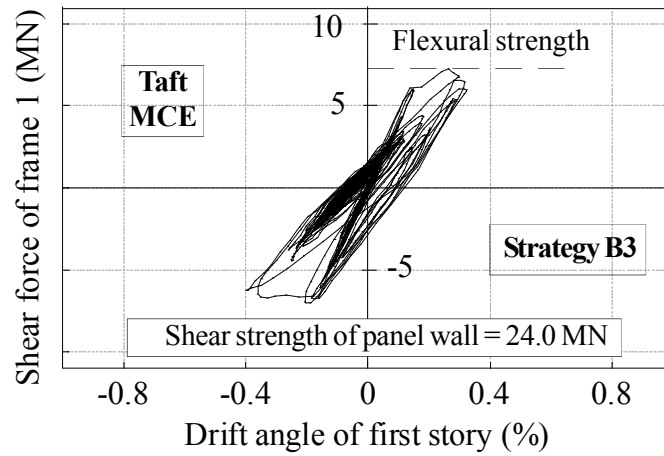**Fig. 4.36 Base shear versus drift angle of first story**

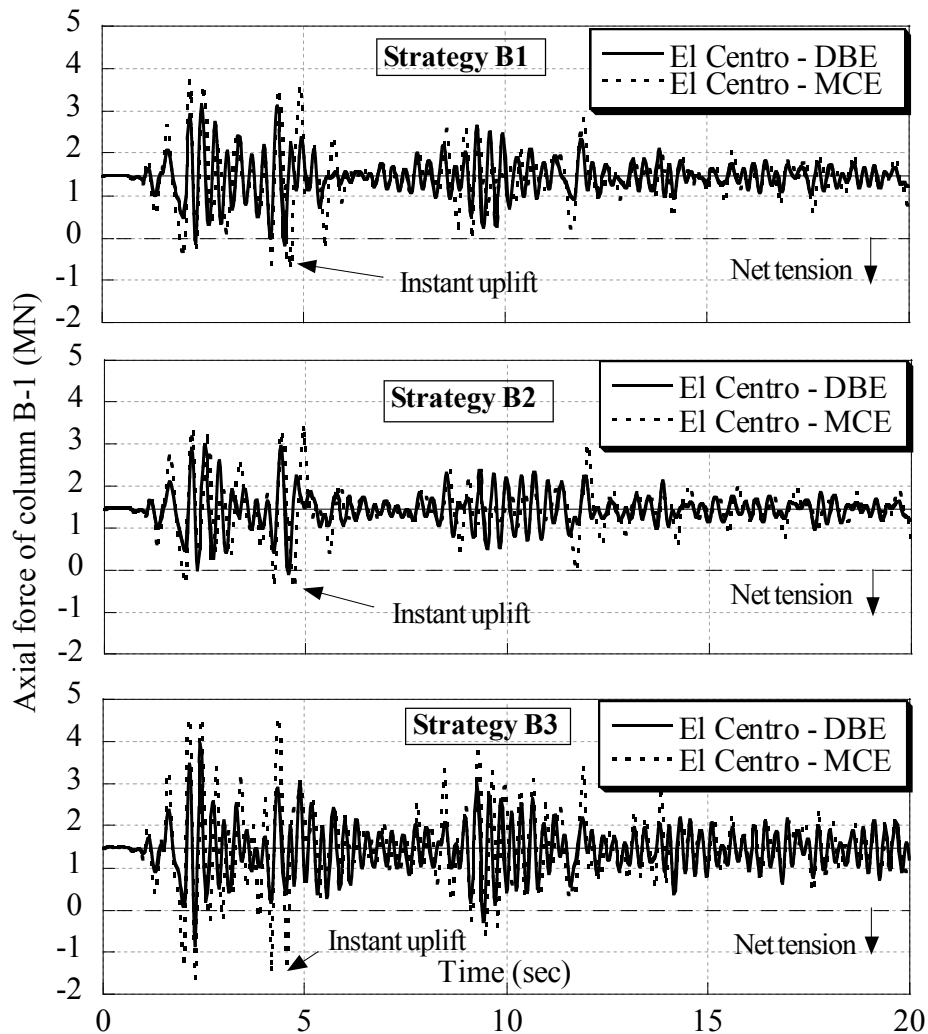**Fig. 4.37 Shear response of frame 1 in strategy B3**

Fig. 4.38 Variation of axial force of column B-1

5. SUMMARY AND CONCLUSIONS

5.1 Summary of thesis

This thesis mainly focuses on seismic evaluation and retrofit of soft-first-story (pilotis) RC buildings. In general, the thesis consists of three main parts. In first part, a series of experimental investigations were conducted to retrofit one-bay one-story pilotis RC frames with thick hybrid wall. The test specimens were retrofitted with wing-wall-type and panel-wall-type thick hybrid wall. The details of retrofitting procedure and loading test are explained in details. Also, the design frameworks for this retrofit type were discussed. After verification of possible mechanisms, the experimental results and the results of suggested design frameworks were compared.

The behaviors of columns retrofitted by wing-wall-type and panel-wall-type thick hybrid wall were modeled by modified Sina hysteresis rules to use in dynamic response analyses. The original Sina hysteresis model was modified based on the experimentally observed mechanism to be suitable for representing the behavior of thick hybrid wall. Furthermore, the behavior of the RC column retrofitted by PC bar was calibrated by Takeda hysteresis rule.

To find out the behavior of soft-first-story buildings retrofitted by thick hybrid wall, an existing soft-first-story building was selected to analyze and assess. The dynamic response analysis and seismic vulnerability assessment of the building were carried out before and after retrofitting of the building. Five strategies for retrofitting of the soft-first-story building were considered. Two strategies are according to conventional method and three strategies are based on the thick hybrid wall technique. The seismic performances of the building retrofitted by different strategies were compared.

5.2 Conclusions

According to the experimental investigations and analytical approach the following conclu-

sion can be derived;

1- Experimental investigations on one-bay one-story RC frames exhibited that by application of thick hybrid wall, the lateral strength and stiffness of the frame significantly increased. In case of wing-wall-type thick hybrid wall, the length of additional wing-wall can be readily decided to provide the required lateral stiffness and strength.

2- The comparison between the results of specimens R06P-WW and R08P-WA, exhibits the influence of jacketing steel plates in shear resistance. Since, in specimen R06P-WW, deck plates were used instead of plain steel plate and deck plates did not have sufficient resistance against in-plane deformation, a diagonal tension crack formed in each wing-wall.

3- The comparison between the governing mechanisms of specimens R08P-WN and R08P-WA, exhibits that the steel plates which were anchored to the top beam had effective contribution in shear-sliding resistance at top of wing-wall.

4- The retrofit plan of specimen R08P-WA can be considered as well-designed scheme that can obtain the desired performance.

5- Simplified design equations are suggested for shear strength and shear sliding of column retrofitted by thick hybrid wing-wall.

6- The columns retrofitted by thick hybrid wall were calibrated by modifying the Sina hysteresis taking into consideration the pinching effect.

7- In all of the nonlinear dynamic analyses including conventional method and proposed method, the building that satisfied the required condition of Japan Building Disaster Prevention Association successfully passed the design basis earthquake at life safety limit state.

8- The results of nonlinear dynamic analyses showed application of thick hybrid wall not only satisfies the demand of design basis earthquake at life safety, but also it readily prevents the collapse of the building even during an extreme level of seismic excitations, while utilizing this technique does not provide architectural limitations in the plan of the soft-first-story building.

REFERENCES

[1]   Otani, S.: Earthquake Resistant Design of Reinforced Concrete Buildings, Journal of Advanced Concrete Technology, JCI, Vol. 2, No. 1, pp. 3-24, Feb. 2004.

[2]   Japan Association for Building Disaser Prevention, Standard for Sesimic Vulnerability Assessment of Existing Reinforced Concerete Buildings, 300 pp., 1977, revised in 1990, 2001. (in Japanese)

[3]   Japan Association for Building Disaster Prevention, seismic Retrofit Design Guidelines for Axisting Reinforced Concrete Building, 337pp., 1977, revised in 1990 and 2001. (in Japanese)

[4]   Japan Association for Building Disaster Prevention, Standard for Post-earthqauke Inspection and Guidelines for Repair and strengthening Technology (in Japanese(, 122 pp., 1991.

[5]   Architectural Institute of Japan, Report on the Damage Investigation of the 1985 Mexico Earthqauke, 599 pp., 1987. (in Japanese)

[6]   Federal Emergency Management Agency & American Society of Civil Engineers: Prestandard and Commentary for the Seismic Rehabilitation of Buildings, FEMA 356, Nov. 2000.

[7]   Folippou. F. C., Ambrisi, A. D. & Issa, A.: Nonlinear static and Dynamic of Reinfiorced Concrete Assemblege, Report No. UCB/EERC-92/08, Earthquake Engineering Research Center, College of Engineering University of California, berkeley, August, 1992.

[8]   Yamakawa, T., Rahman, M. N. & Morishita, Y.: Experimental Investigation and Analytical Approach for Seismic Retrofit of RC Column with Wing-wall, Journal of Structural and Construction Engineering, AIJ, pp. 109-117, 608, Oct., 2006.

[9]   Yamakawa, T., Rahman, M. N., Nakada, K. & Morishita, Y.: Experimental and Analytical Investigation of Seismic Retrofit Technique for a Bare Frame Utilizing Thick Hybrid Walls, Journal of Structural and Construction Engineering, AIJ, pp. 131-138, 610, Dec., 2006.

[10] Rahman, M., D.: An Innovative Seismic Retrofit Technique of Cast-in-site Thick Hybrid Infill Wall into RC Frame -Experimental Investigation and Analytical Approach-, Doctoral thesis, Graduate School of Engineering and Science, University of the Ryukyus, 2007.

[11] Paulay, T. and Priestley, M. J. N.: Seismic Design of Reinforced Concrete and Masonry Buildings, John Wiley & Sons, pp. 129, 480, 1992.

[12] Rahman, M. N. & Yamakawa, T.: Investigation of Hybrid Technique for Seismic Retrofitting of Bare Frames, Journal of Advanced Concrete Technology, JCI, Vol. 5, No. 2, pp. 209-222, June, 2007.

[13] Ramin, M., V., Matamoros, A., B.: Shear Strength of Reinforced Concrete Members Subjected to Monotonic Loads, Structural Journal, American Concrete Institute, V. 103, No. 1, January-February, 2006.

[14] Joint ACI-ASCE Commitee 445, Recent Approach to Shear Design of Structural Concrete, Journal of Structural Engineering, ASCE, V. 124, No. 12, pp. 1375-1417, 1998.

[15] Bazant, Z., P. & Kim, J., K.: Size Effect in Shear Failure of Longitudinally Reinforced Beams, ACI Journal, Proceedings V. 81, No. 5, pp. 456-468, Sep-Oct., 1984.

[16] Collins, M., P. & Mitchell, D.: Prestressed Concrete Structures, Prentice Hall International Series in Civil Engineering and Engineering Mechanics, Prentice Hall, Englewood Cliffs, N.J., 766 pp., 1991.

[17] Kotsovos, M., D. & Pavlovic, M., N.: Size Effects in Beams with Small Shear Span-to-Depth Ratios, Computer and Structures, Elsevier, V. 82, No. 2-3, pp. 143-156, 2004.

[18] Tompos, E., J. and Frosch, R., J.: Influence of Beam Size, Longitudinal Reinforcement, and Stirrup Effectiveness on Concrete Shear Strength, ACI Structural Journal, V. 99, No. 5, pp. 559-567, Sep.-Oct.,2002

[19]   Watanabe, F. & Ichinose, T.: Strength and Ductility Design of RC Members Subjected to Combined Bending and Shear, Preliminary Proceedings, International Workshop on Concrete Shear in Earthquake, University of Houston, Houston , Tex., pp. IV4-1 to IV4-10, 1991.

[20]   Aoyama, H.: Design Philosophy for Shear in Earthquake Resistance in Japan, Earthquake Resistance of Reinforced Structures, T. Okayed, ed., Department of Architecture, Faculty of Engineering, University of Tokyo, pp. 407-418, 1993.

[21]   Architectural Institute of Japan , AIJ Design Guidelines for Earthquake Resistant Reinforced Concrete Buildings Based on Ultimate Strength Concept, with Commentary, 337 pp., 1988.

[22]   Kabeyasawa, T. & Hiraishi, H.: Tests and Analyses of High-Strength Reinforced Concrete Shear Wall in Japan, High-Strength Concrete in Seismic Regions, SP-176, C. W. French and M. E. Kreger, eds., American Concrete Institute Farmington hills, Mich., pp. 281-310, 1998.

[23]   Watanabe, F. & Kabeyasawa, T.: Shear Strength of RC Members with High-Strength Concrete, High strength Concrete in Seismic Regions, SP-176, C. W. French and M. E. Kreger, eds., American Concrete Institute, Farmington Hills, Mich., pp. 379-396, 1998.

[24]   Nielsen, M. P.: Limit Analysis and Concrete in Plasticity, prentice-Hall, 1984.

[25]   Astaneh-Asl, A.: Seismic Behavior and Design of Steel Shear Walls, Steel TIPS, Structural Steel Educational Council, Maraga, CA, January, 2001.

[26]   Bikeland, P. W. & Birkeland, H. W.: Connection in Precast Concrete Construction, ACI J., Vol. 63, No. 3, pp. 345-368, 1966.

[27]   Valluvan, R., Kreger, M. E. & Jirsa, O. J.: Evaluation of ACI 38-95 Shear-friction Provisions, ACI Structural Journal, Proc. V. 96, No. 4, July-Aug., pp. 473-483, 1999.

[28]   Park, R. and Paulay, T.: Reinforced Concrete Structures, John Wiley & Sons, pp.319-325, 1975.

[29]   Otsni, S.: Hysteresis Models of Reinforced Concrete for Earthquake Response Analysis, Journal of the Faculty of Engineering, the University of Tokyo, Vo. XXXVI, No. 2, May, 1981.

[30]   Umemura, H., Editor, Dynamic Design for Earthquakes of Reinforced Concrete Buildings, Giho-do Publishing C., Japan, 1973. (in Japanese)

[31]   Tani, S., Nomura, S., Nagasaka, T. & Hiramatsu, A.: Restoring FOrce Characteristics of Reinforced Concrete Seismic elements-III Influence of Restoring Force Characteristics on dynamic Response of Structure, Transaction, AIJ, No. 228, pp. 39-48, 1975.

[32]   Celebi, M. & Penzien, J.: Experimental Investigation into the Seismic Behavior of the critical Regions of Reinforced Concrete Components as Influenced by Moment and Shear, Earthquake Engineering Research Center, Report No. EERC 73-4, University of California, Berkeley, 1973.

[33]   Yamakawa, T., Rahman, M. N., Nakada, K. & Morishita, Y.: Experimental and Analytical Investigation of Seismic Retrofit Technique for a Bare Frame Utilizing Thick Hybrid Walls, Journal of Structural and Construction Engineering, AIJ, pp. 131-138, 610, Dec., 2006.

[34]   Saiidi, M. & Sozen, M. A.: Simple and Complex Models for Nonlinear Seismic Response of Reinforced Concrete Structures, Report UILU-ENG-79-2031, Department of Civil Engineering, University of Illinois, Urban, Illinois, August, 1979.

[35]   Carr, A. J.: RUAUMOKO Computer Program, Nonlinear Dynamic Analysis, Department of Civil Engineering, University of Canterbury, Christchurch, New Zealand, 1980-2007.

[36]   Yamakawa, T., Kamogawa, S. & Kurashige, M.: An Experimental Study on the Seismic Retrofit Technique for RC Columns Confined with PC Bar Prestressing as External Hoops, Journal of Structural and Construction Engineering, AIJ, No. 526, pp. 141-145, Dec., 1999. (in Japanese)

[37]   Yamakawa, T. & Miyagi, T.: An Emergency Seismic Retrofit Technique for Shear Damaged RC Columns Using Pre-tensioned PC Bars and Steel Plates, Journal of Structural

and Construction Engineering, AIJ, No. 586, pp. 171-178, Dec., 2004. (in Japanese)

[38]   Shinjo, Y. & Yamakawa, T.: Shear Strength of RC Columns Externally Retrofitted by PC Bar Prestressing, AIJ Kyushu Chapter Architectural Research Meeting (Structure), No. 46, pp. 405-408, March, 2007. (in Japanese)

[39]   Otani, S.: SAKE, A Computer Program for Inelastic Response of R/C Frames to Earthquakes, Report UILU-Eng-74-2029, Civil Engineering Studies, Univ. of Illinois at Urbana-Champaign, Nov. 1974.

[40]   Carr, A. J.: RUAUMOKO Computer Program, Nonlinear Dynamic Analysis, Department of Civil Engineering, University of Canterbury, Christchurch, New Zealand, 1980-2007.

[41]   Cook, R. D.: Remarks About Diagonal Mass Matrices, Int. J. Numerical Methods in Engineering, Vol. 17, pp. 1427-1449, 1981.

[42]   Clough, R. W. & Penzien, J. Dynamic of Structures, Second Edition, McGraw-Hill, New York, 735pp., 1993.

[43]   Crisp, D. J., Damping Models for Inelastic structures, M. E. Report, Department of Civil Engineering, University of Canterbury, Feb. 1980.

[44]   Caughey, T. K.: Classical Normal Modes in Damped Linear Systems, J. Appl. Mech., Vol. 27, pp. 269-271, 1960.

[45]   Sharpe, R. D.: The Seismic Response of Inelastic Structures, PhD Thesis, Department of Civil Engineering, University of Canterbury, Nov. 1974.

[46]   Stewart, W. G.: The Seismic Design of Plywood Sheathed Shear Walls, PhD Thesis, Department of Civil Engineering, University of Canterbury, 395 pp., March, 1987.

[47]   Architectural Institute of Japan: Design Guidelines for Earthquake Resistant Reinforced Concrete Buildings Based on Inelastic Displacement Concept, 1999. (in Japanese)

[48]   Carr, A. J.: Dynamic analysis of Structures, Bull., NZ Nat. Soc. Earthquake Engineering, Vol. 27, No. 2, 129-146 pp., June 1994.

[49]   Clough, R. W. & Penzien, J. Dynamic of Structures, Second Edition,McGraw-Hill, New York, 735pp., 1993.

[50]   Tobita, T., Ghayamghamian, M. R., Kang, G. C. & Iai, S.: Preliminary Report of the July 16, 2007 Niigata Prefecture Chuetsu Off Shore (Niigata-Ken Chuetsu-Oki), Japan, Earthquake, Disaster Prevention Research Institute, Kyoto University, Japan, 2007.

[51]   Public Building Association: Standard for Structural Design of Buildings, 1997.

[52]   Abe, H.: Outline of Japanese Seismic Design Review Guide of Nuclear Power Reactor Facilities, Japan Nuclear Energy Safety Organization, Sept. 2007.

[53]   Kabeyasawa, T., Shiohara, H., Otani, S. & Aoyama, H.: Analysis of the Full-scale Seven-story Reinforced Concrete Test Structure, Journal of the Faculty of Engineering, University of Tokyo, (B), pp. 432-478, Vol. XXXVII, No. 2, 1983.

[54]   Tomii, M. & Takeuchi, M.: The Relations between the Deformed Angle and the Shearing Force Ratio (0.80~1.00) with Regard to 200 Shear Walls, Trans. of AIJ, No. 153, Nov. 1968.

LIST OF PUBLICATIONS

Refereed Papers:

1. **Javadi, P.** & Yamakawa, T.: Seismic Analyses of a Soft-first-story RC Building Retrofitted by Thick Hybrid Wall Technique During Strong Earthquake Excitations, Journal of Structural and Construction Engineering, AIJ, No. 636, pp. 339-349, Feb., 2009.

2. **Javadi, P.**, Yamakawa, T., Kobayashi, M. & Gaja, M.: Cyclic Loading Tests on Soft-first-story RC Frames Retrofitted with Thick Hybrid Wing-wall, Proceedings of Japan Concrete Institute (JCI), July, 2009. (in press)

3. Kobayashi, M., Yamakawa, T., Maeda K. & **Javadi, P.**: Seismic Performance of 1-bay 2-story Pilotis Frame Retrofitted by Thick Hybrid Wall, Proceedings of Japan Concrete Institute, pp. 415-420, Vol. 30, No. 2, 2008. (in Japanese)

4. Maeda, K., Yamakawa, T., Rahman, M. N. & **Javadi, P.**: Investigation of 1-bay 2-story Pilotis Frame Retrofitted by Non-reinforced Thick Hybrid Wall, Proc. of JCI, pp. 289-294, Vol. 29, No. 3, 2007. (in Japanese)

International Conferences:

5. Yamakawa, T. & **Javadi, P.**: A Convenient Seismic Retrofit Technique of Soft Story RC buildings, Fifth International Conference on Urban Earthquake Engineering, March 4-5, 2008, Tokyo Institute of Technology, Tokyo, Japan, pp. 155-160, March, 2008.

6. **Javadi, P.**, Shinya, T., Yamakawa, T., Rahman, M. N. & Carr, A. J.: Nonlinear Dynamic Analysis of Soft-first-story Building before and after Retrofitting, 8th Pacific Conference on Earthquake Engineering, Singapore, Paper No. 257, Dec. 2007.

Other Publications:

7. Kobayashi, M., Yamakawa, T. & **Javadi P.**: Cyclic loading Tests on One-bay One-story Pilotis Frames Retrofitted by Steel Braced Frames, Annual Meeting of AIJ, Vol.C-2, August, 2009. (in Japanese) (in press)

8. Taira, K., Yamakawa, T., **Javadi, P.** & Kobayashi, M.: Cyclic Loading Test on One-bay Two-story Pilotis RC Frames Retrofitted by Thick Hybrid Wing-wall, Annual Meeting of AIJ, Vol. C-2, August, 2009. (in Japanese) (in press)

9. **Javadi, P.**, Yamakawa, T., Gaja, M. & Kobayashi, M.: Experimental Investigation on Soft-first-story RC Frame Retrofitted by Thick Hybrid Wing-wall, AIJ Kyushu Chapter Architectural Research Meeting (Structure), No. 48, pp. 509-512, March, 2009.

10. Gaja, M., Yamakawa, T., **Javadi, P.**, Yamashiro, K.: Experimental Investigation on Shear-sliding Resistance of RC Bare Frame Retrofitted by Thick Hybrid Wall, AIJ Kyushu Chapter Architectural Research Meeting (Structure), No. 48, pp. 505-508, March, 2009.

11. Taira, K., Yamakawa, T., Kobayashi, M. & **Javadi, P.**: Seismic Performance of one-bay one-story Pilotis Frames Retrofitted by Steel Braced Frames – Part 1: Test Plan -, AIJ Kyushu Chapter Architectural Research Meeting (Structure), No. 48, pp. 537-540, March, 2009. (in Japanese)

12. Kobayashi, M., Yamakawa, T., **Javadi, P.** & Taira, K.: Seismic Performance of one-bay one-story Pilotis Frames Retrofitted by Steel Braced Frames – Part 2: Experiemntal Result and Discussion -, AIJ Kyushu Chapter Architectural Research Meeting (Structure), No. 48, pp. 537-540, March, 2009. (in Japanese)

13. **Javadi, P.** & Yamakawa, T.: Seismic Response Analysis of an Existing Soft-first-story RC Building Before and After Retrofitting by Thick Hybrid Wall Technique, Annual Meeting of AIJ, Vol.C-2, August, 2008.

14. Kobayashi, M., Yamakawa, T. & **Javadi, P.**: Cyclic Loading Test on One-bay Two-story Pilotis RC Frames Retrofitted by Thick Hybrid Wall, Annual Meeting of AIJ, Vol.C-2, August, 2008.

15. Maeda, K., Yamakawa, T. & **Javadi, P.**: Seismic Performance of a 1-bay 2-story Pilotis Frame Retrofitted by Thick Hybrid Wall, AIJ Kyushu Chapter Architectural Research Meeting (Structure), No. 47, pp. 337-340, March, 2008. (in Japanese)

16. **Javadi, P.**, Yamakawa, T., Rahman, M. N. & Takara, S.: Nonlinear Dynamic Response of an Existing Pilotis-type RC building Before and After Retrofitting, Annual Meeting of AIJ, Vol.C-2, August, 2007.

17. Maeda, K., Yamakawa, T., Rahman, T. & **Javadi, P.**: Experimental Investigation of a Hybrid Technique of Seismic Retrofit for 2-story 1-bay Pilotis Frame, Annual Meeting of AIJ, Vol.C-2, August, 2007.